CONDUCTION BLOCK IN PERIPHERAL NERVES: EFFECT OF HIGH FREQUENCY STIMULATION ON DIFFERENT FIBER TYPES

A Dissertation
Presented to
The Academic Faculty

By

Laveeta Joseph

In Partial Fulfillment
Of the Requirements for the Degree
Doctor of Philosophy in the
Interdisciplinary Bioengineering Graduate Program
Department of Biomedical Engineering

Georgia Institute of Technology
December 2010

CONDUCTION BLOCK IN PERIPHERAL NERVES: EFFECT OF HIGH FREQUENCY STIMULATION ON DIFFERENT FIBER TYPES

Approved by:

Dr. Robert J. Butera, Advisor
School of Electrical and Computer Engineering
Georgia Institute of Technology

Dr. Ronald L. Calabrese
Department of Biology
Emory University

Dr. T. Richard Nichols
School of Applied Physiology
Georgia Institute of Technology

Dr. Ravi V. Bellamkonda
Department of Biomedical Engineering
Georgia Institute of Technology & Emory University

Dr. Robert Lee
Department of Biomedical Engineering
Georgia Institute of Technology & Emory University

Date Approved: 16 June 2010

To my parents –my inspiration and my strength

ACKNOWLEDGEMENTS

This PhD work was possible due to the support of a number of special people whom I would like to acknowledge. First, I would like to thank my PhD advisor, Dr. Robert J. Butera. His advice and guidance over the past 6 years helped transform me from a naïve undergraduate into a competent researcher. He was always just an email or a phone call away for professional or personal advice. Thank you for giving me the freedom to pursue the projects I wanted and to travel whenever I needed. Thank you for being a great mentor and teaching me the importance of time-management and work-life balance. This PhD would not have been possible without your supervision and thank you for making it a 'painless' experience for me.

Next, I would like to thank my PhD committee members- Dr. Ronald Calabrese, Dr. Richard Nichols, Dr. Ravi Bellamkonda and Dr. Bob Lee - for their innovative ideas that helped shape this work. Each of them has also been instrumental in helping me navigate the various stages of the PhD process. I want to thank Ravi for introducing me to the Neurolab and Bob for leading me to Rob's lab. The classes I took with Ron and Richard were among the best classes I have ever taken and their passion for science and teaching will always inspire me. I would also like to thank Richard and Bob for their help during my preparation for the PhD qualifying exam and the PhD proposal. Each of my committee members has been ever willing to meet with me individually and their inputs have been indispensable to the success of my projects.

I would also like to acknowledge all the members of the Butera Group – especially Dr. Amanda Preyer, Dr. Luke Purvis, Murat Sekerli, "Mouse" Tsao and Isaac Clements, who besides being exceptionally intelligent colleagues, have been an extremely fun group to work with.

Thanks to Ben Haeffele for the simulation work described in this dissertation and thanks to all the undergraduates I have had the opportunity to mentor and learn from over the past few years. I would like to thank a number of people from the Laboratory for Neuroengineering at Georgia Tech and the Neuroscience program at Emory University, who taught me various skills and techniques that made me a good researcher. Thanks to Dr. Carrie Williams, Edgar Brown and Dr. Stefan Clements for the various technical discussions that helped in the design of some of my PhD experiments. Thanks to Kartik Sundar, Liang Guo, Essy Behravesh and Angela Albrecht for their help with the frog room maintenance. Thanks to Sarah Jones, Bob Lee and other members of the Lee and Nichols group for their help with experiments on cat nerves. Special thanks to Dr. Angela Wenning-Erxleben and other members of the Calabrese group for teaching me techniques to obtain great electrophysiological recordings. Thanks to Dr. Astrid Prinz for discussions related to culturing Lymnaea axons and to Dr. Naweed Syed for being a great host during our brief visit to the University of Calgary.

Special thanks to all the administrative staff in the Neurolab, the BME and the Bioengineering programs, specially - Amber Massey, Brian Williams, Jon Hall, John Holthaus, Chris Ruffin, Sally Gerrish, Beth Bullock, Shannon Sullivan, Sandra Wilson, May-Lin Chang, Steven Marzec and Jesus Mata-Acosta - whose help at various points in the PhD program enabled me to complete my PhD efficiently and smoothly. I would also like to acknowledge the National Science Foundation (NSF) and the Schlumberger Foundation Fellowship that supported my graduate education and provided me the freedom to pursue the projects I wanted.

I would like to dedicate this work to my parents- Dr. Mercy Joseph and Mr. Joseph Chacko, whose endless sacrifices and hard work have helped me become what I am today. I would specially like to thank my Mom, whose immense love and untiring strength will always amaze and inspire me. My family is my biggest strength and I couldn't have done this without their love and support. The past 6 years of my PhD have also been the toughest years for my family, yet they always pushed me to keep persevering with the PhD. Thank you Mom and Dad for supporting me in my every decision and I hope I can always make you proud. I would also like to thank my sister, Dr. Joveeta Joseph Ruben, who was always available to lend an ear or a shoulder to lean on, despite the distances. Her honest advice, in both personal and professional matters, has been invaluable to me. Thank you for constantly cheering me on over the years and I am extremely grateful to have you as my sister. I would also like to thank my brother-in-law, Christopher Ruben, for being extremely supportive and for making all my vacations in India really enjoyable. Thanks also to my niece and nephew, Rhea and Neil Ruben, who have unwittingly been a source of joy and entertainment for my family and helped us laugh through the tough times. Over the past 2 years, I have also been blessed with the support of another family, my in-laws – Olga and Dominic Maladen, and Michelle, Dennis and Diya Percy. Thank you for your love and constant words of encouragement.

I have also had the good fortune of finding an extremely great group of friends, who have made the PhD process really pleasant. I would specially like to thank the 'SLARP' ladies- Dr. Swathi Ravi, Dr. Abbey Wojtowicz, Dr. Rekha Nair and Dr. Priya Santhanam, for the crazy halloween costume parties, the annual outlet mall shopping trips, the movies nights and the various occasions we celebrated together. Our frequent hangouts helped me survive the rigors of

graduate school and I am delighted to have such a close group of friends. Thanks for also making my wedding day very special by flying down all the way to India despite your hectic schedules. A few additional friends in the Bioengineering program that deserve special mention are Dr. Radhika Madhavan, Komal Rambani, Sandeep Prabhakara, Dr. Mahesh Dodla, Dr. Kartik Sundar, Dr. Murali Padala, Dr. Kartik Balachandran, Dr. Kartik Sundareswaran and Dr. Yash Kolambkar, who have not only helped me personally at various points over the past few years, but have also made the PhD experience really memorable. I also want to thank Fr. Mario Di Lella, for caring and supporting me through some tough times. He has been a great spiritual mentor and friend and his dynamism and optimism will always inspire me. I would also like thank my undergraduate friends for over 10 years, Smruta Koppaka and Tarun Saxena, for always finding time to stay in touch and supporting each other through the good and the bad times. Thanks also to my extended family, especially Dr. Anthony Chacko and Dr. Susan Anthony, and to all my friends for their love and support during the entire PhD process.

Finally, I want to thank the one person who made it all easy for me– my husband, Ryan Maladen. Thank you for being extremely patient with me and for always giving priority to my needs, however irrational they were. Your love and support helped me glide through the toughest years of graduate school. Thank you for challenging and pushing me, especially when I was down. Thank you for knowing how to always bring a smile on my face. I could not have done it without you. Thank you my love. Georgia Tech and the PhD will always be special, because of you!

TABLE OF CONTENTS

LIST OF TABLES

LIST OF FIGURES

LIST OF ABBREVIATIONS

HFAC	High Frequency Alternating Current
AC	Alternating Current
DC	Direct Current
DBS	Deep Brain Stimulation
FES	Functional Electrical Stimulation
AP	Action potential
CAP	Compound Action Potential
HH	Hodgkin-Huxley
FDC	Frequency-Dependent Capacitance
MRG	McIntyre, Richardson and Grill model
A-fiber	Myelinated nerve fiber with conduction velocity > 6 m/s
C-fiber	Unmyelinated nerve fiber with conduction velocity < 1 m/s

Chemical Ions/Compounds:

Na^+	Sodium ion
K^+	Potassium ion
Ca^{2+}	Calcium ion
Cl^-	Chloride ion
Mg^{2+}	Magnesium ion
Ag	Silver
AgCl	Silver Chloride

Units:

Hz	hertz (seconds $^{-1}$)
kHz	kilohertz (milliseconds^{-1})
ms	millisecond
m/s	meter per second
μA	microamperes
mA	milliamperes
V	volt
dB	decibel

SUMMARY

Selective stimulation and conduction block of specific nerve fibers has been a major area of research in neuroscience. The potential clinical and neurophysiological applications related to spasticity suppression, pain management, bladder control and graded motor control for neural prostheses have warranted reliable techniques for transiently blocking conduction through nerves. High Frequency Alternating Current (HFAC) waveforms have been found to induce a reversible and repeatable block in peripheral nerves; however the effect of these waveforms on the neural activity of individual fiber types is currently unknown. Understanding this effect is critical if clinical applications are to be pursued. This dissertation work utilized extracellular electrophysiological techniques to characterize the activity of different fiber type populations in peripheral nerves during application of HFAC waveforms. First, we investigated the phenomenon in the homogeneous unmyelinated nerves of the sea-slug, *Aplysia californica.* Although complete reversible block was demonstrated in these nerves, a non-monotonic relationship of block threshold to frequency was found which differed from previously published work in the field. We then investigated the effect of HFAC waveforms on amphibian mixed nerves and studied the response of specific fiber types by isolating different components of the compound action potential. We validated our results from the *Aplysia* nerves by determining the block thresholds of the larger diameter, myelinated A-fibers and comparing them with those of the smaller diameter, unmyelinated C-fibers, at different frequencies. We also showed that block threshold behavior during application of the HFAC waveform depends on the nerve fiber type, and this property can be used to selectively block specific fiber types at certain frequencies. Finally, we examined the recovery time after block induction in unmyelinated nerves and found

that recovery from block was dependent on the duration of application of the HFAC waveform. The time-dependent distribution of the recovery time and the non-monotonic threshold behavior in the smaller diameter unmyelinated nerves indicate that multiple mechanisms are involved in block induction using HFAC waveforms, and these mechanisms are dependent not only on the blocking stimulus but also on the characteristics of the nerve fiber. Overall, this work demonstrates that HFAC waveforms may enable inherent peripheral nerve properties to be exploited for potential clinical applications related to the treatment of unwanted neural activity.

CHAPTER 1

INTRODUCTION

Defects in the nervous system resulting from accidents, damages inflicted during medical procedures and autoimmune diseases can lead to a loss in control of motor systems and/or to the improper functioning of sensory systems. These disruptions in the neural communication pathways are difficult to treat because functionality is not often restored even if complete regeneration of the nerve occurs (Chen *et al.*, 2007). Neural interface systems have emerged as viable solutions for use in various debilitating conditions to restore or supplement nerve functionality and thus enhance the quality of life (Hatsopoulos & Donoghue, 2009). The ultimate goal of most neural interface systems is to electrically bridge the gap in neural signaling after nerve transection and replicate normal behavior (Prochazka *et al.*, 2001) . Natural behavior can be mimicked by providing an appropriate electrical stimulus to the severed nerve after deciphering the neural activity of the response to a know behavior. Isolating the right neural activity for a desired action and stimulating specific fibers in an appropriate order to obtain a physiologically analogous behavior has been extremely challenging for researchers in the field of neural interfaces (Rushton, 1997; Lertmanorat *et al.*, 2006).

Selective activation of specific fibers of the transected nerve is essential to replicate the normal behavior and restore functionality. Selective stimulation can be achieved either by spatial selectivity or fiber diameter selectivity, but they are difficult to realize using extracellular electrical stimulation. Spatial selectivity of nerve fibers is only

possible by modulation of stimulation procedures and parameters due to the complex anatomical intermingling of sensory and motor fibers (Peng *et al.*, 2004). Fiber diameter selectivity is also difficult to achieve, particularly due to the reverse recruitment order of nerves during extracellular stimulation. Physiologically the smaller motor units are recruited before the larger ones, as described by the 'size principle'. This graded recruitment enables dexterous control of motor systems and prevents muscle fatigue (Henneman & Olson, 1965; Mendell, 2005). But neural prostheses and external stimulation devices, like functional electrical stimulation (FES) systems, recruit individual fibers in the reverse physiological order (Baratta *et al.*, 1989). Larger diameter fibers are recruited first and then the smaller diameter fibers due to the lower resistivity and in turn lower activation threshold of the larger diameter fibers (Blair & Erlanger, 1933) . This reverse recruitment order during external stimulation often leads to a poor grading of muscle force, rapid muscle fatigue and an inefficient stimulation system (Baratta *et al.*, 1989; Lertmanorat *et al.*, 2006).

Developing techniques that could enable the activation of the smaller diameter fibers first while preventing excitation of the larger diameter fibers would be critical for generating a physiologically relevant stimulus. Transient conduction block would also be advantageous for neurophysiological studies involving complex neural circuitry. Reversible block of specific pathways within a neural circuit (consisting of multiple feedback loop pathways) would enable the detachment of specific components of the circuit to study its function in isolation or its effect on the entire system (Tanner, 1962; Solomonow, 1984). Hence, besides enhancing control in neural prosthetic systems,

selective blocking of specific nerve fibers would also provide a useful neurophysiological tool for investigating the behavior of specific neurons or pathways.

Application of high frequency alternating current (HFAC) waveforms on peripheral nerves has been found to be a potential clinical method for blocking conduction of action potential through nerves (Tanner, 1962) and achieving selective stimulation (Baratta *et al.*, 1989). However, most experimental work in the field has been focused on motor block applications where the progression of block in each fiber type population within whole nerves is difficult to detect. Characterizing the behavior of individual fiber types during HFAC stimulation is critical for the clinical implementation of this technique. It is the objective of this work to evaluate the effect of HFAC waveforms on individual fiber type populations in peripheral nerves and determine the feasibility of this technique to selectively stimulate specific fibers.

1.1 Specific Aims

The overall goal of this work is to characterize neural activity in different fiber type populations during application of HFAC waveforms for the development of a clinical technique that might enable selective stimulation of specific fibers. High Frequency Alternate Current (HFAC) waveforms have been known to induce a local, reversible conduction block in motor nerves but their effect on isolated fiber types and the biophysical mechanism through which block induction occurs is currently debated. Direct monitoring of neural activity using extracellular electrophysiological techniques should enable us to study the effect of the HFAC waveforms on different fibers and gain

a better understanding of the phenomena. To achieve our objective, three studies were undertaken as outlined below and detailed in subsequent chapters of this work.

Specific Aim 1: Characterize the effect of HFAC waveforms on unmyelinated nerves. High Frequency Alternate Current (HFAC) waveforms have been shown to block the conduction of action potentials in motor nerves but the response of isolated unmyelinated nerves in isolation has not been previously studied. We investigated the effect of sinusoidal HFAC waveforms on the purely unmyelinated nerve fibers of *Aplysia californica*. In this aim, we varied the frequency and amplitude of the HFAC waveform and monitored the response before, during and after application of the HFAC waveform. Neural activity during these phases was characterized by monitoring the propagation of the compound action potential along the nerve and the block thresholds were determined for various frequencies. This was the first study to specifically investigate the effect of HFAC waveforms on unmyelinated nerves. A unique behavior not previously observed in literature was found in these nerves. The results for this study are discussed in Chapter 2.

Specific Aim 2: Characterize the effect of HFAC waveforms in mixed nerves and specifically investigate selective stimulation. Results of Specific Aim 1 indicated that the threshold behavior of unmyelinated nerves to HFAC stimulation differed from published literature on the threshold behavior of myelinated nerves during application of HFAC waveforms, especially for higher frequencies. This disparity in the behaviors of myelinated and unmyelinated nerves could potentially enable selective stimulation of specific fiber types. In order to validate our results from Aim1, we investigated the difference between myelinated and unmyelinated nerves by studying the effect of HFAC

stimulation on the compound action potential of mixed nerves of frogs and cats. We specifically investigated the A- fiber and the C-fiber components of the compound action potential, which corresponds to the signal propagating through the myelinated and the unmyelinated fibers respectively. We expected the threshold behavior of the unmyelinated C-fibers to be analogous to that of the *Aplysia* fibers, while the A-fibers were expected to have a linear threshold behavior, as observed in previously published studies on motor fibers. The results of this study are further elaborated and the clinical implications discussed in Chapter 3.

Specific Aim 3: Investigate the physiological mechanism of inducing block induction using HFAC waveforms. In this aim, we attempted to understand the physiological mechanisms that impede action potential propagation through nerve fibers during application of HFAC waveforms by exploring the recovery time from block induction. Simulation studies aimed at identifying the ionic mechanisms of block induction by HFAC waveforms have provided inconclusive results with block being attributed to a variety of mechanisms, depending on the type of computational model used. Physiological experiments with animal nerves have not been previously employed to identify HFAC induced blocking mechanisms. In this study, the frequency of the waveform and the duration of application of the HFAC waveforms were varied to discern if these factors played a role in block induction. This aim identifies factors of block induction using HFAC waveforms that were never previously considered. These results are elaborated and discussed in Chapter 4 of this dissertation.

1.2 Background and Significance

This section provides a brief introduction to conduction block induced by HFAC waveforms and a review of previous work that provides both the foundation and the motivation for the stated specific aims.

1.2.1 Conduction block

Neuromuscular pathologies commonly involve neuronal hyperactivity that cause undesirable sensations and hinder dexterous motor control. Undesired motor activity occurs in spasticity conditions and affects patients suffering from spinal cord injuries (Levi *et al.*, 1995), multiple sclerosis (Beard *et al.*, 2003), cerebral palsy (Flett, 2003) and stroke (O'Dwyer *et al.*, 1996). Dystonia, choreas, tics and intractable hiccups are other conditions that result from extraneous motor neural activity. Unwanted afferent activity also occurs in various conditions associated with chronic pain, like neuromas, neuralgias etc. Arresting or blocking these kinds of superfluous activity through peripheral nerves can be useful for alleviating the disease symptoms and eliminating the debilitating nature of these conditions.

Current methods of blocking the conduction of neural activity include pressure application (Perot & Stein, 1956; Perot & Stein, 1959), local changes in temperature (Franz & Iggo, 1968; McMullan *et al.*, 2004) and various surgical and pharmacological methods (Strichartz, 1976; Ashburn & Staats, 1999; Abbruzzese, 2002; Guven *et al.*, 2005; Martinov & Nja, 2005; Guven *et al.*, 2006). But these methods have several disadvantages in that they are not quick acting and quick reversing and possibly

irreversible, are non-specific and cause serious side-effects with possible nerve destruction. Though used for selective blocking they are unsuitable for chronic clinical applications. Their low success rates have warranted alternate methods of effectively blocking nerve conduction.

1.2.2 Electrical current stimulation

For almost a century now, high frequency electrical currents have been known to affect action potential conduction (Cattell & Gerard, 1935; Reboul & Rosenblueth, 1939; Rosenblueth & Reboul, 1939). High frequency alternating currents (AC) and direct currents (DC) have been used as method of inducing block in whole nerves (Tanner, 1962; Woo & Campbell, 1964; Bowman & McNeal, 1986; Petruska *et al.*, 1998; Bhadra & Kilgore, 2004; Kilgore & Bhadra, 2004). One study on DC induced conduction block (Petruska *et al.*, 1998), even demonstrated the ability of the DC stimulation technique to selectively block the conduction in peripheral myelinated A-nerve fibers while allowing propagation only in the unmyelinated C- fibers. However methodological problems related to polarization, inability to reproduce effective separation in larger nerves and generation of undesired synchronous and asynchronous activity by the polarization itself, limited the method's usefulness. High frequency AC stimulation, on the other hand, has been shown to be physiologically better then DC stimulation since it does not causes polarization of the electrode and the nerve after a few minutes of continuous application and has been employed in various chronic clinical applications (Woo & Campbell, 1964; Ishigooka *et al.*, 1994; Bhadra & Kilgore, 2005; Tai *et al.*, 2005; Bhadra *et al.*, 2006; Tai *et al.*, 2006)

Electrical currents have also been used to block conduction in other neurophysiological applications. In the Deep Brain Stimulation (DBS) field, frequencies in the 100-500 Hz range are used to block conduction through the central nervous system fibers (Durand & Bikson, 2001; Jensen & Durand, 2007). In these studies, extracellular stimulation at frequencies less than 500Hz are termed 'high frequency' stimulation and are used to reset the firing of neurons when unwanted neural activity is detected. In invertebrates, conduction block in axonal branches has been observed when the firing frequency of the neuron (Smith, 1983) or the frequency of the applied extracellular stimulus (Grossman *et al.*, 1979) is in the range of 30-100 Hz. This differential block of conduction is useful for transmitting information along axons that branch. Though these stimuli have been termed 'high-frequency' in literature, the mechanism involved in inducing conduction block in these fields differs from the local block observed in peripheral nerves where the frequency of stimulation is typically above 3 kHz.

1.2.3 High Frequency Alternating Current

High frequency alternating current (HFAC) waveforms, typically in the range of 3-30kHz, have been shown to induce a completely effective, repeatable, relatively localized and quickly reversible conduction block in various amphibian and mammalian animal models (Tanner, 1962; Ishigooka *et al.*, 1994; Kilgore & Bhadra, 2004; Tai *et al.*, 2004; Bhadra & Kilgore, 2005; Tai *et al.*, 2005; Williamson & Andrews, 2005; Bhadra *et al.*, 2006; Tai *et al.*, 2006). A schematic of the phenomena of locally blocking the conduction of action potentials along a nerve using HFAC waveforms is depicted in Figure 1.1. For frequencies below 1 kHz it is possible to induce a fatigue type block

caused by muscle fatigue or neurotransmitter depletion at the neuromuscular junction (Solomonow *et al.*, 1983). However, for frequencies above 3kHz, it has been demonstrated that the block obtained is not caused by nerve fatigue, but is a true neural block occurring around the local area of application of the high frequency waveform, since action potentials were shown to propagate at a distance away from the site of block (Kilgore & Bhadra, 2004). Figure 1.2 depicts a typical experimental setup used in published studies where the muscle force, measured by a force transducer, was used as an output measure of block status. A distal stimulator was used to verify that the nerve could be excited even when proximal stimulation could not activate the nerve. This distal stimulation technique indicated that the block induced by HFAC waveforms was a local block around the site of stimulation.

1.2.3.1 Block threshold

Even though conduction block induced by HFAC waveforms has been demonstrated on nerves from different species, the ideal frequency for block induction is still debated. This disparity can be attributed to the difference in the experimental conditions used to induce block in these investigations. The optimum frequency of block was found to be anywhere in the range of 3 kHz to 30 kHz. The experimental conditions of the different published studies where conduction block could be induced using HFAC waveforms are summarized in Table 1.1.

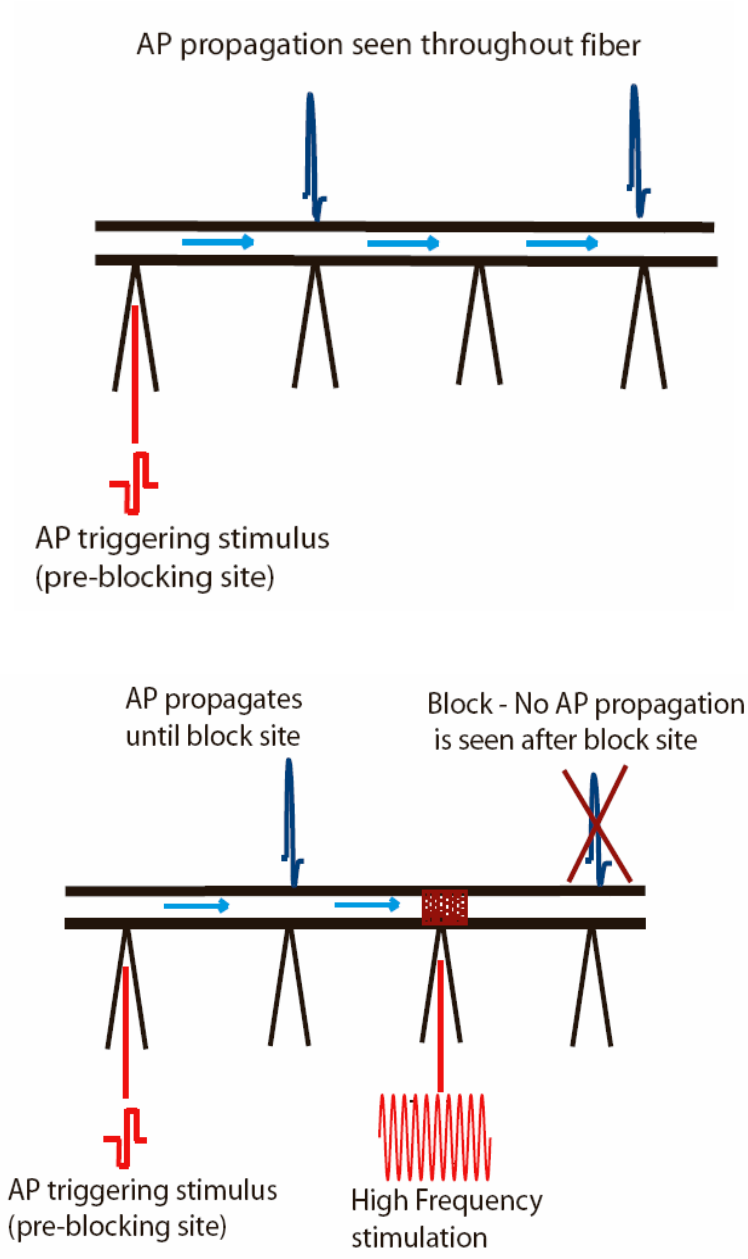

Figure1.1: Schematic of local conduction block induced by application of HFAC stimulation. A triggered action potential propagates along the length of the axon when no HFAC waveform is applied. Application of HFAC waveforms induces a local block at the site of stimulation preventing the action potential from propagating beyond the HFAC stimulating site.

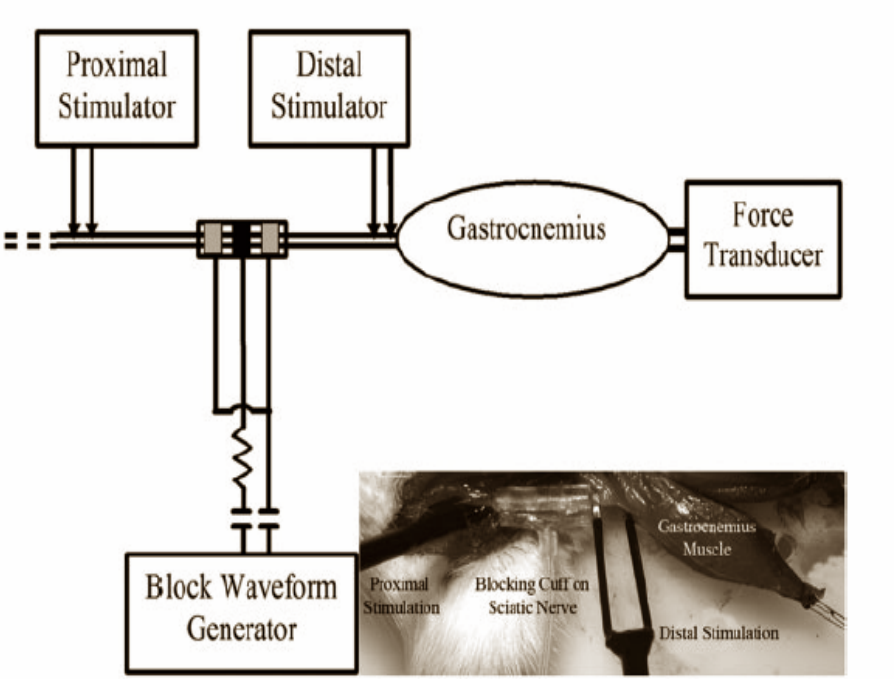

Figure 1.2: A typical experimental arrangement used to investigate the effect of HFAC waveforms in inducing conduction block. The proximal stimulator was used to activate the sciatic nerve and neural activity was monitored using force transducer measurements of the gastrocnemius muscle. Distal stimulating electrode was used in some experiments to verify continued function of the neuromuscular junction. (Adapted from (Bhadra & Kilgore, 2005)

Table 1.1: Summary of different animal studies demonstrating conduction block induced by HFAC waveforms.
*The bottom two rows list studies that were undertaken as part of this dissertation.

Author / Year	*Species*	*Waveform*	*Block frequency (kHz)*	*Proof of conduction block*
Tanner (1962)	Frog	Sine	20	Nerve recording
Woo and Campbell (1964)	Frog /Cat	Sine	20	Nerve recording
Bowman and McNeal (1986)	Cat	Square	4-10	Nerve recording
Kilgore and Bhadra (2004)	Frog	Sine	1-20	Distal stimulation
Tai et.al. (2004)	Cat	Sine/ Square	6-10	Sphincter pressure
Williamson and Andrews (2005)	Rat	Sine	10-20	Distal stimulation
Bhadra and Kilgore (2005)	Rat	Sine	10-30	Distal stimulation
Bhadra et.al. (2006)	Cat	Sine	1-30	Distal stimulation
Miles et.al. (2007)	Rat	Sine	10-30	Distal stimulation
Joseph and Butera (2007) & (2009)*	Sea-slug	Sine	5-50	Nerve recordings
Joseph and Butera (2010)*	Frog	Sine	5-50	Nerve recordings

In some cases, block could not be observed below 6 kHz (Tai *et al.*, 2004) while physical limitations of the equipment bounded the maximum frequency to 30 kHz (Bhadra & Kilgore, 2005; Bhadra *et al.*, 2006). Various experimental factors including the species and nerve studied, electrode characteristics, electrical parameters used and the outcome measures used to identify block could affect the mechanism and efficiency of conduction block.

Block threshold, defined as the minimum amplitude of the HFAC waveform below which complete block cannot be obtained, was found to increase linearly with an increase in the waveform frequency in the myelinated animal model systems considered (Kilgore & Bhadra, 2004; Bhadra & Kilgore, 2005; Tai *et al.*, 2005; Williamson & Andrews, 2005; Bhadra *et al.*, 2006). Block thresholds obtained at different frequencies in one such study is shown in Figure 1.3. Of the various waveforms studied, sinusoidal and rectangular biphasic waveforms have been found to be the most efficient and useful; however the linear block threshold trend exists regardless of the waveform type. One study (Williamson & Andrews, 2005) demonstrated that after block induction, a reduction in the amplitude of the HFAC waveform to a level that was initially insufficient to initiate block, could subsequently be used to sustain block. This hysteresis type effect could potentially be useful during clinical applications.

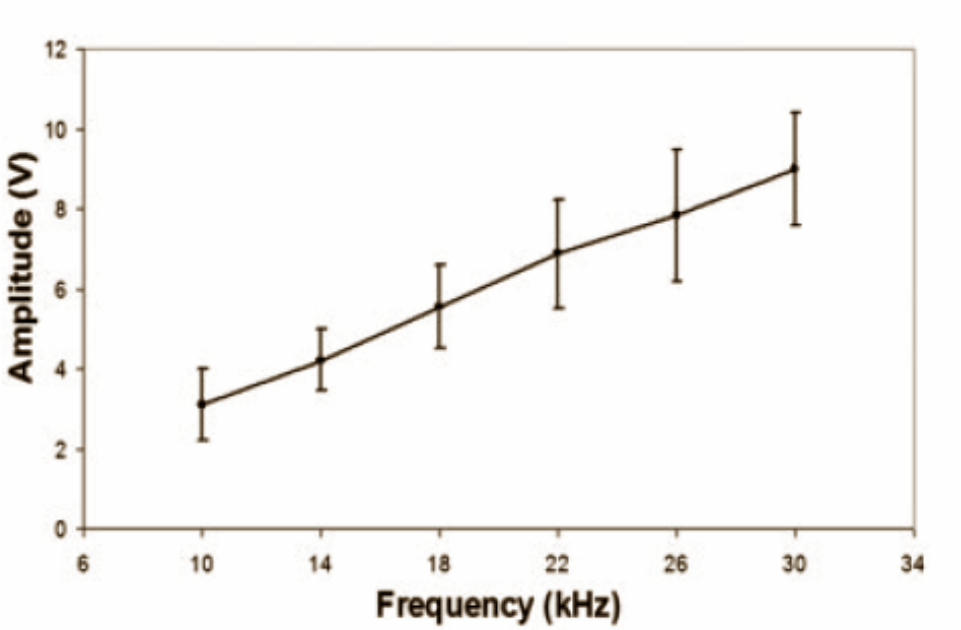

Figure 1.3: Relationship of block thresholds to frequency. Each dot is the average of 18 block threshold trials from 6 animals. (Adapted from (Bhadra & Kilgore, 2005).

1.2.3.2 Onset response

Prior studies have found that application of HFAC waveforms cause repetitive stimulation followed by a local block of the propagation of action potentials in single axon simulations (Tai *et al.*, 2005; Tai *et al.*, 2005; Williamson & Andrews, 2005; Zhang *et al.*, 2006; Zhang *et al.*, 2006; Bhadra *et al.*, 2007). The observed HFAC response had a variable period of repetitive firing, just prior to block induction, that increased initially and then decreased as the amplitude or frequency of the waveform increased (Rosenblueth & Reboul, 1939; Bhadra & Kilgore, 2005; Miles *et al.*, 2007). Application of the HFAC waveform resulted in an onset response consisting of several summed muscle twitches with a peak of 1-8 times the normal muscle twitch, a variable period of repetitive firing and a final steady state of complete or partial block (Bhadra & Kilgore, 2005). The first two phases had a characteristic relationship in the amplitude-frequency space where the repetitive firing was minimized at the highest frequencies and highest amplitudes. The magnitude of the onset response has been found to be dependent on the experimental variables or conditions including the amplitude and frequency of the HFAC waveform (Rosenblueth & Reboul, 1939; Bowman & McNeal, 1986; Bhadra & Kilgore, 2005; Bhadra *et al.*, 2006; Joseph & Butera, 2007; Joseph *et al.*, 2007; Miles *et al.*, 2007; Gaunt & Prochazka, 2009).

Elimination or reduction of the onset response and the transient repetitive firing behavior observed prior to block induction will be critical if clinical applications utilizing HFAC waveforms for conduction block are to be pursued. Various investigations are currently underway to develop methods to circumvent this response, either by coupling DC with AC waveforms for block induction or by changing the temperature of the nerve

(Ackermann *et al.*, 2009; Bhadra *et al.*, 2009; Foldes *et al.*, 2009; Kilgore *et al.*, 2009; Ackerman, 2010; Ackermann *et al.*, 2010). For the purpose of this dissertation work we will assume that eventually a clinically feasible solution, to reduce or eliminate the transient onset response during conduction block induced by HFAC waveforms, will be developed.

1.2.3.3 Computational studies

Computational models based on the Hodgkin-Huxley (HH) model or the McIntyre, Richardson and Grill model (MRG) model have been used to characterize the effect of HFAC waveforms on peripheral nerves and identify potential ionic mechanisms of conduction block induced by HFAC waveforms (Kilgore & Bhadra, 2004; Tai *et al.*, 2005; Tai *et al.*, 2005; Williamson & Andrews, 2005; Zhang *et al.*, 2006; Zhang *et al.*, 2006; Bhadra *et al.*, 2007; Haeffele & Butera, 2007; Miles *et al.*, 2007; Wang *et al.*, 2008) . The frequency and amplitude of the waveform, axon diameter, electrode-to axon distance, polarity of stimulation and the position of the block electrode longitudinally over the axon were individually modulated in simulations to understand the various factors affecting conduction block induced by HFAC waveforms. Simulation results from these studies show that the block threshold is inversely proportional to axon diameter similar to the reverse recruitment order observed with extracellular stimulation. Block threshold was also found to be linearly increase with the frequency of the HFAC waveform and was found to be directly proportional to the distance of the electrode from the axon. These results are depicted in Figure 1.4.

Computer simulations of nerve membrane models, coupled with *in vivo* experiments have failed to identify the mechanism and principle of nerve conduction block. (Kilgore & Bhadra, 2004; Tai *et al.*, 2005; Tai *et al.*, 2005; Williamson & Andrews, 2005; Zhang *et al.*, 2006; Zhang *et al.*, 2006; Bhadra *et al.*, 2007). The membrane voltage, ionic currents and gating potentials near the high frequency current source were examined in the various simulation studies, to understand how the high frequency current could produce either rapid excitation of the axon or localized block but no conclusive mechanism was found. Inconsistencies appear in literature regarding whether the block is produced by net membrane hyperpolarization, depolarization caused by the activation of potassium channels (Tai *et al.*, 2005; Tai *et al.*, 2005; Zhang *et al.*, 2006; Zhang *et al.*, 2006), the deactivation of sodium channels (Kilgore & Bhadra, 2004; Williamson & Andrews, 2005; Bhadra *et al.*, 2007) or through some other mechanism.

1.2.4 Limitations of published work

Computational studies investigating HFAC induced block have been based on models that are perhaps not valid for the frequencies studied and hence cannot be used to reliably predict the physiological mechanisms of block induction. Some studies (Bhadra & Kilgore, 2005) have used the MRG (McIntyre *et al.*, 2002) mammalian axon model to simulate the response of nerves to HFAC conduction block.

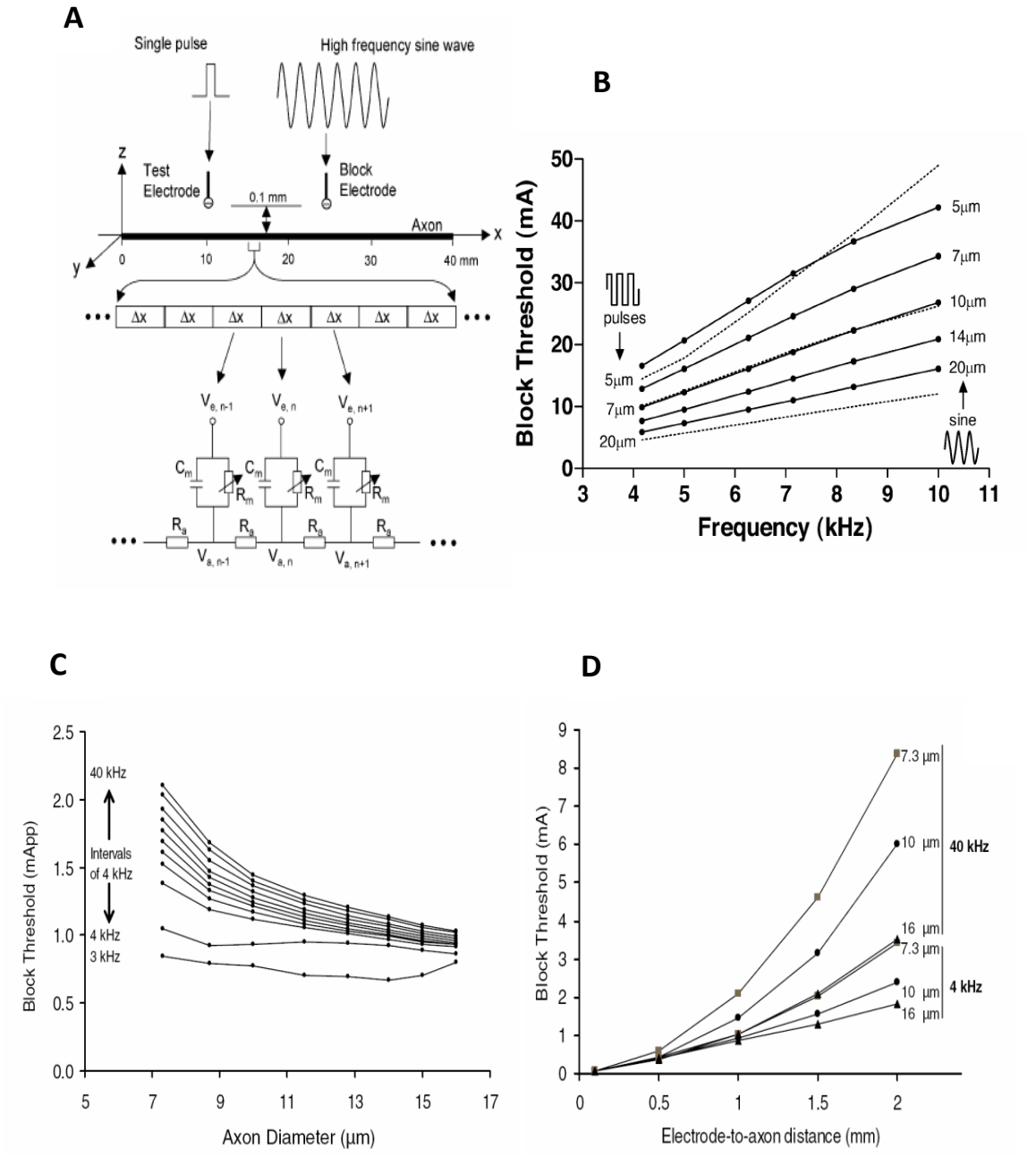

Figure 1.4: A: A simple HH cable model commonly used to investigate the mechanism of HFAC block. (B-D) The relationship between block threshold and frequency, axon diameter and electrode-to axon distance was studied in various computational studies. B: Block threshold was found to linearly increase with frequency. C: Block threshold was inversely proportional to axon diameter. D: Block threshold was proportional to the electrode-to-axon distance. Adapted from (Tai *et al.*, 2005; Bhadra *et al.*, 2007)

The model was able to demonstrate similar behavior as seen in motor fibers during application of the HFAC waveforms. Although the MRG model is a topologically detailed mammalian model based on human, cat and rat data, it was found to give reliable responses for frequencies in the 100 Hz range (Richardson *et al.*, 2000; Bhadra *et al.*, 2007). Studies based on the HH model are also not valid for determining the physiological mechanism of block induction using HFAC waveforms. The HH model assumes that capacitance is constant even at higher frequencies, when actually experimental data from the giant squid axon shows that capacitance decreases as frequencies increase (Haydon & Urban, 1985). No model used for investigating HFAC induced conduction block has been validated for frequencies in the kHz range. In addition, since the HH model was developed for large axons (500-1000 μm in diameter), it ignores ionic fluxes across the membrane and ionic pumps that are essential for maintaining the differential concentration across the membrane in small unmyelinated fibers (<100μm in diameter) (Scriven, 1981). Furthermore, causality of the proposed block induction mechanisms using HFAC waveforms was never shown in any of the models used to simulate nerve behavior during application of HFAC waveforms.

Animal experiments investigating HFAC induced block have been conducted on mixed nerves that contain different types of fiber populations including myelinated and unmyelinated nerves but only the motor nerve properties have been monitored in these studies. The isolated response of a particular fiber type has not been experimentally investigated even though the simulation studies have been based on nerve models of either only myelinated or unmyelinated nerves. Significant differences exist between the excitation properties and ion channel distribution of myelinated and unmyelinated nerve

fibers. The active membrane properties as well as the effects of surrounding extracellular environment may also account for the disparity in the ideal frequency range suggested and the hypothesized mechanisms of block induction in the different experimental and computational studies (Rosenblueth & Reboul, 1939; Tanner, 1962; Woo & Campbell, 1964; Bowman & McNeal, 1986; Kilgore & Bhadra, 2004; Bhadra & Kilgore, 2005; Tai *et al.*, 2005; Tai *et al.*, 2005; Williamson & Andrews, 2005; Zhang *et al.*, 2006; Zhang *et al.*, 2006; Bhadra *et al.*, 2007) .

Failure of action potential propagation during repetitive stimulation with frequencies less than 1000 Hz, has been reported in central and peripheral axons of both vertebrates and invertebrates (Grossman *et al.*, 1979; Smith, 1983; Gu, 1991; Jensen & Durand, 2007). In the crayfish, differential conduction block was observed in the branches of axons, where propagation of action potentials was seen in one branch of the axon and not in the other (Grossman *et al.*, 1979). Conduction block in these studies was found to be caused by the accumulation of K^+ in the extracellular space, while the differential nature of action potential conduction was attributed to the early activation of the Na^+-K^+ electrogenic pump and increased an intracellular Ca^{2+} concentration in the thinner branch of the axon. In the small sensory fibers of the leech, the large increase in internal sodium concentration $[Na^+]_I$, strongly activated the Na^+-K^+ electrogenic pump and prevented axonal firing (Grossman & Kendig, 1987). The above studies indicate that during extracellular stimulation, a variety of physiological mechanisms can alter the membrane voltage and gating variables, to prevent action potential propagation along the nerve.

Block induction using HFAC waveforms in peripheral nerves could possibly be attributed to any of above mechanisms. In addition, it is possible that conduction block using HFAC stimulation in mixed nerves of varying diameter is produced by a combination of different mechanisms that are indirectly influenced by the nerve studied, the electrode type, the size and shape of the electrode and the amount of chloride on the silver wires. Published studies in literature have failed to quantify these extraneous factors that could potentially affect the block thresholds and the ionic mechanisms of block induction. Obtaining a better understanding of the mechanisms underlying HFAC block induction would enable the design and development of a clinically feasible technique for effectively managing or eliminating various nervous disorders.

1.3 Summary

Disparate results in published literature make it difficult to determine the physiological mechanism of HFAC induced block or its potential for clinical applications. Differences between the axon diameters, myelination properties and the surrounding extracellular environment affect the conduction and blocking mechanisms in nerves. Experimentally testing only the motor nerve response indirectly through a force transducer hides the effect on the different fiber type populations in peripheral nerves. Characterizing the behavior of each fiber type population under HFAC stimulation, and specifically of the smaller-diameter pain conducting unmyelinated nerve fibers, is critical if clinical applications are to be pursued.

This dissertation work investigates the fundamental characteristics of different nerve population types during application of HFAC waveforms. Extracellular

electrophysiological techniques will be used to examine some of the assumptions and predictions from computational modeling of conduction block induced by HFAC waveforms. These studies will improve our understanding of using HFAC waveforms as a technique for selective stimulation or selective blocking. Arresting the propagation of superfluous signals through specific nerve fibers, using HFAC waveforms, will be useful for various neuroprosthetic and neurophysiological studies, and will be significant in alleviating disease symptoms such as blocking chronic peripheral pain and stopping pathological hyperactivity of neuronal signals.

CHAPTER 2

HFAC INDUCED BLOCK IN UNMYELINATED NERVES [1]

Fundamental mechanisms of nerve conduction are known to be highly conserved across different species (Kandel *et al.*, 2000). However, the properties of electrically excitable membranes depend on the properties of the ion channels present in the membrane. High Frequency Alternating Current (HFAC) waveforms have been shown to reversibly block the conduction of action potentials through amphibian and mammalian myelinated nerve fibers (Tanner, 1962; Woo & Campbell, 1964; Ishigooka *et al.*, 1994; Kilgore & Bhadra, 2004; Bhadra & Kilgore, 2005; Tai *et al.*, 2005; Williamson & Andrews, 2005; Bhadra *et al.*, 2006; Tai *et al.*, 2006). Most experiments demonstrating HFAC induced conduction block have been conducted on mixed nerves that contain both myelinated and unmyelinated nerve fibers, but only the motor nerve response has been reported. Experimentally testing only the motor nerve response hides the effect on the unmyelinated nerves, which is critical if clinical applications are to be pursued.

We know that significant differences exist between the excitation properties of myelinated and unmyelinated nerve fibers and these differences along with the surrounding extracellular environment could affect the nerve activity around the HFAC stimulus regimes. Experimental data observing the motor response from mixed nerves

---

[1] Most of the work described in this chapter has been published in **Joseph L and Butera R J. 2009.** Unmyelinated Aplysia nerves exhibit a nonmonotonic blocking response to high-frequency stimulation. *IEEE Transactions on Neural Systems and Rehabilitation Engineering*, **17**:537-544.

have previously been used to validate computational models based on unmyelinated nerve models (even when they consider ion channels found in myelinated nerves) with limited success. The active membrane properties as well as the effects of myelination may account for the disparity in the ideal frequency range suggested and the hypothesized mechanism of block induction in the different experimental and computational studies (Rosenblueth & Reboul, 1939; Tanner, 1962; Bowman & McNeal, 1986; Kilgore & Bhadra, 2004; Bhadra & Kilgore, 2005; Tai *et al.*, 2005; Tai *et al.*, 2005; Williamson & Andrews, 2005; Zhang *et al.*, 2006; Zhang *et al.*, 2006; Bhadra *et al.*, 2007). To complete our understanding of the phenomena of conduction block using HFAC waveforms, we must be able to understand the effect of high frequency waveforms on isolated fiber types and especially on the smaller diameter, unmyelinated nerve fibers.

The goal of this study was to determine whether complete nerve conduction block could be consistently and repeatedly obtained in purely unmyelinated nerves using HFAC stimulation and to characterize the effect of HFAC waveforms on the homogenous unmyelinated nerves by varying the amplitude and frequency of the blocking waveform and monitoring the neural activity. Some molluscan species have individually identifiable cells and easily identifiable axons that make them amenable for direct electrophysiological analysis at a resolution unapproachable in other species (Kandel, 1979; Meems, 2005). The sea-slug *Aplysia californica* has been widely used to understand the various functions and mechanisms involved in the nervous system (Kandel, 1979; Kandel *et al.*, 2000). It has large identified neurons and long easily accessible nerve connectives from the pleural-pedal ganglia to the abdominal ganglion

that allow for the monitoring of neural activity at various points along the nerve and served as an ideal preparation for our experiments. We acknowledge that though these experiments were not conducted on mammalian unmyelinated fibers, the results will provide insight into the effect of high frequency stimulation on small diameter axons.

2.1 Material and Methods

2.1.1 Animal preparation

In vitro experiments were performed on the unmyelinated nerves of *Aplysia.* The propagation of impulses along the nerve was used as an output measure to monitor block status. The animals were dissected according to standard protocol where the animals are anesthetized with isotonic $MgCl_2$ (30% of body weight). The body cavity was incised to expose the nerve connectives leading from the abdominal ganglion. The nervous system, including the circumesophageal ring or head ganglia and the abdominal ganglion, was isolated and pinned to a petri dish with a Sylgard base (Dow Corning). Acute experiments were performed on the left or right pleuroabdominal connectives, which are usually about 4-6 cm in length and provide ample distance for the placement of four suction electrodes. Care was taken to ensure that the nerves of interest were not stretched or damaged during dissection. Spontaneous bidirectional neural activity was present between the ganglia. A high-magnesium, low-calcium saline solution was used in the bath to synaptically isolate the neurons in the ganglia (Nowotny *et al.*, 2003) and suppress the spontaneous activity. The preparation typically allowed for 3-4 hours of experimentation time. Experiments were also conducted on the isolated nerve preparation (excluding the ganglia to prevent neuronal effects) with normal ASW (artificial sea

water) in the bath, but this preparation was typically viable for only about an hour or less. All experiments were conducted at room temperature.

2.1.2 Electrophysiological setup

Suction electrodes, commonly used for extracellular recording and stimulation, were used in our experiments. Glass electrodes with tip diameters about the same as that of the nerve fiber (200-500 μm) were pulled and attached to an electrode holder. Typical electrode impedances for suction electrodes are in the kOhms range. A 400μm tip electrode was found to have an impedance of 30 kOhm. The suction electrodes were positioned along the nerve by micromanipulators (SD Instruments, Narishige). Negative pressure was applied via a syringe mechanism to draw the nerve into the electrode for *en passant* recording and stimulation. Bath solution drawn into the electrode maintained electrical contact and minimized noise in the recordings. Suction electrodes allow for the continuous immersion of the nerve in the saline solution, thus preventing the nerve from drying out. These electrodes also allow localized stimulation and a higher signal to noise ratio for recording. A total of four electrodes were used in our experiments. Two suction electrodes were used for the continuous monitoring of the propagation of action potentials (APs) along the nerve. One suction electrode, placed between the recording electrode and the head ganglia, was used to trigger an action potential in the nerve. Another electrode positioned between the two recording electrodes, was used to provide the block-inducing HFAC stimulus. The distance between each of the suction electrodes was 5-10 mm. A schematic of the experimental setup is shown in Figure 2.1.

A healthy and viable preparation was identified as one in which the activity observed in one electrode was reflected in the other with a delay proportional to the conduction velocity. We used a 10k gain on the amplifier and the bandwidth was limited from 100Hz-1 kHz to filter out the noise that would arise from the high frequency stimulation without affecting the unmyelinated nerve signal. This range of band pass filtering also allowed for recording of traces that did not require any averaging or post-data digital filtering. Our experimental set up had the advantage of providing direct access to monitor the neural activity along the nerve, unlike other studies where the activity of the innervated muscle was used as an indicator of nerve block (Kilgore & Bhadra, 2004; Bhadra & Kilgore, 2005; Williamson & Andrews, 2005).

The input stimuli were transmitted through battery-powered stimulation isolation units (AM Systems-Analog Stimulus Isolator, Model 2200, Carlsborg, WA) that provided voltage controlled current waveforms. We verified the apparatus response and found that it matches with the advertised specifications, including at frequencies up to 50 kHz (above the specs of 40 kHz).1-3 dB attenuation was found at frequencies above 30 kHz. For the range of parameters in our experiments, the output was not limited by the slew rate. A suprathreshold stimulus pulse of 2V for 0.4ms, converted to current stimulation through the stimulus isolation unit (0.1mA/V), was used to trigger an action potential.

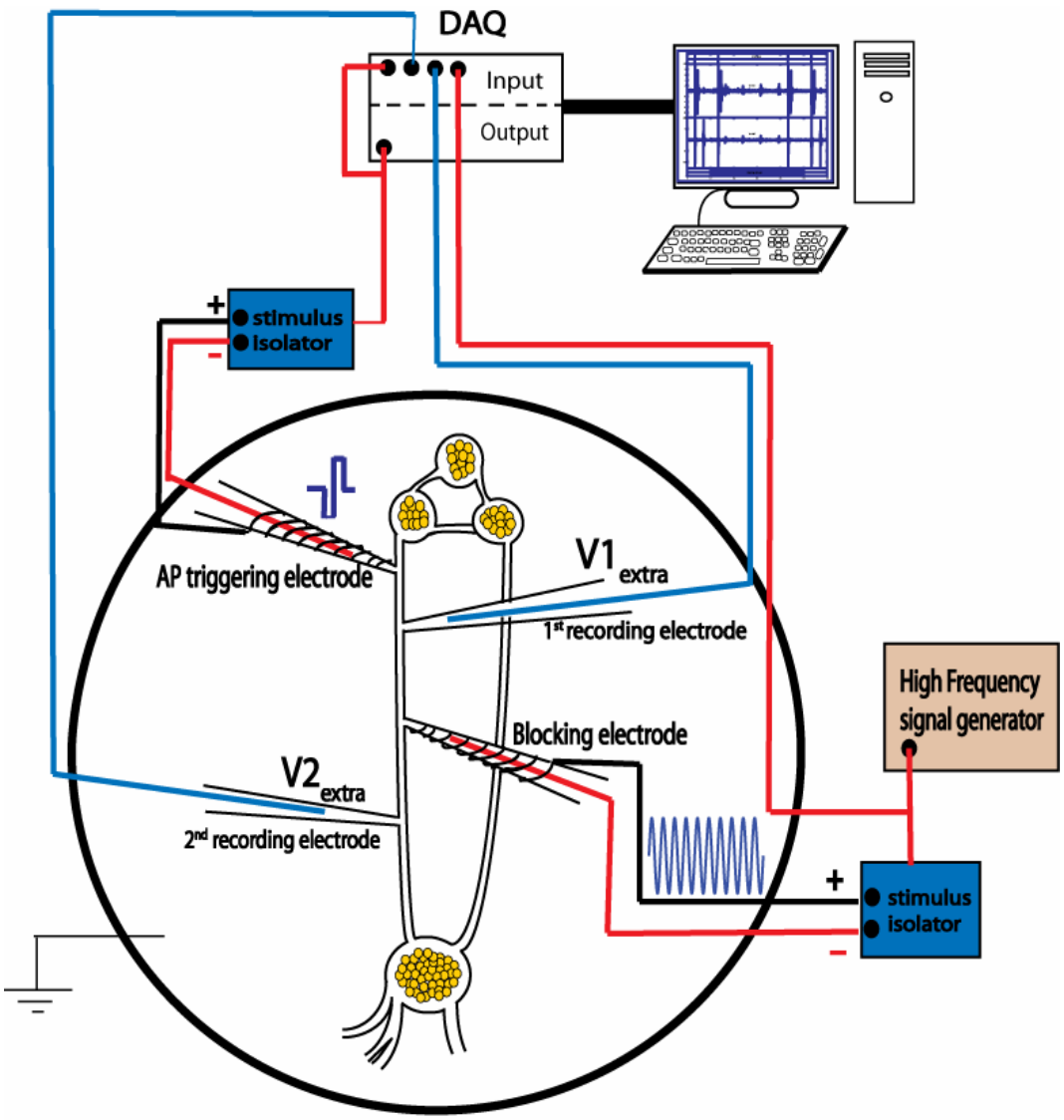

Figure 2.1: Schematic of the experimental setup used for studying HFAC induced conduction block in the unmyelinated nerves of *Aplysia*. The pleura-abdominal nerves along with the attached ganglia were transferred to a saline filled petri-dish. Four suction electrodes were placed along the triggered neural activity was monitored using the depicted apparatus.

Based on previously published work, current-controlled, sinusoidal or biphasic rectangular waveforms in the frequency range of 3 kHz-20 kHz were hypothesized and found to produce the most effective block (Kilgore & Bhadra, 2004). Higher frequencies had not been previously tested due to physical limitations of the instrument. In our study, sinusoidal waveforms in the frequency range of 5-50 kHz, generated by a function generator (Stanford Research Systems, Model DS345) were used to induce block. These waveforms were sent to a similar stimulus isolation unit (1mA/V) to produce current waveforms which were found to be more effective in inducing block than voltage waveforms. This experimental set up (Figure 2.1) was used to investigate the effect of HFAC waveforms in the unmyelinated pleuro-abdominal nerves of *Aplysia*.

2.1.3 Block Threshold

For each frequency, the amplitude of the waveform was varied until the propagation of action potentials could not be observed. A range of amplitudes was tested to identify the threshold at which block was observed, beginning at lower amplitudes and incrementing the amplitude in discrete steps of 0.1-0.5mA. Our method differs from other studies where the amplitude of the HFAC waveform was initially at its maximum value and was then linearly decreased until action potentials appeared in the fiber (Kilgore & Bhadra, 2004; Bhadra *et al.*, 2006). We chose this approach to avoid potential unknown remnant effects of stimulating the nerve at higher amplitudes of current or voltage.

In our experiments, after the HFAC stimulus was applied on the nerve, a test pulse was injected at the proximal end near the head ganglia to trigger an action potential in the nerve. If the amplitude of the HFAC waveform was at or above the threshold for

inducing conduction block, the action potentials were arrested at the site of injection of the blocking stimulus. The minimum amplitude of the HFAC waveform at which an action potential was not observed in the distal recording electrode, though observed in the proximal recording electrode, was identified as the threshold for inducing block and termed as the 'block threshold'. By monitoring the arrival of action potentials at the distal end, axonal conduction block was detected and the minimum threshold for blocking propagation was determined for a particular frequency. This procedure of identifying block threshold was repeated for different frequencies. The order of frequency tested was randomized to avoid any cumulative effects of fatigue or time. The nerve was allowed to rest for at least a minute between individual trials.

The response of the nerve before, during and after high-frequency block was recorded in individual trials. Based on the neural activity when the high frequency waveform was applied, the nerve response was further classified as 'No change', 'Repetitive firing', 'Partial Block' and 'Block'. 'Repetitive firing' was identified as the amplitudes below the block threshold where the nerve spontaneously and repetitively fired. 'Partial block' was identified as the amplitudes below the block threshold where part of the compound action potential appeared to be blocked or distorted. Multiple trials, for each randomly chosen frequency, were performed on every nerve to evaluate the repeatability and reversibility of applying the HFAC stimulus. These multiple trials enabled the complete characterization of the response of the nerve to different HFAC waveforms.

2.2 Results

2.2.1 Verification of normal conduction properties

All experimental preparations were initially tested for normal conduction properties to determine if action potentials could be repetitively triggered and transmitted along the axon. The nerve preparations in which either an action potential could not be triggered successively or in which the triggered action potential could not be observed in both the recording electrodes, were terminated and the preparation discarded. The triggered action potential appeared in the recording electrodes with a small latency between them, due to the propagation delay. As shown in Figure 2.2, the stimulus artifact also appeared in the recording traces but was usually well separated from the action potentials due to the slow conduction velocity in unmyelinated nerves.

The distance between the two recording electrodes was noted for determining the conduction velocity. The conduction velocity in the *Aplysia* nerves was in the range of 0.4-1m/s, typical of most unmyelinated nerves (Kandel *et al.*, 2000). The conductive properties of the preparation were also constantly tested during the experiment in the absence of the HFAC stimulus to determine whether the preparation was healthy and viable. The nerve was tested prior to each application of the HFAC stimulus and block was determined by comparing with the recording taken prior to switching on the HFAC stimulus. If a dramatic change in the AP amplitude or shape was observed or if the AP could not be observed in both the recording electrodes or if recovery of the AP did not occur to its pre-block amplitude and shape, the experiment was terminated and the last dataset deleted.

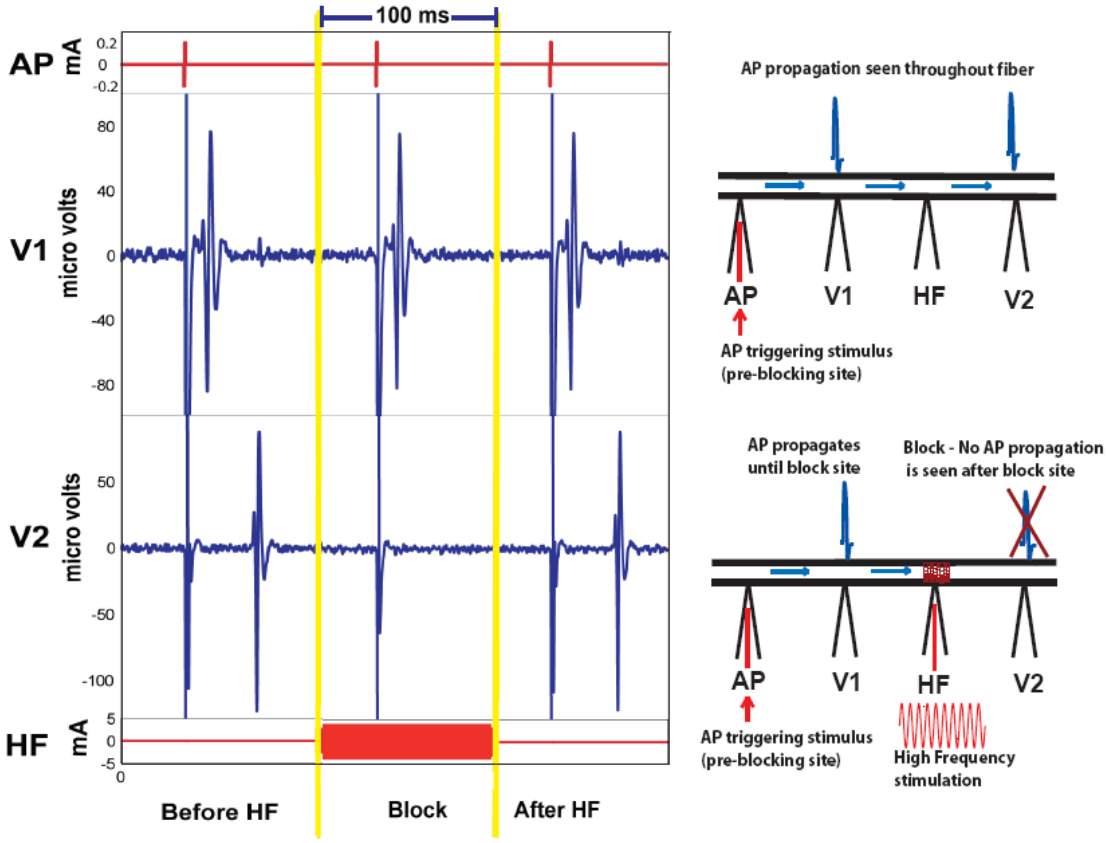

Figure 2.2: The left panel indicates an example of a trial where propagation can be seen before and after application of the high frequency stimulation. When the high frequency waveform is applied above a certain threshold, conduction is blocked as evidenced by the absence of the action potential in the second recording electrode. The right panel shows a schematic of the experiment with and without application of the high frequency stimulus.

2.2.2 Complete reversible block

Axonal conduction block induced by high frequency stimulation was demonstrated in nerves from 20 animals. In 14 animals, the threshold for inducing block was identified for at least 6 different frequencies ranging from 5-50 kHz. The other animals produced data for only 2 or 3 different frequencies, after which the recording in one electrode stopped echoing the recording in the other electrode even in the absence of the high frequency stimulus. Data from all 20 animals were pooled for analysis of block threshold. Complete and reversible block was achieved in all the 20 animals tested and for all the frequencies in the range of 5-50 kHz. In the absence of the high frequency AC current and for stimulus intensities below the block threshold, normal conduction of the action potential i.e. propagation of the action potential from the electrode proximal to the head ganglia (1^{st} recording electrode) to the distal recording electrode (2^{nd} recording electrode) closer to the abdominal ganglion was observed. Action potentials were intermittently triggered and axonal propagation along the nerve was monitored to identify whether conduction was blocked or not as the amplitude of the HFAC waveform was varied.

For current intensities at and above the identified blocking thresholds, the action potential appeared only in the proximal recording electrode and not in the distal recording electrode as seen in Figure 2.2. This was indicative of local conduction block. Only the stimulus artifact could be observed in the trace obtained from the distal electrode for amplitudes greater than the blocking threshold. A trial showing complete block when the high frequency stimulation is applied while normal conduction can be observed before and after application of the high frequency waveform is displayed in Figure 2.2. The

current for inducing complete block across all frequencies was in the range of 1-6 mA peak. Action potential conduction returned within 5 s of switching off the high frequency current and was instantaneous in some cases. Lower frequencies had greater delays in the reversibility of nerve conduction after the HFAC stimulation was stopped.

2.2.3 Block onset and repetitive firing

The initiation of the HFAC stimulus usually triggered multiple transient bidirectional action potentials in the nerve fiber that propagated away from the site of the HFAC stimulating electrode. Figure 2.3 shows that as the amplitude of the high frequency waveform was increased, spontaneously generated action potentials with varying firing frequencies are observed just before the onset of conduction block. The range of the amplitude of the HFAC waveform for generating spontaneous action potential firing was found to vary inversely with frequency as shown in Figure 2.5. Higher frequencies had a smaller range below the block threshold, where spontaneous firing of action potentials was observed compared to lower frequencies.

2.2.4 Partial block

In some cases a decrease in the amplitude or a notable change in the shape of the compound action potential was observed, suggesting conduction block of some of the axons in the nerve fiber. This was noted as partial block of the nerve fiber. The partial block response and the spontaneous firing of nerve activity occurred at amplitudes of the high frequency waveform that were immediately below the threshold for inducing block as can be seen in Figure 2.4.

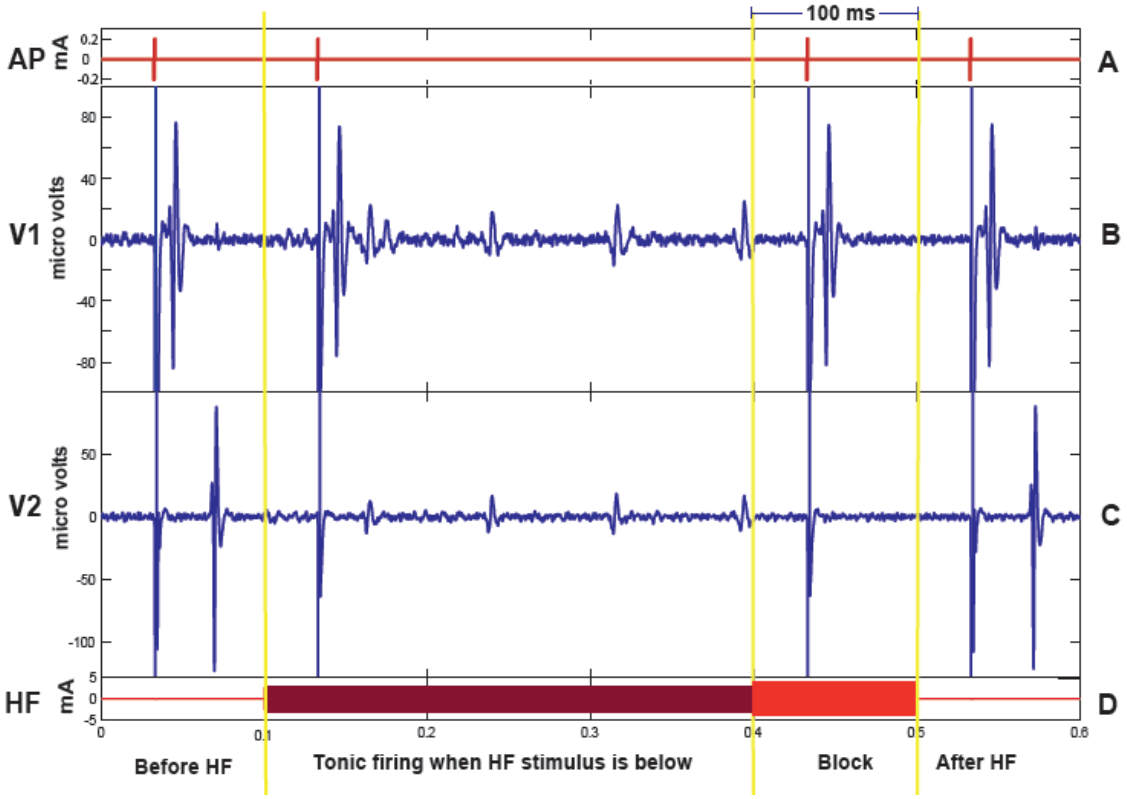

Figure 2.3: Response of an unmyelinated nerve recorded for 600ms before, during and after the application of the sinusoidal HFAC waveform. **A**. Spikes indicate the time instant when the stimulus to trigger an action potential in the nerve was given and appear as stimulus artifacts in other panels. **B.** Extracellular voltage recordings of the electrode proximal to the head ganglia. **C.** Extracellular voltage recordings of the distal electrode. **D.** Amplitude of the sinusoidal HFAC stimulation. The dark brown region of the HFAC waveforms, indicate amplitudes below block threshold where tonic firing was observed. The red region of indicates amplitudes of the HFAC waveforms where complete block of the triggered action potential was observed.

The nerve fiber was said to be totally blocked when the triggered compound action potential and the spontaneously generated spikes completely disappeared in the second recording electrode. In most cases, partial block occurred simultaneously as the spontaneous tonic firing in the nerve. When the HFAC amplitude of the waveform was about 0.5-0.9 times the block threshold, the nerve exhibited spontaneous firing and the triggered action potential appeared to be partially blocked, evident by the absence of the large amplitude peak in the compound action potential. The neural activity of the nerve changed depending on the amplitude and frequency of the HFAC waveform.

2.2.5 Block thresholds

The minimum thresholds for inducing block using HFAC sinusoidal waveforms were obtained for frequencies in the range of 5-50 kHz and amplitudes varying from 1-6 mA. Unlike previous results utilizing mixed nerves of amphibians (Kilgore & Bhadra, 2004) and mammals (Bhadra & Kilgore, 2005; Williamson & Andrews, 2005), the minimum amplitude of the high frequency waveform required to block axonal conduction in unmyelinated nerves did not linearly increase with an increase in frequency as depicted in Figure 2.6. The current intensity required to block conduction through these unmyelinated nerves increased until about 12 kHz and then decreased until 50 kHz, which was the maximum frequency tested. These frequencies were tested in a random order, indicating that this non-monotonic frequency-amplitude relationship is not a time-dependent phenomenon.

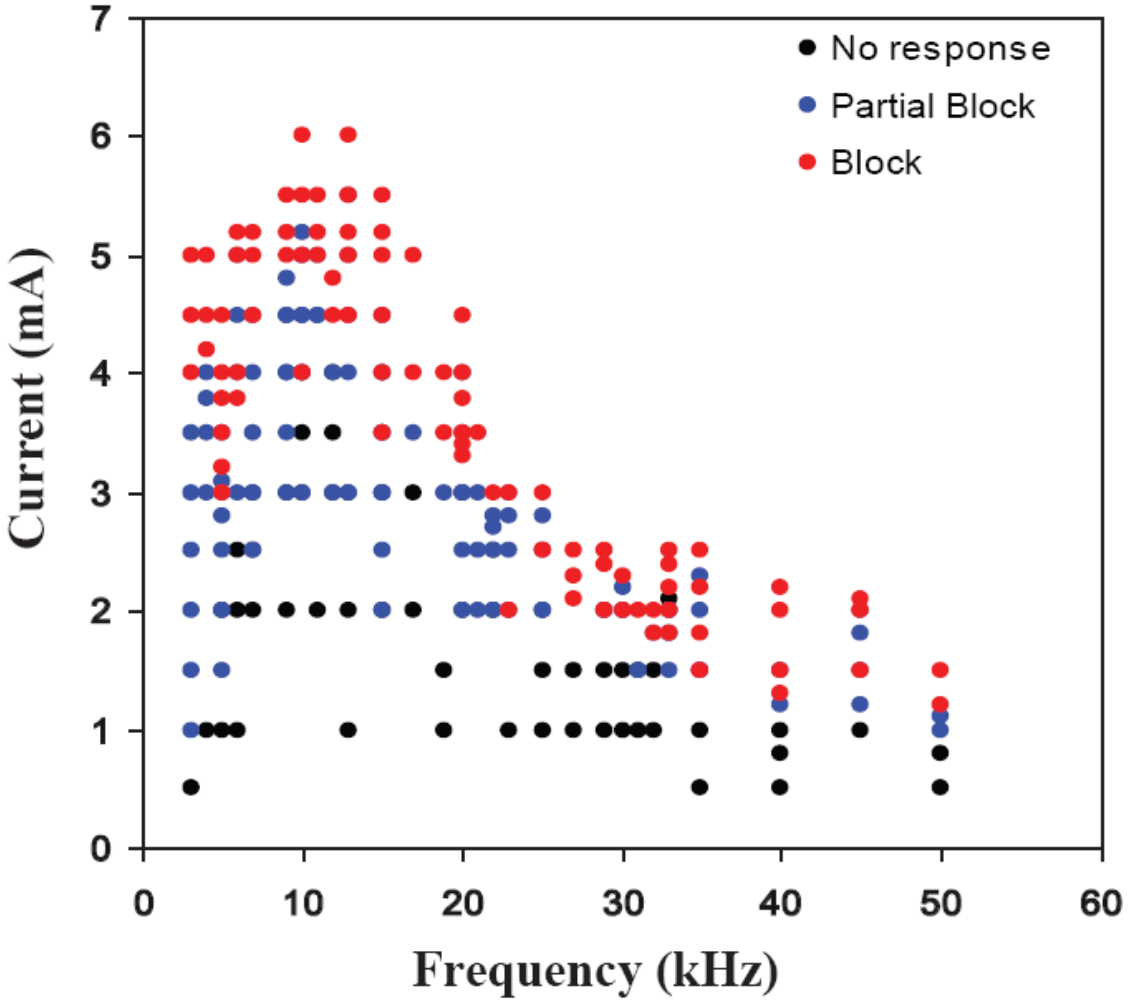

Figure 2.4: The response of the nerve to application of high frequency waveforms as the amplitude of the waveform is changed. Pooled data obtained from all experiments is shown. The black dots indicate no change to the shape or amplitude of the CAP compared to that prior to application of the HFAC waveform. The blue dots indicate when repetitive firing and partial block were seen. The red dots indicate when conduction was blocked and the CAP did not appear in the second recording electrode, though it was present in the first recording electrode. Repetitive firing and partial block always occurred at amplitudes below block threshold.

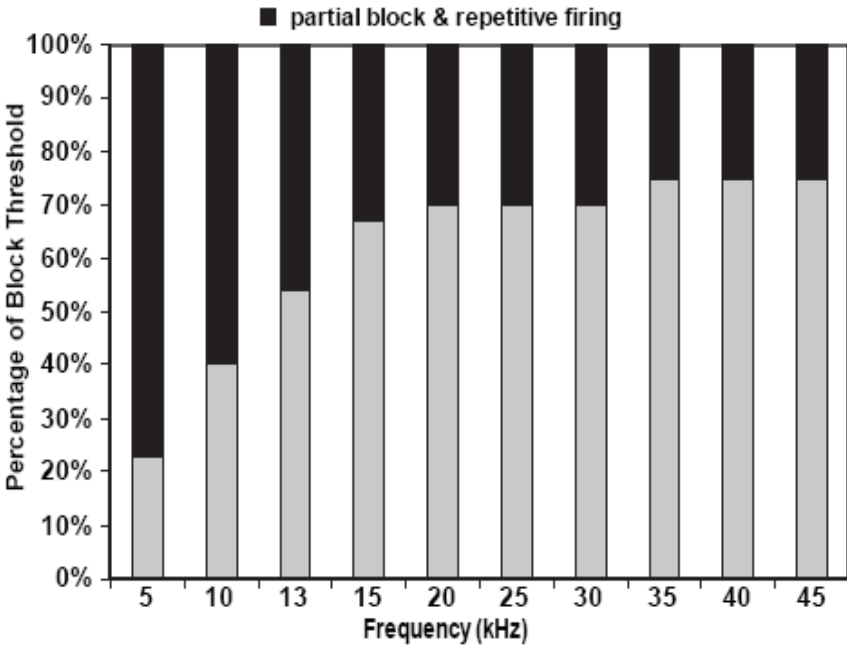

Figure 2.5: Range of partial block as a percentage of the block threshold for different frequencies. As frequency increased the range of amplitudes for observing repetitive firing and partial block decreased.

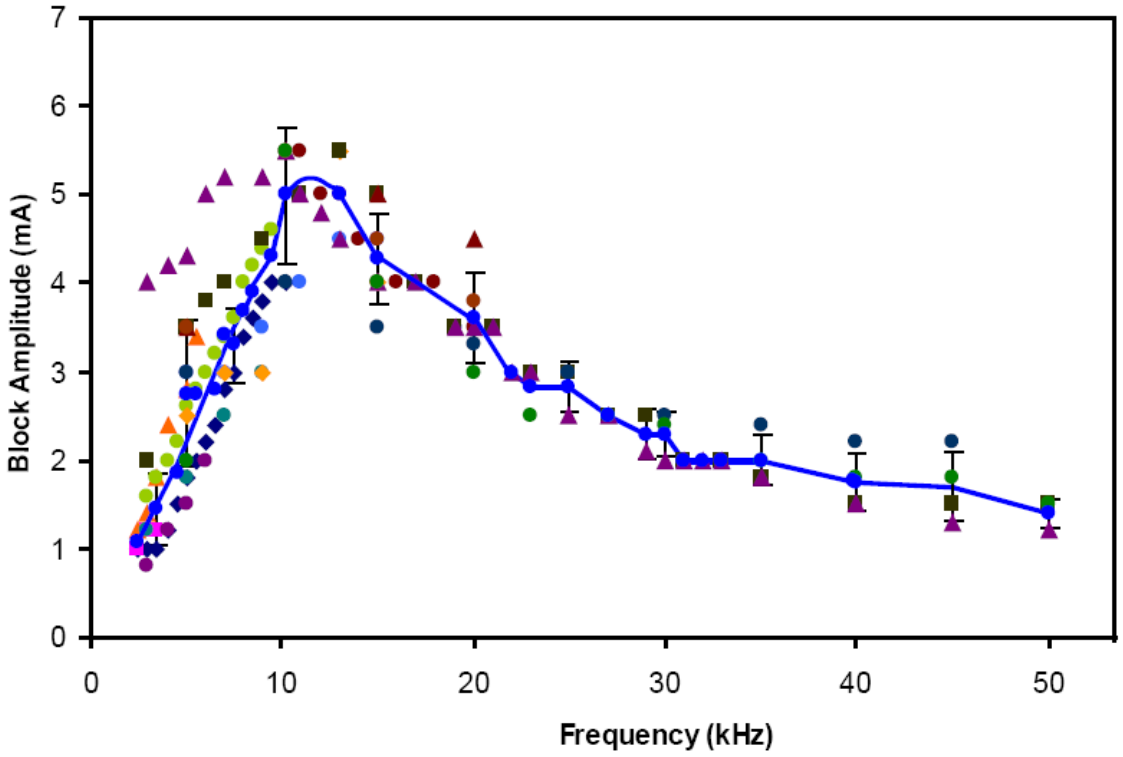

Figure 2.6: Block thresholds in *Aplysia* nerves. Each point indicates the blocking threshold for a particular frequency obtained from the unmyelinated nerves of *Aplysia*. Different symbols and colors indicate data from different animals. The blue solid trace indicates the average extrapolated block threshold at each frequency. The error bars indicate the standard deviation of the block thresholds at a particular frequency.

2.3 Discussion

The phenomenon of conduction block induced by high frequency waveforms has been shown in several preparations of mixed nerves. However it has not been studied by direct measurements of neural activity on homogeneous nerves for a wide frequency range. In the present study, purely unmyelinated nerves of *Aplysia* were used to investigate the changes in the excitability of the nerve during high frequency activation. This study has shown that 5-50 kHz HFAC waveforms can reversibly block the conduction of action potentials in unmyelinated nerves. Although it has been previously demonstrated that the mechanism of HFAC conduction block is not due to a distal effect at a neuromuscular junction or muscle, such as neurotransmitter depletion or muscle fatigue but is due to a local neural block at the site of stimulation (Kilgore & Bhadra, 2004) , our experiments provide conclusive evidence of the same since we use an isolated nerve preparation with no muscle attached.

Conduction block was obtained for all frequencies tested between 5 and 50 kHz at stimulation strengths varying from 1-6 mA peak. The block induction was reversible and repeatable at all the frequencies tested. No other study has tested for frequencies above 30 kHz. Our experiments reveal that in *Aplysia* fibers, for frequencies above 12 kHz, the minimum HFAC amplitude for block decreases as frequency increases which differs from the frequency-amplitude relationship seen in other modeling and experimental studies (Kilgore & Bhadra, 2004; Bhadra & Kilgore, 2005; Tai *et al.*, 2005; Tai *et al.*, 2005; Zhang *et al.*, 2006; Bhadra *et al.*, 2007). The non-monotonic relationship was found in all the animals tested where the entire frequency range was randomly spanned.

This non-monotonic relationship is possibly a unique property of these unmyelinated nerves that has not been formerly observed.

All other features of HFAC induced block, like the onset response and repetitive firing observed just prior to the conduction block, were consistent with published literature even though we used suction electrodes unlike other studies on HFAC block. Most invertebrate neurophysiologists use suction electrodes since they provide highly localized stimulation along with providing a high signal to noise ratio. Also, high resolution recordings of the neural activity can be obtained with them. Since the preparation is always immersed in saline solution, suction electrodes maintain the viability of the preparation for longer durations by preventing the nerves from drying out. They also enable good tubular contact which is essential for achieving neural block.

HFAC block was almost always preceded by a period of asynchronous tonic firing of the nerve which appeared at intensities that were just below the block thresholds. The duration of asynchronous firing varied inversely with frequency. Higher frequencies (>35 kHz) had minimal asynchronous firing and appeared to have the quickest onset of block. Lower frequencies had greater delays in reversibility of nerve conduction after the HFAC stimulation was stopped. For current intensities at and above the blocking thresholds, the action potential appeared only in the proximal recording electrode and not in the distal recording electrode as depicted in Figure 2.3, which was indicative of block.

The onset activity produced when the HFAC waveform is initiated can be a significant disadvantage for clinical applications. Miles et. al. (Miles *et al.*, 2007), looked into the effect of using ramped waveforms to suppress the transient onset response when the HFAC waveform is turned on and found that the transient onset response was not

eliminated with slowly ramping HFAC waveforms. Unlike the long periods of transient activity observed with ramped waveforms (Miles *et al.*, 2007), we found that when the HFAC amplitude was stepped from an amplitude of zero to an amplitude above the block threshold, on average, only about 1-3 spikes occurred within the first 30ms of switching on the HFAC waveform. Hence, clinical applications using HFAC waveforms to block conduction would warrant the use of a step waveform to an amplitude above the block threshold for that frequency. Based on our experimental results, frequencies above 30 kHz might be ideal for clinical applications since they have lower thresholds for block induction and have a smaller range for the steady-state repetitive firing activity. We cannot state with certainty whether our results are unique to the *Aplysia* preparation or to unmyelinated nerves in general, however, we also note that this is the first experimental study of this phenomena using purely unmyelinated nerves.

Modeling studies, to date, have been based on single fiber type axon models, where the models have not been extensively tested with high frequency signals. It is unknown how well these existing axon models correlate to the physical axon behavior at these higher frequencies that are above the normal electrophysiological range. This could also explain the disparity in results of published studies about the ideal frequency range and hypothesized mechanism. Modeling studies were conducted in our lab to investigate the possible mechanisms for the observed non-monotonic behavior at higher frequencies. The Hodgkin-Huxley (HH) model assumes that the membrane capacitance is constant at all frequencies. However, measurements of membrane capacitance taken on squid axons show that the membrane capacitance decreases for frequencies above 1kHz (Haydon & Urban, 1985), as shown in Figure 2.7. Incorporating this frequency-dependent membrane

capacitance into the HH model rectified the frequency-threshold relationship in the model while still preserving the standard characteristics of action potential propagation (Haeffele & Butera, 2007). Figure 2.8 shows that the blocking thresholds of the FDC model were similar to the HH model at low frequencies, up to 12 kHz, but deviated significantly from the HH model at higher frequencies. These results suggest that the classical HH model is insufficient to describe the effect of HFAC waveforms on unmyelinated nerves. A non-linear capacitance may partially account for the experimentally observed non-monotonic behavior at the higher frequencies in *Aplysia* nerves. Further experiments along with modifications of the HH model are required to comprehensively understand the non-monotonic threshold behavior observed in the unmyelinated *Aplysia* nerves.

2.4 Feather duster worm experiments

The above study on the unmyelinated nerves of the sea-slug *Aplysia*, showed that HFAC waveforms can reversibly and repeatedly block nerve conduction in purely unmyelinated nerves. The minimum amplitude to induce block proportionately increased with frequency in these nerves until 12 kHz. For frequencies above 12 kHz, the blocking threshold for these nerves was inversely proportional to frequency. This behavior contradicts the frequency-threshold relationship reported in published literature (Kilgore & Bhadra, 2004; Bhadra & Kilgore, 2005; Tai *et al.*, 2005; Tai *et al.*, 2005; Tai *et al.*, 2005; Bhadra *et al.*, 2006; Tai *et al.*, 2006; Zhang *et al.*, 2006; Zhang *et al.*, 2006; Bhadra *et al.*, 2007).

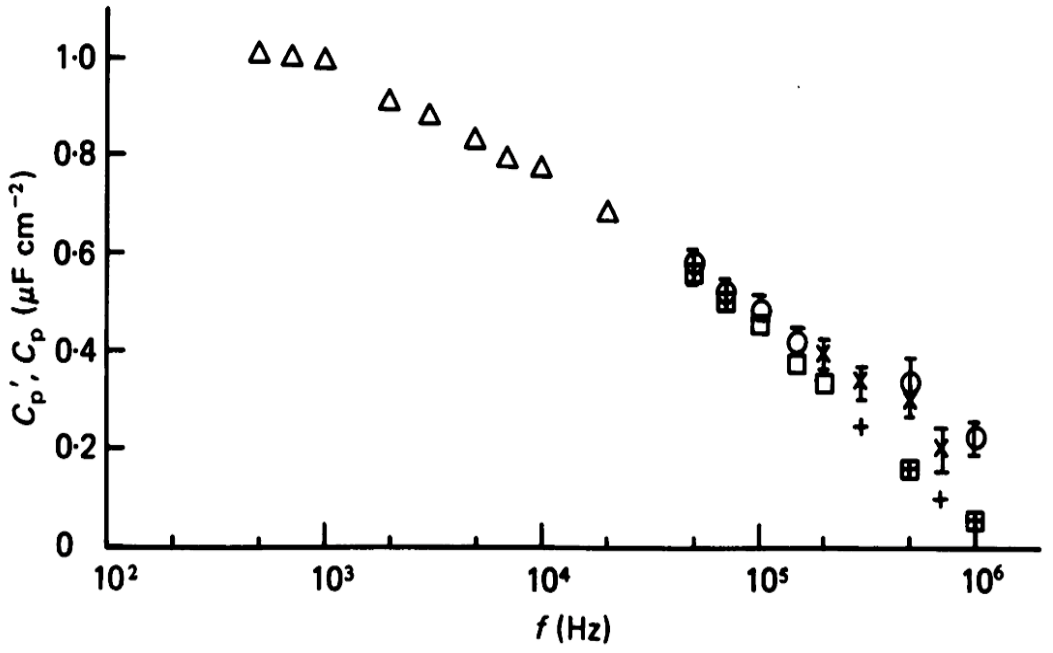

Figure 2.7: Capacitance measurements for different frequencies in a giant squid axon. Adapted from (Haydon & Urban, 1985)

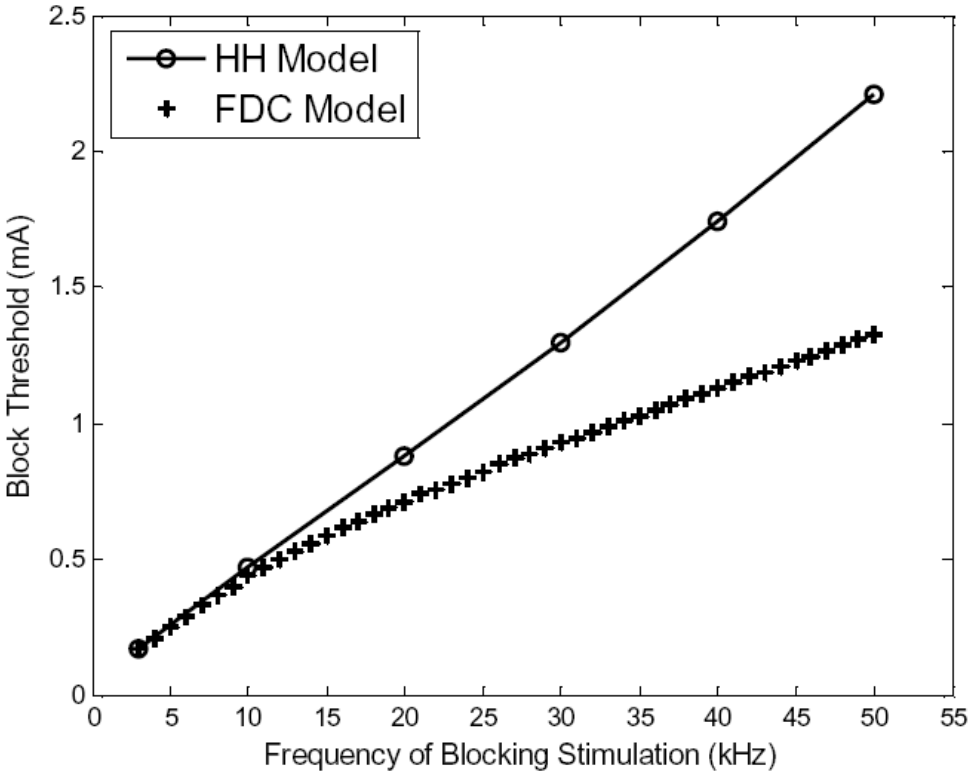

Figure 2.8: Blocking thresholds of the HH (Hodgkin-Huxley) and FDC (frequency-dependent capacitance) models for an axon with diameter = 3μm
(Adapted from Haeffele & Butera, 2007)

In order to validate our results obtained from the *Aplysia* fibers and investigate whether the non-monotonic behavior is unique to *Aplysia* or is a property of all unmyelinated fibers, we attempted to replicate the experiments in the unmyelinated nerve fibers of the feather-duster worm.

The giant axons of the marine polychaete feather duster worm, *Myxicola infundibulum*, are known to be upto 900 μm in diameter, and are usually about 500-700 μm (Binstock & Goldman, 1967; Binstock & Goldman, 1969). Most of the nerve cord is the giant axon which dominates the dorsal aspect of the cord. This preparation has been shown to have similar conduction properties as the squid giant axon (Binstock & Goldman, 1967; Binstock & Goldman, 1969) and since it is available year round at most pet stores in the US, unlike the seasonal nature of the giant squid, the featherduster worm was found to be a useful animal to study nerve activity and conduction block using HFAC waveforms.

We wanted to repeat the experiments, previously performed on the unmyelinated Aplysia nerves, to characterize the effect of HFAC waveforms on the nerve of the featherduster worm. If the threshold behavior in these nerve fibers is similar to the trends seen in the *Aplysia* nerves, then we can conclusively state that the observed non-monotonic behavior in the *Aplysia* nerves is a characteristic of all unmyelinated nerves that could potentially be significant for clinical applications related to pain management. If the results obtained on *Aplysia* nerves during HFAC stimulation can be obtained in another unmyelinated nerve preparation, then the study would also prove that the classical Hodgkin-Huxley model does not adequately describe nerve behavior at higher frequencies. Sufficient modification of the HH model will then be required to investigate

the physiological mechanisms of block induction using HFAC waveforms. If the blocking characteristics of the worm are not similar to the *Aplysia* results then we can conclude that the non-monotonic frequency-amplitude behavior is a property specific to the nerve bundle of *Aplysia* that could be attributed to its unique ion channel distribution or its surrounding extracellular environment.

Unfortunately we could not use the feather duster nerve model to validate our results. After dissecting the worm and testing its conduction properties, we found that in the feather duster nerve cord, even though action potentials could be triggered, 'sputtering decline' in the conduction properties occurred along the length of the nerve (Bullock & Turner, 1950). Several discontinuities in action potential propagation were observed along with random responses to successive stimulation that prevented detection of the triggered action potential. This preparation could not be used to validate our results from the *Aplysia* nerve since faithful reproduction of the action potential propagation could not be observed in the two recording electrodes. We could not conclusively state whether the absence of the action potential in the second recording electrode was solely due to the local conduction block induced by the HFAC waveforms or due to other changes in the conduction properties along the length of the nerve and hence had to abandon the study. Future experiments aimed at replicating the results in other unmyelinated nerves are described in Chapter 5.

2.5 Conclusion

The study described in this chapter, characterizing the effect of HFAC waveforms on the unmyelinated nerves of *Aplysia*, demonstrated that sinusoidal HFAC waveforms

from 5-50 kHz can successfully induce a local, reversible and repeatable block in unmyelinated nerve fibers. This study also demonstrated that extracellular compound action potential recordings can be a useful technique for monitoring and investigating nerve behavior during application of HFAC waveforms. The isolated response of unmyelinated nerves to HFAC stimulation had not been previously studied, though many computational models investigating the mechanism of the conduction block were based on the unmyelinated nerve model by Hodgkin-Huxley. This study is the first to investigate the effect of HFAC waveforms on purely unmyelinated nerves. It is also the first to investigate such a broad range of frequencies and including higher frequencies in the 30-50 kHz range.

We found that unlike myelinated nerves, the block threshold in *Aplysia* nerves did not have a monotonically increasing relationship with frequency. The block threshold increased linearly until 12 kHz and then exponentially decayed until 50 kHz. This difference in the response of unmyelinated nerves could not be validated in another unmyelinated nerve due to the lack of an easily accessible and amenable unmyelinated nerve preparation. In the following chapter, we intend to quantify the effect of the HFAC waveforms by observing the compound action potential of mixed nerves and isolating the components of the myelinated and unmyelinated nerve activity. Studying the different components of the compound action potential should enable us to compare our results with published literature. If our results in *Aplysia* nerves can be validated in another nerve preparation, then HFAC induced conduction block may potentially be advantageous in various neurophysiological and clinical applications related to pain management and selective stimulation.

CHAPTER 3

HFAC INDUCED BLOCK IN MIXED NERVES

High frequency alternating current (HFAC) waveforms in the range of 1-40 kHz have been shown to induce complete and reversible local block in whole nerves with minimum side effects (Tanner, 1962; Kilgore & Bhadra, 2004; Bhadra & Kilgore, 2005; Williamson & Andrews, 2005; Bhadra *et al.*, 2006; Joseph & Butera, 2009). The block threshold, defined as the amplitude of the HFAC waveform below which complete block did not occur, was found to monotonically increase with frequency in myelinated animal model systems of frog, rat and cat nerves, where muscle force was used as an indirect measure of block status (Kilgore & Bhadra, 2004; Bhadra & Kilgore, 2005; Williamson & Andrews, 2005; Bhadra *et al.*, 2006). The block threshold was found to be dependent on the electrode design, nerve type and the frequency of the HFAC waveform (Bhadra *et al.*, 2007; Ackermann *et al.*, 2009).

Traditionally only the myelinated response of the nerve and its effect on muscle force has been studied, while the effect on the smaller diameter, slower conducting unmyelinated nerves has not been experimentally considered. Simulation studies have shown that smaller diameter axons have higher blocking thresholds than the larger diameter axons at the same frequency (Bhadra & Kilgore, 2005; Tai *et al.*, 2005; Tai *et al.*, 2005; Williamson & Andrews, 2005; Bhadra *et al.*, 2007). Prior studies have also shown that for certain amplitudes of the HFAC waveform below block threshold, the nerve shows repetitive firing activity (Kilgore & Bhadra, 2004; Bhadra & Kilgore,

2005; Tai *et al.*, 2005; Williamson & Andrews, 2005; Bhadra *et al.*, 2006; Bhadra *et al.*, 2007; Joseph & Butera, 2009). Therefore, if HFAC block induction of the larger diameter fibers causes activation of the smaller diameter pain fibers, this method of conduction block would be clinically inapplicable. Hence, understanding the response of the unmyelinated nerves to HFAC stimulation is critical if clinical applications are to be pursued.

Previous experimental work in our lab on the unmyelinated nerves of the sea-slug, *Aplysia californica,* showed that HFAC stimulation could induce complete and reversible conduction block for frequencies in the range of 5-50 kHz (Joseph & Butera, 2009). The minimum HFAC amplitude for block (called the blocking threshold) was between 1 mA and 6 mA in our experiments. Although, the characteristics of the neural activity during HFAC stimulation in these unmyelinated nerves mimicked the characteristics of the myelinated nerves, the minimum amplitude for inducing block in these nerves decreased for frequencies above 12 kHz. This nonmonotonic behavior of unmyelinated nerves differed from published experimental and modeling studies on the response of myelinated nerves to high frequency stimulation (Ishigooka *et al.*, 1994; Kilgore & Bhadra, 2004; Bhadra & Kilgore, 2005; Tai *et al.*, 2005; Tai *et al.*, 2005; Tai *et al.*, 2005; Williamson & Andrews, 2005; Bhadra *et al.*, 2006; Tai *et al.*, 2006; Zhang *et al.*, 2006; Zhang *et al.*, 2006; Bhadra *et al.*, 2007). If this disparity to HFAC stimulation exists in all myelinated and unmyelinated nerves, then the ability to block the smaller diameter pain fibers while allowing conduction though the larger diameter myelinated nerves would provide a novel means for selective blocking of specific fibers, especially for applications related to pain management.

To further investigate this difference in the response of myelinated and unmyelinated nerves to conduction block induced by HFAC stimulation, we decided to characterize the effect of high frequency stimulation on mixed nerves comprising of both myelinated and unmyelinated nerves. The sciatic nerve of frogs, composed of myelinated and unmyelinated fibers, is frequently used in nerve conduction studies. Supramaximal stimulation of the sciatic nerve should produce a compound action potential consisting of the A-fiber and C-fiber response corresponding to the myelinated and unmyelinated nerve fibers' response.

3.1.1 Compound Action Potential of mixed nerves

Peripheral nerves are composed of many fibers of varying diameters and conduction velocities and serve different functions as shown in Table 3.1 and detailed in Figure 3.1. The Roman numeral (Lloyd-Hunt) system is mostly used for sensory fibers while the alphabet (Erlanger and Gasser) system is used for sensory and motor fibers. Conduction velocities of peripheral nerves are measured clinically using compound action potential (CAP) recordings. Electrically stimulating a peripheral nerve at different intensities activates different populations of nerve fibers. The action potentials of all the nerves activated by a particular current stimulus, when summed produce the compound action potential. The conduction velocity of each fiber group is then computed by dividing the latency of the peaks by the distance along the nerve between the stimulating and the recording electrodes.

Larger diameter fibers have lower axonal resistance and hence have a lower activation threshold during extracellular stimulation than the smaller diameter fibers. For

this reason, during application of an extracellular stimulus, the larger diameter fibers are recruited first and then the smaller diameter fibers which is opposite of the normal physiological recruitment order (Blair & Erlanger, 1933). As the stimulus strength increases, the largest axons are first activated followed by the other smaller axons as shown in Figure 3.2. This causes the compound action potential (CAP) to display a graded nature as opposed to the all-or-none nature of action potentials. It is also known that conduction velocity is directly proportional to fiber diameter. Consequently, the response of the smaller diameter axons occurs after a longer latency than the larger diameter axons. This latency enables the response of the smaller diameter fibers to be well separated in time from the larger diameter axons, if the nerve response is recorded at a sufficient distance from the stimulating electrode. The above stated characteristic features of the CAP make it an attractive technique for studying the response of different fiber type populations to HFAC stimulation. Figure 3.2 shows sample traces of CAP where the A-fibers response corresponds to the myelinated nerve fibers while the slower unmyelinated fibers are responsible for the C-wave. In our experiments, the C-fiber response and the A-fiber response to HFAC stimulation will be compared. We hypothesize that there exists a difference in the behavior of myelinated and unmyelinated nerves to high frequency stimulation and the C-fiber response to HFAC stimulation will be similar to that seen in the unmyelinated nerve fibers of *Aplysia*. Our hypothesis will be validated if the block thresholds of the C-fibers display the non-monotonic behavior with frequency while the A-fibers display the monotonically increasing threshold behavior as shown in Figure 3.3.

Table 3.1: Classification of peripheral nerve fibers according to their diameters. Adapted from (Kandel *et al.*, 2000)

Nerve	Fiber diameter (μm)	Conduction Velocity (m/s)	General function
Aα Large myelinated	12-20	72-120	Alpha-motoneurons, muscle spindle primary endings, golgi tendon organs, touch
Aβ Medium myelinated	6-12	36-72	Touch, kinesthesia, Muscle spindles secondary endings
Aδ Small myelinated	1-6	4-36	Pain, crude touch, pressure, temperature
B Thinly myelinated	1-3	3-15	Preganglionic autonomic
C Unmyelinated	0.2-1.5	0.2-2.0	Pain, touch, pressure, temperature, postganglionic autonomic

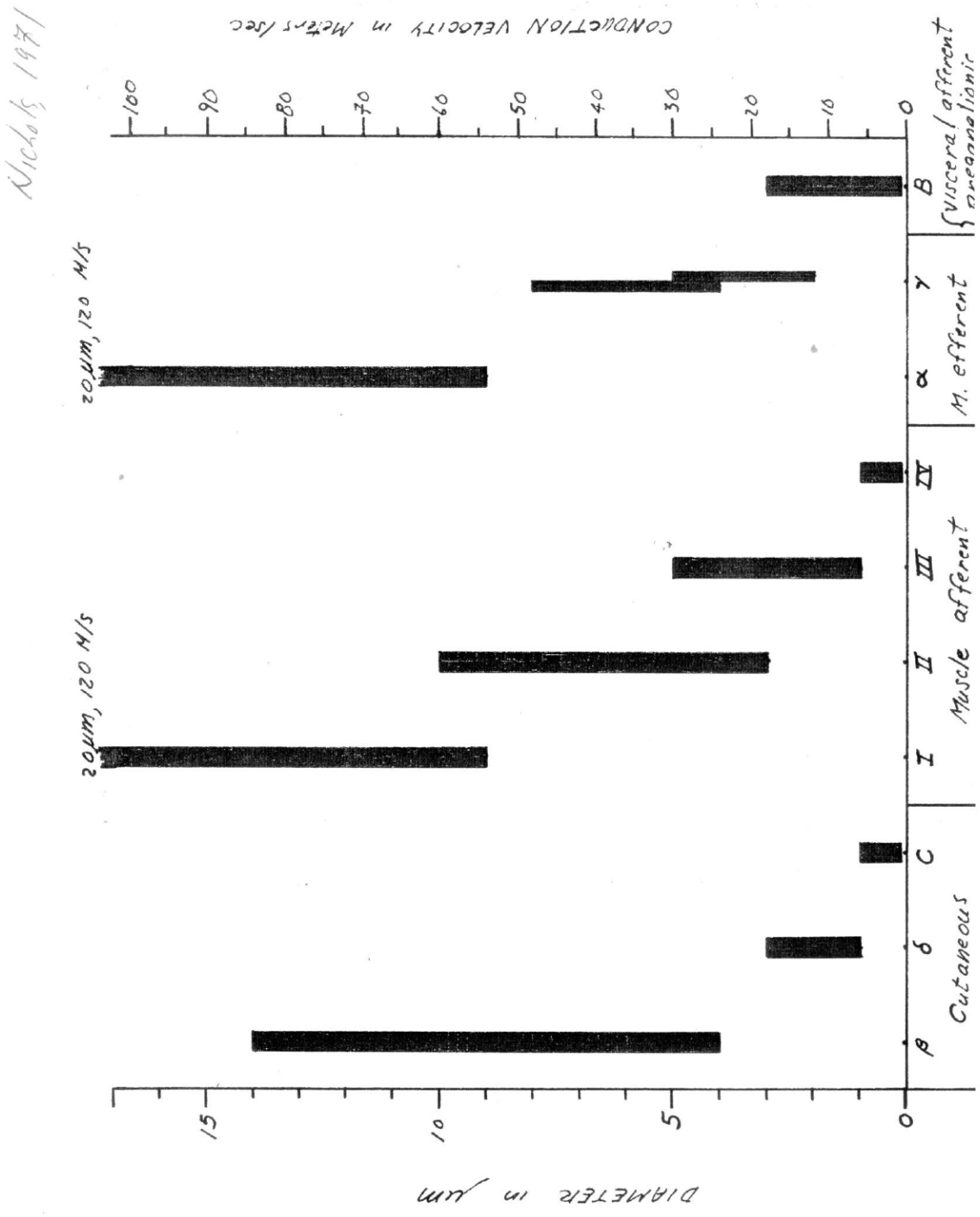

Figure 3.1: Detailed classification of peripheral nerve fibers based on fiber diameter and conduction velocity. (Personal communication with Dr. T. Richard Nichols)

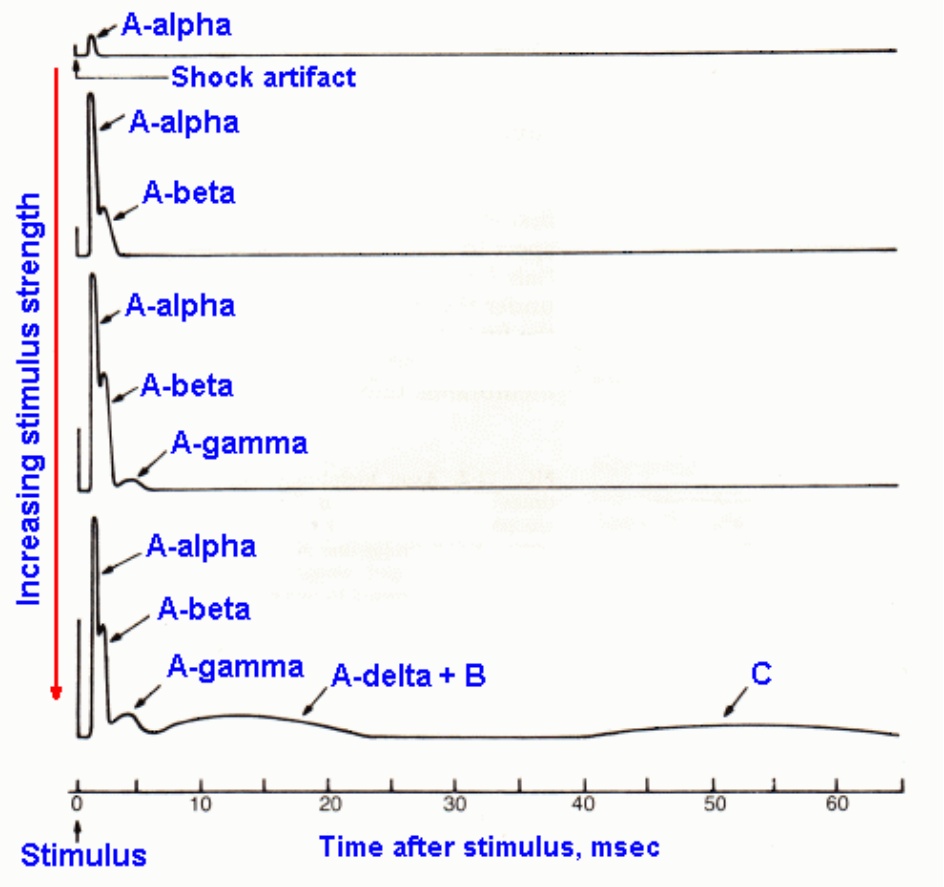

Figure 3.2: Recruitment of different types of nerve fibers in a mixed nerve with increasing stimulus strength.

(Adapted from: http://unmc.edu/Physiology/Mann/mann12.htm)

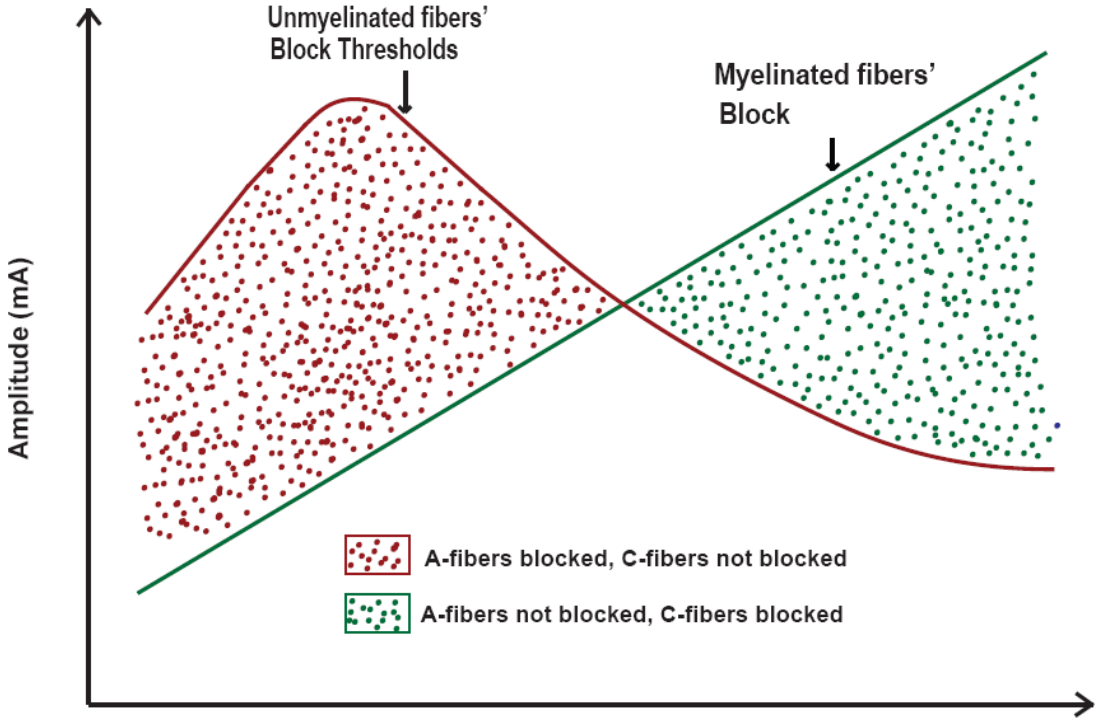

Figure 3.3: Hypothesized block threshold behavior for myelinated and unmyelinated nerves at different frequencies based on data from *Aplysia* nerves and amphibian and mammalian nerves. The brown dots indicate the region where A-fibers can be selectively blocked while conduction in C-fibers persists. In the region with green dots, the C-fibers can be blocked while conduction through the A-fibers exists.

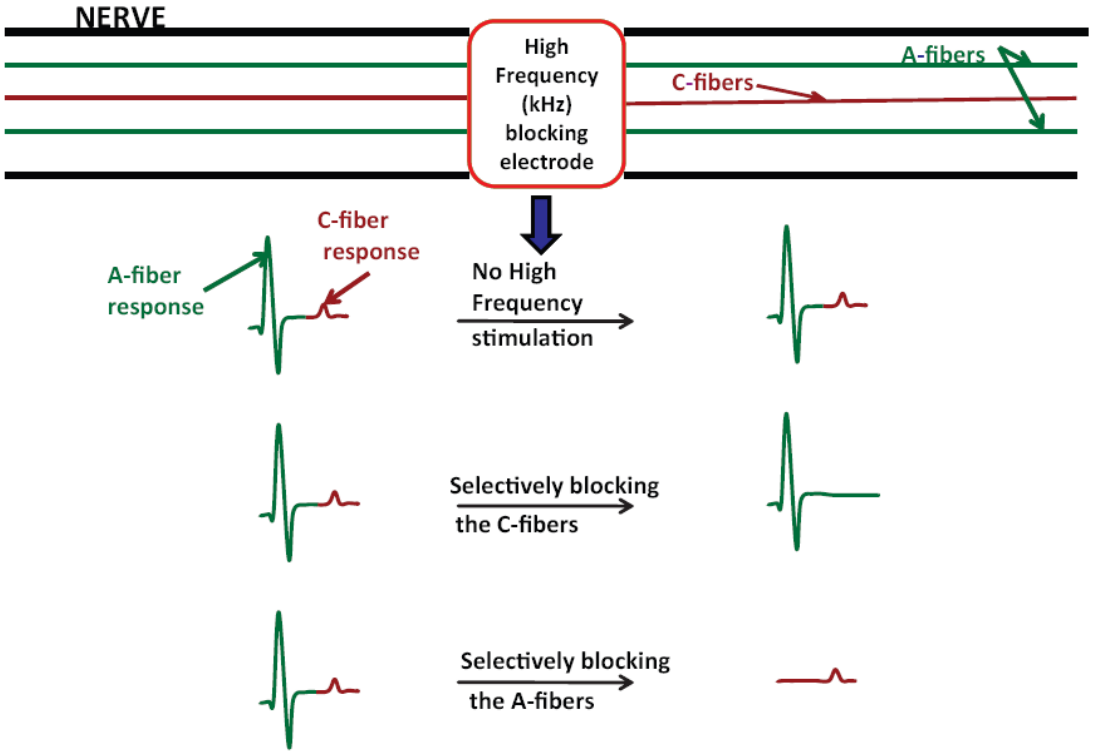

Figure 3.4: Expected traces of the CAP during application of HFAC waveforms. Based on the the hypothesized blocking regimes for myelinated and unmyelinated fibers,HF stimulation should enable selective block the A-fibers or the C-fibers. We hypothesize that specific components of the CAP might be selectively blocked with HFAC waveforms.

If validated, this property of differential thresholds for inducing block in myelinated and unmyelinated nerves can be extremely advantageous for various clinical applications, as we could potentially find two regions where one component of the CAP could be selectively blocked while the conduction of action potential is maintained in the other types of fibers. Figure 3.4 demonstrates the hypothesized results where specific components of the CAP can be selectively blocked using HFAC waveforms. HFAC waveforms can be used to selectively block conduction through the unmyelinated pain fibers and thus reduce or eliminate the sensation of pain. HFAC block can also be utilized for selective stimulation of specific fiber types, especially in motor prosthetic applications, to achieve the normal recruitment order of nerve fibers. For example, slow variation of the stimulation frequency can cause the blocking and unblocking of the larger diameter fibers while allowing conduction trough the smaller diameter fibers. This mechanism would provide more control on the extracellular stimulation used to restore functionality and can thus improve the current state of motor prostheses.

3.1.2 Preliminary data from cat nerves

Preliminary experiments conducted on the sciatic nerve of cats, using the same equipment as that used for the unmyelinated *Aplysia* nerves, demonstrated that conduction block can be induced in the nerve fiber using 10-30 kHz HFAC waveforms. Only the larger diameter motor nerve response of the compound action potential was studied in these nerves. Partial block and complete block of the compound action potential was observed when high frequency sinusoidal waveforms with frequencies of 10 kHz, 20 kHz and 30 kHz sinusoidal were applied. Hook electrodes were used in these

experiments and so complete encapsulation of the nerve fiber was not possible. Figure 3.5A depicts two such trials of application of HFAC waveforms on the nerve and Figure 3.5B shows the relationship of block threshold to frequency for these mammalian nerves. A linear relationship of block threshold to frequency was observed in these nerves even at higher frequencies (above 20 kHz). These experiments proved that the non-monotonic behavior observed in the Aplysia nerves was a property of the unmyelinated nerves and not an experimental artifact.

To validate our results from the *Aplysia* fibers and investigate whether the nonmonotonic response is unique only to the *Aplysia* nerves or is applicable to all unmyelinated nerves, we studied the effect of HFAC stimulation on the compound action potential (CAP) of amphibian mixed nerves. The sciatic nerve of frogs, frequently used in experimental studies, is composed of myelinated and unmyelinated fibers. Investigating the effect of HFAC waveforms on the different components of the CAP would enable us to detect the progression of block in each fiber type population within the whole nerve. In this paper, we describe the i*n vitro* experiments performed on the sciatic nerve of the frog where neural activity was directly observed to determine the block status. For simplicity, we grouped the fast-conducting myelinated fibers with conduction velocities greater than 20m/s as the A-fiber response and the slow-conducting unmyelinated fibers with conduction velocities less than 1m/s as the C-fiber response. If the A-fiber and C-fiber components are found to have different blocking threshold behaviors at high frequencies, then this method of block induction could be significant for a variety of clinical and neurophysiological applications.

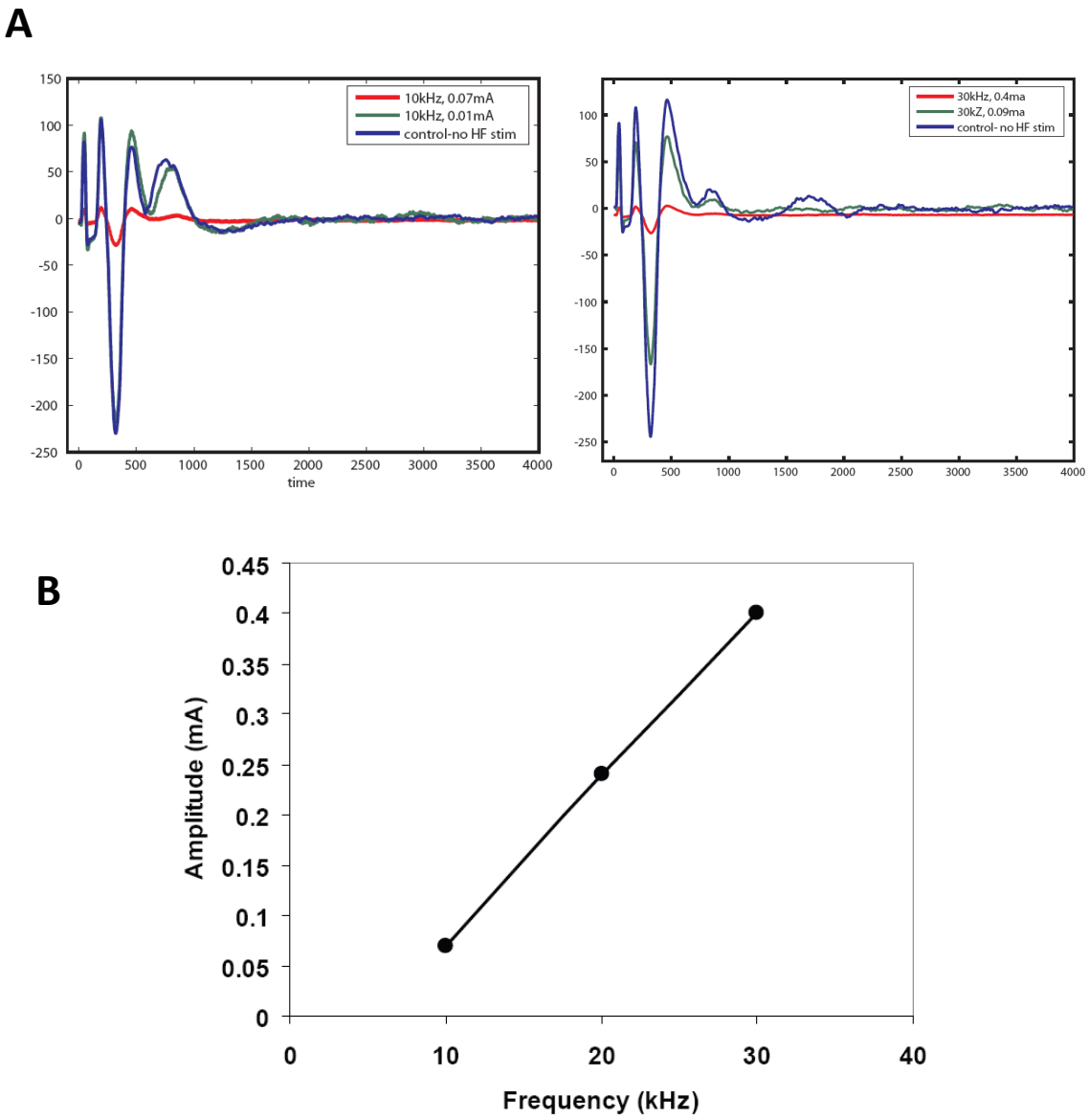

Figure 3.5: A: Block of the compound action potential obtained during application of 10, and 30 kHz, sinusoidal waveforms on the sciatic nerve of cats. CAP recording during application of 20 kHz is not shown but displayed similar properties. B: Plotting thresholds at the 3 different frequencies demonstrated that the CAP nerves displayed a linear block threshold to frequency relationship. Hook electrodes were used in these experiments.

3.2 Materials and Methods

3.2.1 Animal preparation

In vitro acute experiments were performed on the sciatic nerve of 14 leopard frogs, *Rana pipiens*. Prior to surgery, the frogs were anestheized with tricaine methanesulfonate (MS-222, 1 g/L) and then the frogs were double pithed. The sciatic nerve was exposed along its entire length through a dorsal incision and cut at the level of the spinal cord as shown in Figure 3.6. The nerve, usually about 5 cm long, was ligated at both ends with silk threads. The threads were pinned to a petri dish with a Sylgard base (Dow Corning), and the dish was filled with normal frog Ringer's solution (NaCl 83.89mM, NaHCO3 28.11 mM, KH2PO4 1.2mM, KCl 1.5mM, MgSO4 1.2mM, CaCl2 Dihydrate 1.3mM, Glucose 10 mM, pH adjusted to 7.4) . The frogs were decapitated at the end of the dissection. All experiments were conducted at room temperature and all protocols involving animal use were approved by the Georgia Tech Institutional Animal Care and Use Committee.

3.2.2 Electrophysiological setup

Glass suction electrodes, with tip diameters about the same as that of the nerve fiber (0.5-1mm), were used in our experiments. Figure 3.7 illustrates the experimental setup used for recording CAPs triggered in the sciatic nerve. This experimental setup was similar to that previously used for the *Aplysia* nerves (Joseph & Butera, 2009). Two electrodes were used for recording the propagation of the CAP along the nerve. One electrode was used to trigger a CAP while another electrode, placed between the two

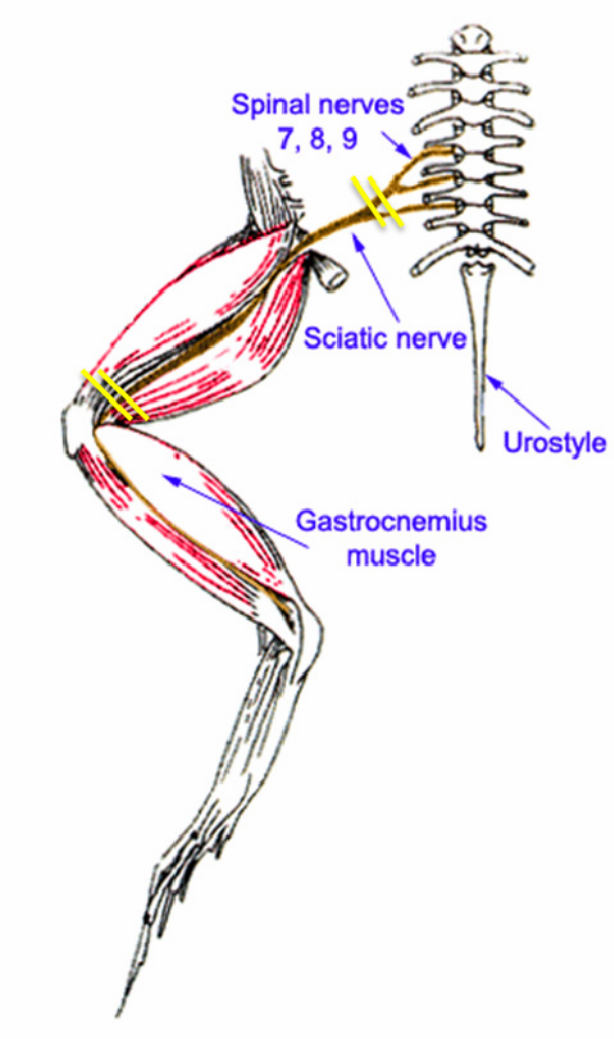

Figure 3.6: Anatomical features of the frog leg highlighting the sciatic nerve used for our experiments. The yellow double lines indicate the positions where the sciatic nerve was severed.

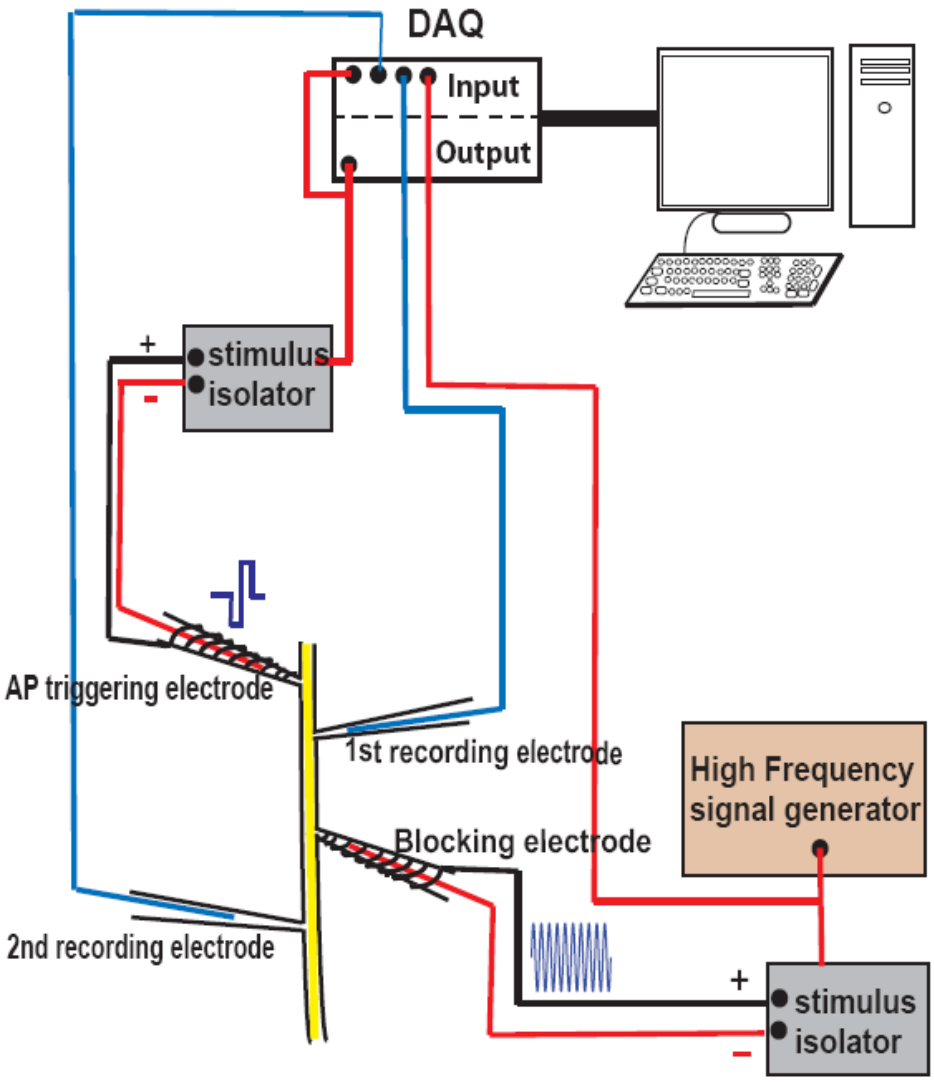

Figure 3.7: Experimental setup for recording the compound action potential from the sciatic nerve and blocking conduction by application of HFAC waveforms.

recording electrodes, was used to provide the block-inducing HFAC waveform. The distance between the electrodes was optimized for maximizing separation between the stimulus artifact and the recorded CAP without temporally dispersing the signal, and was usually about 5mm. The propagation of impulses along the nerve was used as an output measure to monitor block status. A suprathreshold bipolar stimulus pulse of 10V for 0.2ms, converted to current stimulation (0.1mA/V), through a stimulus isolation unit (AM Systems-Analog Stimulus Isolator, Model 2200, Carlsborg, WA) was used to trigger the CAP. High frequency sinusoidal waveforms generated by a function generator (Stanford Research Systems, Model DS345) and sent through a similar stimulus isolation unit (0.1mA/V) were used to produce HFAC waveforms for block induction.

Each trial consisted of an average of 20 runs. The signal was differentially amplified (gain=1000) and the bandwidth was restricted to 100Hz-5 kHz for recording the A-fiber response. Similarly, an amplifier gain of 10K and bandwidth of 100Hz-1 kHz was used to record the C-fiber response. In 5 animals where both the A-fiber and C-fiber components were recorded, a gain of 1000 and bandwidth of 100 Hz-5 kHz was used. Additional post-data filtering in Clampfit (bandpass filter = 100Hz-3 kHz), enabled detection of block status of the C-fiber components. These optimal settings filtered out the noise from the high frequency waveforms and enabled identification of the different components of the CAP. Our experimental set up had the advantage of providing direct monitoring of the neural activity along the nerve, unlike other published studies where muscle force or sphincter pressure was used as an indirect measure of nerve block.

3.2.3 Experimental procedures

Repeated, randomized trials were conducted for various frequencies in the range of 5-50 kHz and amplitudes in the range of 0.1-1 mA. For each frequency, the amplitude of the waveform was varied until the propagation of APs could not be observed. A range of amplitudes was tested to identify the threshold at which block was observed. The amplitude was incremented in discrete steps initially of 0.1-0.3mA and then of 0.01-0.05mA closer to block threshold. After the HFAC stimulus was applied on the nerve, a test pulse was injected to trigger an AP in the nerve. If the amplitude of the HFAC waveform was at or above the threshold for inducing conduction block, the CAP was arrested at the site of injection of the blocking stimulus. The minimum amplitude of the HFAC waveform at which the CAP was not observed in the distal recording electrode was identified as the 'block threshold'.

The procedure of identifying block threshold was repeated for different frequencies in a random order. The response of the nerve before, during and after high-frequency block was recorded in individual trials. Based on the recorded CAP when the high frequency waveform was applied, the nerve response was further classified as 'No change', 'Partial Block' and 'Block'. This classification was done for both the C-fiber and A-fiber components of the CAP. 'No change' was identified as the amplitudes of HFAC stimulation when the CAP component was similar to the CAP prior to switching on the HFAC waveform. 'Partial block' was identified as the amplitudes below the block threshold where part of the CAP appeared to be blocked or distorted and the CAP component was less than 50% of the amplitude of the component prior to switching on the HFAC waveform. 'Block' was identified as the amplitudes of the HFAC waveform

when the component of the CAP was less than 10% of the CAP component prior to switching on the HFAC waveform. Multiple trials, for each randomly chosen frequency, were performed on every nerve to evaluate the repeatability and reversibility of applying the HFAC stimulus. These multiple trials enabled the complete characterization of the response of the nerve to different frequencies and amplitudes.

3.3 Results

All experimental preparations were initially tested for normal conduction properties to determine if a CAP could be repetitively triggered and transmitted along the axon. The triggered CAP appeared in the recording electrodes with a small latency between them, due to the propagation delay. The conduction velocities were greater than 20m/s for the A-fiber component and in the range of 0.4-1m/s for the C-fiber components. The stimulus artifact also appeared in the recording traces but was usually well separated from the A-fiber component of the CAP in the second recording electrode due to the longer distance from the stimulating electrode. The C-fiber component of the CAP due to the slower conduction velocity appeared at a latency greater than 20 ms after the A-fiber response. Detection of these waveforms was essential for determining the A-fiber and C-fiber block thresholds. A sample recording from which the A-fiber and C-fiber component are extracted is shown in Figure 3.8.

Conduction block induced by HFAC stimulation was demonstrated in all the nerves tested for at least 2 different frequencies in the range of 5-50 kHz. In the absence of the high frequency AC current and for stimulus intensities below the block threshold, normal conduction of the CAP was observed.

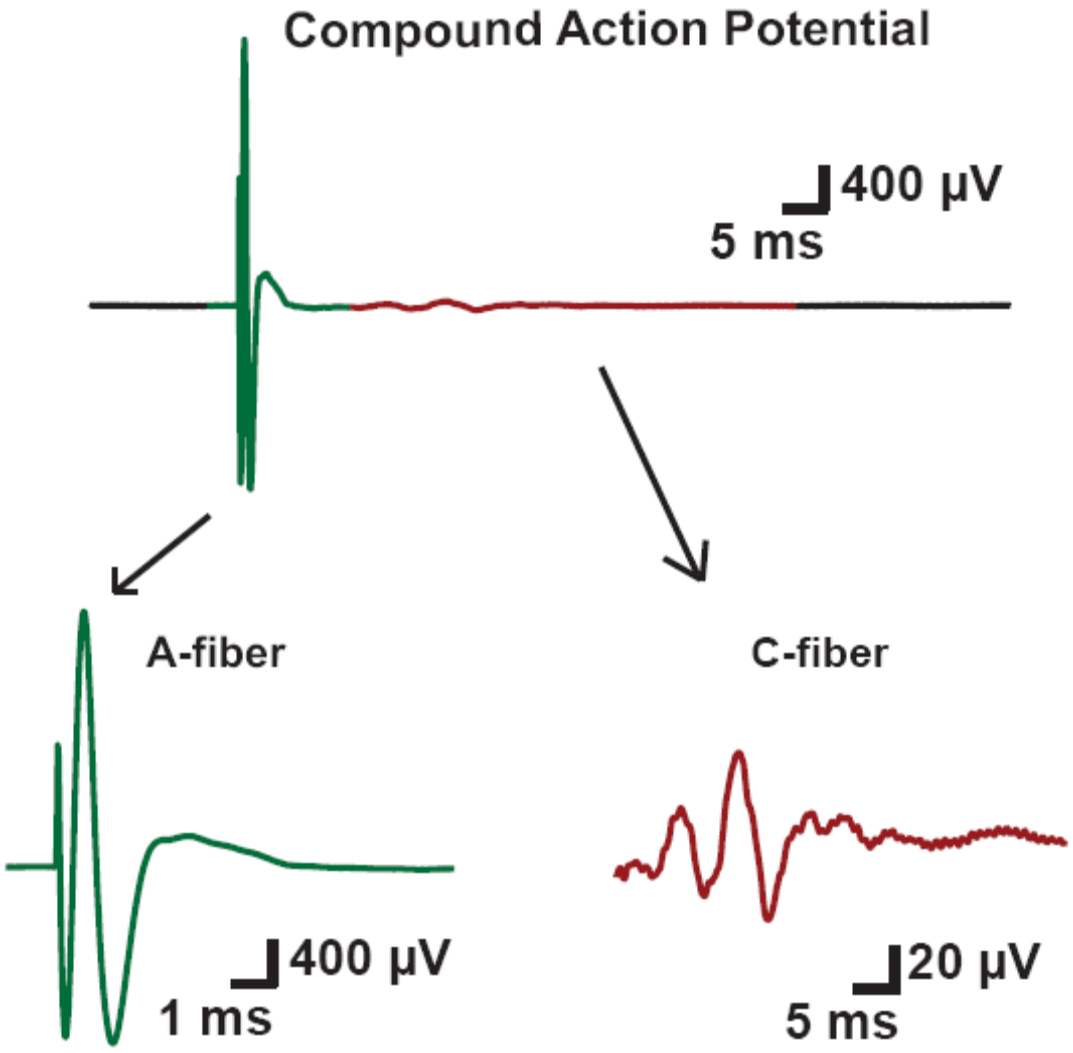

Figure 3.8: Sample recording from which the A and C-fiber components can be extracted.

The nerve was tested before each application of the HFAC waveform and block was determined by comparing with the recording taken prior to switching on the HFAC stimulus. The presence or absence of the different components of the CAP was used to determine block status. Figure 3.9 shows two different trials where the A-fiber or the C-fiber component of the CAP could be separately blocked. The nerve fiber was said to be blocked when the CAP completely disappeared or was smaller than 10 % of the amplitude of the pre-block CAP. 100 % block of A-fiber could not be obtained in some cases due to incomplete encircling of nerve fiber (Petruska *et al.*, 1998; Bhadra & Kilgore, 2005).

In cases where conduction block could be observed, CAP conduction returned within a few seconds of switching off the high frequency current and was instantaneous in some cases. The neural activity of the nerve changed depending on the amplitude and frequency of the HFAC waveform. A decrease in the amplitude or a notable change in the shape of the CAP, during application of the HFAC waveform, was indicative of block of only few axons in the nerve fiber and was noted as 'partial block'. Figure 3.10 shows a sample trace of the C-fiber component where partial block was observed. The CAP components prior to, during and after application of the HFAC waveform are also displayed for comparison. We also note, as in Figure 3.11, that partial block always occurred at amplitudes of the HFAC waveform that were immediately below the block thresholds. If a dramatic change in the amplitude or shape of the CAP was observed, or if recovery of the CAP did not occur to its pre-block amplitude and shape after the HFAC stimulus was switched off, the experiment was terminated and the last dataset deleted.

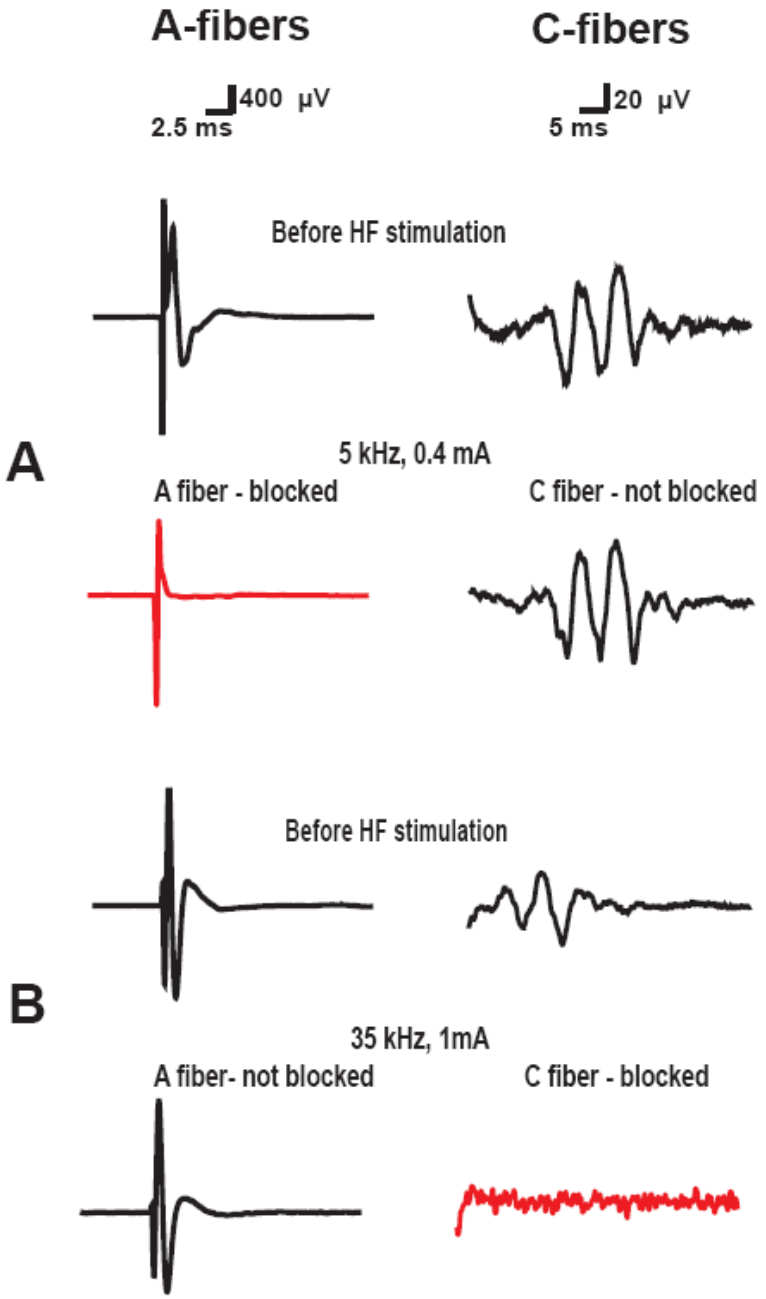

Figure 3.9: Selective block of A fibers and C-fibers. Two different trials showing selective block of the components during application of HFAC waveforms A: The topmost trace shows the CAP before application of HFAC waveforms. Application of a 5 kHz waveform blocked the A-fiber and not the C-fiber component. B: Application of a 35 kHz waveform blocked the C-fiber and not the A-fiber component.

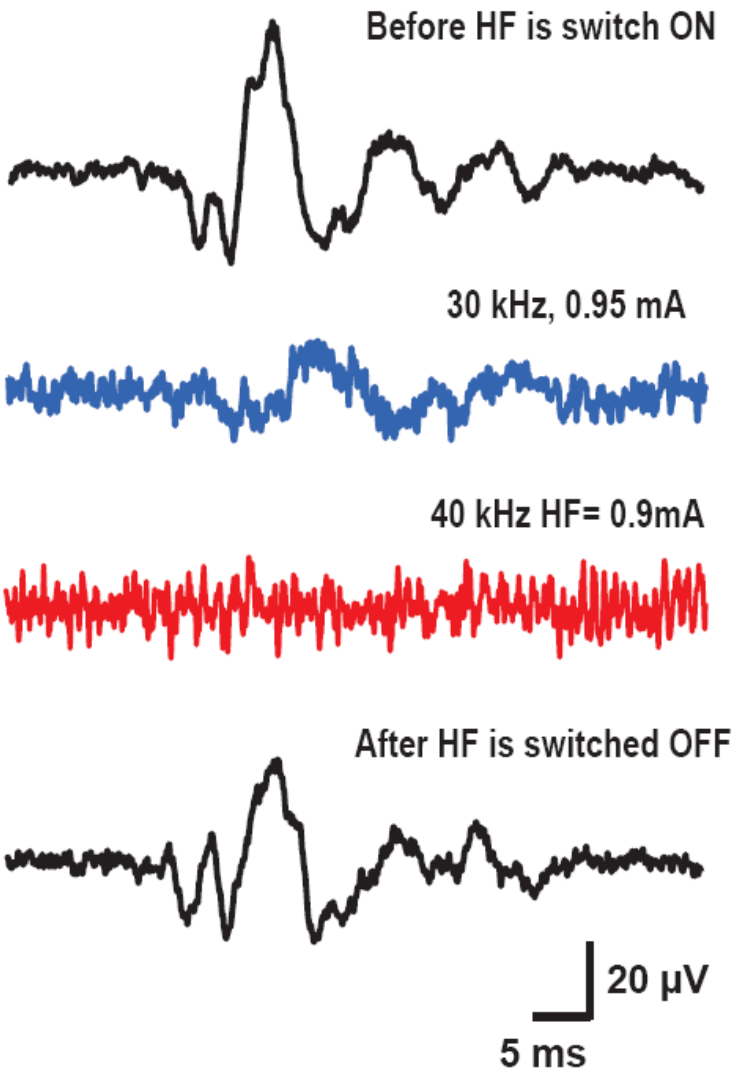

Figure 3.10: Sample traces showing the C-fiber response, before, during and after application of HFAC waveforms. Partial block (blue trace) was noted in certain cases when the amplitude of the component of the CAP was less than that prior to application of the HFAC waveform (black trace). Changing the amplitude or the frequency eliminated the response completely and this was noted as complete block (red trace). After switching off the HFAC waveform, the C-fiber component of the CAP could again be observed.

Failure of these trials was attributed to improperly constructed electrodes, electrodes that had a degraded AgCl coating, a weak battery in the stimulus isolator or degrading health of the nerve preparation.

A mapping of the neural activity of the A and C-fiber components for different frequency and amplitude combinations is shown in Figure 3.12. The amplitudes of the HFAC waveform required to induce block in the A-fiber component of the CAP appeared to linearly increase with frequency as shown in Figure 3.12 A. In contrast, as observed in Figure 3.12 B, the amplitudes of the HFAC waveform required to block conduction of the C-fiber component of the CAP did not monotonically increase with frequency. The current intensity required to block conduction through the unmyelinated nerves increased until about 20 kHz and then decreased until 50 kHz, which was the maximum frequency tested. The minimum amplitude of the HFAC waveform for inducing block at a particular frequency was termed the block threshold. Figure 3.13 compares the average block thresholds obtained for the A and C-fiber components at different frequencies in the range of 5-50 kHz.

3.4 Discussion

This paper is the first study to demonstrate that the unmyelinated and myelinated components of the mixed nerve can be consistently, repeatedly and separately blocked in peripheral amphibian nerves. It is also the first to experimentally investigate the frequency-amplitude relationship of the different components of the CAP of a mixed nerve to HFAC stimulation. Block induced through HFAC waveforms can be obtained in whole nerves for frequencies from 5-50 kHz and amplitudes from 0.1-1 mA.

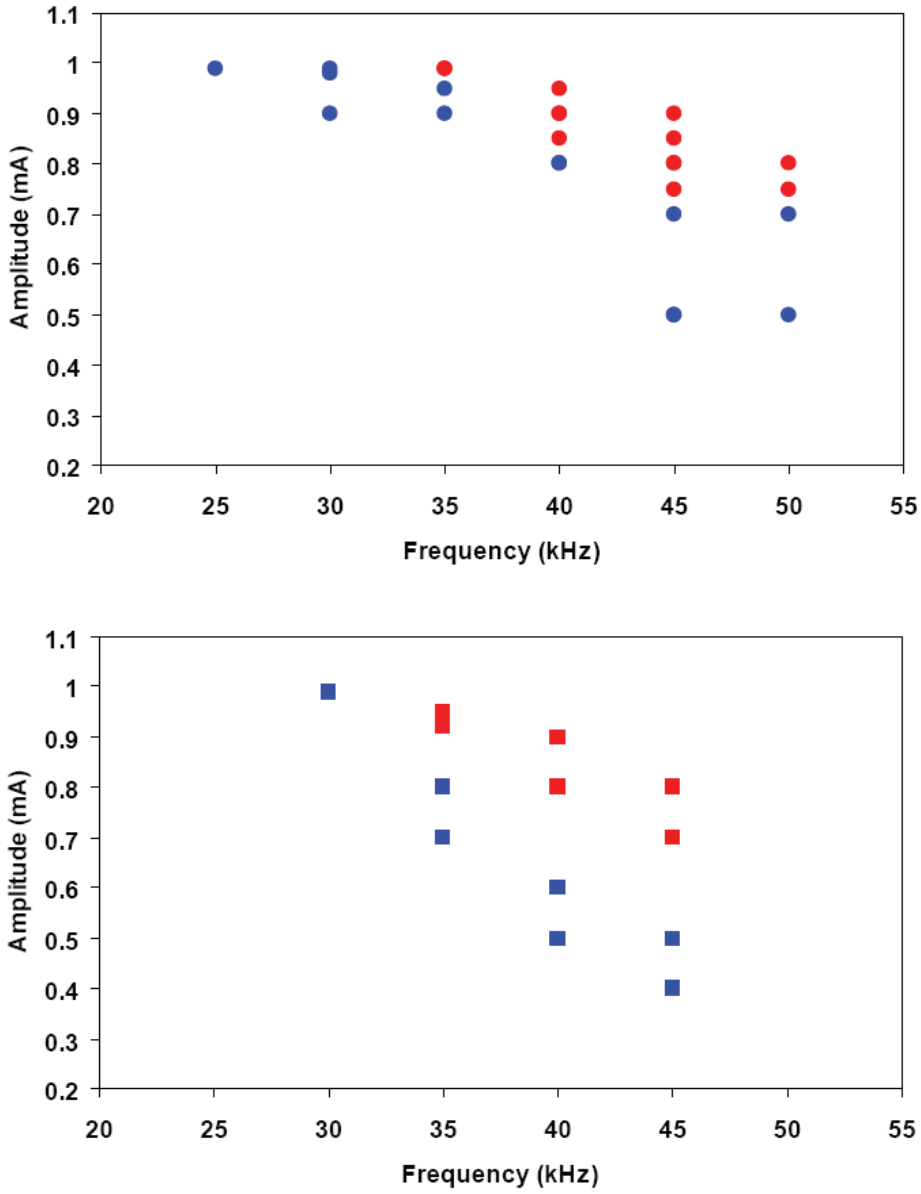

Figure 3.11: Partial block occurs at amplitudes below block. Trials on two different nerves showing amplitudes when partial block and block occurred. The red points indicate amplitudes at which conduction was blocked and the blue points indicate amplitudes at which partial block was observed.

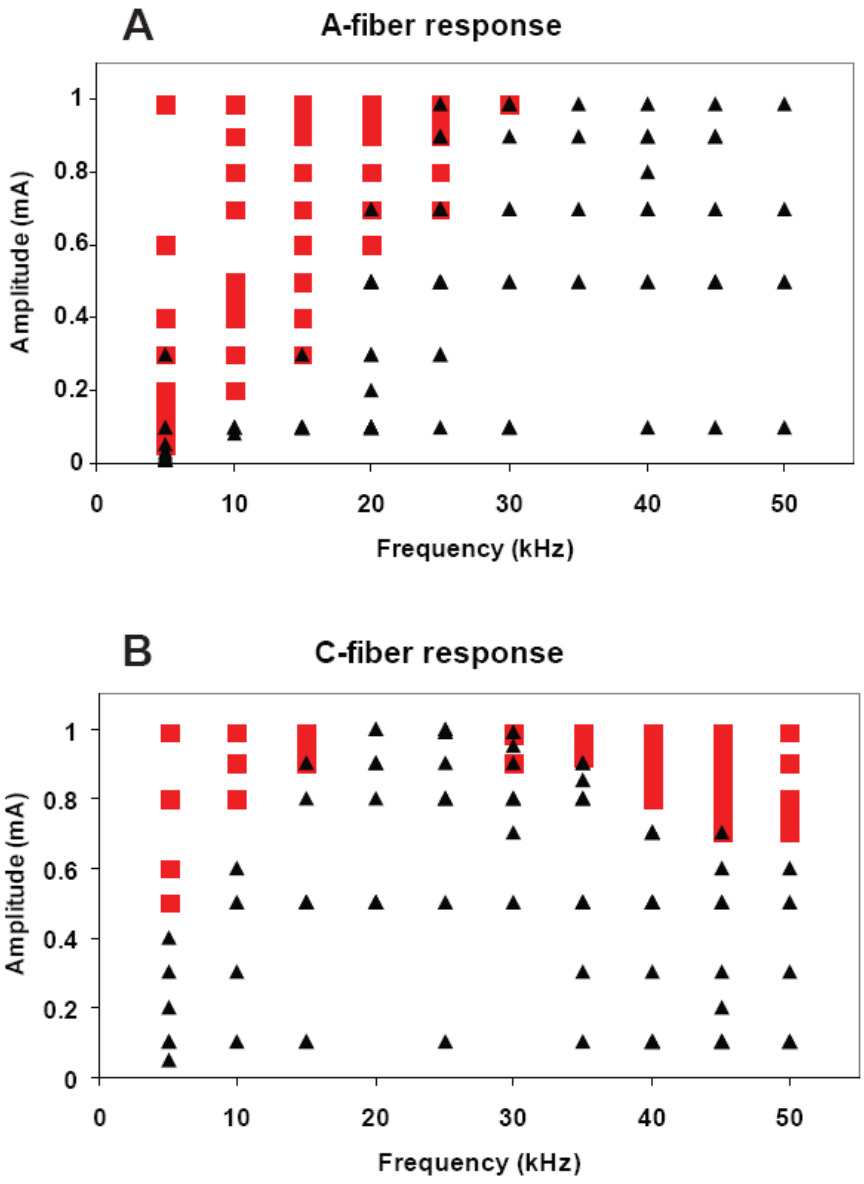

Figure 3.12: The A-fiber and the C-fiber response for different frequencies and amplitudes. A: The A-fiber response shows a monotonically increasing trend for blocking amplitudes. B: The C-fiber response demonstrates a non-monotonic trend for blocking amplitudes. The red squares indicate amplitudes at which the component was blocked. The black triangles indicate amplitudes at which the amplitude and shape of the CAP was similar to the CAP prior to application of the HFAC stimulus

The block threshold was a repeatable measure both within animals and between animals and showed a strong linear relationship with frequency for the A-fiber component of the CAP and a nonmonotonic relationship with frequency for the C-fiber component of the CAP. Published models have shown that the block threshold using HFAC waveforms is inversely proportional to axon diameter (Bhadra & Kilgore, 2005; Tai *et al.*, 2005; Tai *et al.*, 2005; Williamson & Andrews, 2005; Bhadra *et al.*, 2007). However, in our experiments a pure diameter dependence of threshold on frequency was not observed. A nonmonotonic relationship was found in the smaller diameter unmyelinated fibers, with block thresholds decreasing as frequency increased above 30 kHz. These results are consistent with the results previously obtained from the purely unmyelinated nerves of the sea-slug *Aplysia* (Joseph & Butera, 2009) . Since the frequencies were tested in a random order and the nonmonotonic relationship was observed only in the C-fiber component of the CAP and not in the A-fiber component, it can be concluded that the negative slope relationship observed at higher frequencies was an inherent property of the unmyelinated nerves and was not due to fatigue over time or an artifact of the experimental set-up.

Simulation work in our lab has attempted to understand this decrease in block thresholds at higher frequencies and a modified Hodgkin-Huxley model with a frequency- dependent capacitance was able to partially account for the nonmonotonic behavior (Haeffele & Butera; Joseph *et al.*, 2007). Previous work in the field has indicated that the frequency of the waveform, the computational model used, and the possible interactions between the nodes of Ranvier, are key issues in achieving the localized electrical nerve block (Tai *et al.*, 2005; Williamson & Andrews, 2005; Zhang

et al., 2006; Bhadra *et al.*, 2007; Ackermann *et al.*, 2009). We hypothesize that the active and dielectric membrane properties as well as the effects of myelination may account for the disparity in the behavior between the two types of nerve fibers. Additional experimental and simulation studies will be required to completely understand the mechanisms of block induction and future work in our lab is aimed at understanding this difference. The average block thresholds for different fiber types are markedly distinct at certain frequencies, as evident in Figure 3.13. Our study conclusively demonstrates that selective block of either the A-fiber component of the CAP (Figure 3.9A) or the C- fiber component of the CAP (Figure 3.9B) can be obtained by choosing the right frequency and amplitude combination, shown in Figure 3.13. In our experiments block thresholds for certain frequencies could not be precisely determined due to physical limitations of the equipment that restricted the maximum current output to 1mA, but other features of nerve activity, like partial block or no change in the features of the CAP for amplitudes below 1mA helped deduce that the block thresholds at those frequencies were above 1mA. Nerve block might also be obtainable over a wider frequency range for amplitudes that could not be tested with our apparatus.

Our experimental set-up, using direct measures of nerve activity through compound action potential recordings, offers a powerful technique to investigate the effect of HFAC waveforms on the different types of nerves fibers and identify regions where specific fiber types can be blocked. Selective blocking of conduction through the pain fibers has been the goal of many researchers and our study has conclusively shown that HFAC waveforms can be used to selectively and reversibly induce block in the C-fibers, thus decreasing or eliminating the sensation of pain through these fibers.

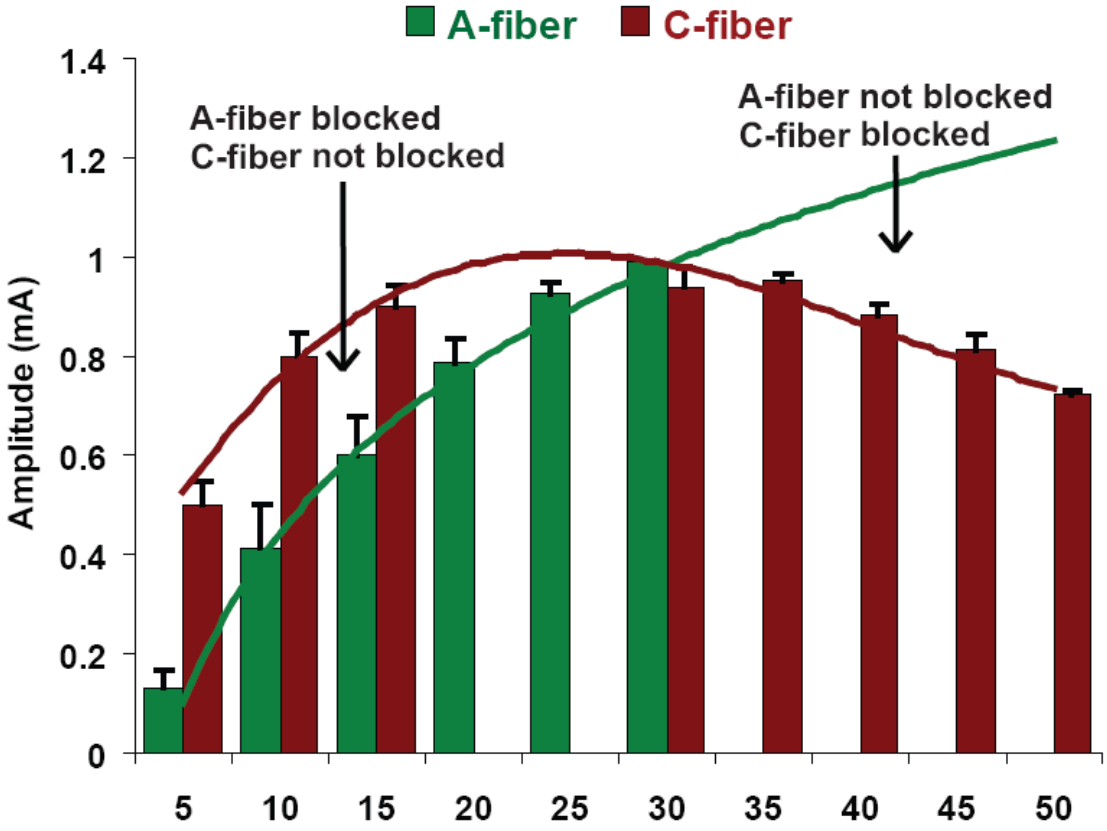

Figure 3.13: Plot of the trend lines and average block thresholds for the A and C-fiber components of the CAP for different frequencies. The block thresholds for the A-fibers directly increased with frequency while the block thresholds for the C-fibers increased and then decreased above 35 kHz. Average block thresholds at certain frequencies could not be denoted since they were above 1 mA, the maximum amplitude tested. We note that there are two regions with different frequency-amplitude combinations, where one fiber type can be selectively blocked. For frequencies from 5-15 kHz, and amplitudes from 0.5-0.8 mA, only the A-fibers can be blocked without blocking the C-fibers and for frequencies from 35- 50kHz and amplitudes from 0.8-1mA, only the C-fibers can be blocked without affecting the A-fibers.

Future studies in our lab are aimed at understanding how A-delta fibers, respond to high frequency stimulation. This study is also significant for the field of selective stimulation as it demonstrates that HFAC waveforms can be used in neural prosthetic applications to achieve graded block. Block induced by HFAC waveforms could facilitate functional recruitment of nerve fibers, thus enabling dexterous control of muscle activity.

3.4 Conclusion

This study characterizing the effect of HFAC waveforms on individual fiber type populations of mixed nerves has demonstrated that larger diameter myelinated fiber and smaller diameter unmyelinated nerves fibers have different blocking thresholds at different frequencies and the threshold behavior is non-uniform across the frequency range. This is the first study on animal nerves to describe the effect of HFAC waveforms on different types of fibers using compound action potential recordings. It is also the first study to demonstrate that unmyelinated nerves can be selectively blocked using HFAC waveforms, while maintaining conduction in the myelinated fibers. The nonmonotonic threshold behavior of the unmyelinated nerves compared to the linear threshold behavior of myelinated nerves offers distinct frequency-amplitude combinations where specific fiber types can be selectively blocked or stimulated. These results are significant for potential clinical applications related to blocking C-fiber conduction while stimulating the larger diameter myelinated fibers. Future studies in our lab are aimed at identifying the response of other nerve fiber types, especially the A-delta and B fibers to gain an appreciation of the non-monotonic behavior displayed by the C-fibers.

CHAPTER 4

EFFECT OF DURATION OF APPLICATION OF HFAC WAVEFORMS [2]

High frequency alternating current (HFAC) electrical waveforms are capable of inducing a fully reversible conduction block in myelinated and unmyelinated axons (Rosenblueth & Reboul, 1939; Tanner, 1962; Richardson *et al.*, 2000; Bhadra & Kilgore, 2005; Tai *et al.*, 2005; Tai *et al.*, 2005; Tai *et al.*, 2005; Williamson & Andrews, 2005; Bhadra *et al.*, 2006; Tai *et al.*, 2006; Zhang *et al.*, 2006; Zhang *et al.*, 2006; Bhadra *et al.*, 2007; Joseph & Butera, 2007; Joseph *et al.*, 2007; Ackermann *et al.*, 2009; Joseph & Butera, 2009). This ability to temporarily block the propagation of action potentials along an axon using electrical current can be significant for various neurophysiological applications. However, the ionic mechanism underlying block induction using HFAC waveforms is not well understood.

Several computational studies investigating HFAC waveforms have proposed various mechanisms of block induction. Some modeling studies have attributed the mechanism to the constant activation of the potassium channels (Tai *et al.*, 2005; Tai *et al.*, 2005; Zhang *et al.*, 2006; Zhang *et al.*, 2006) while others have claimed that a depolarizing mechanism brought about by the deactivation of the sodium gate is responsible for block induction (Kilgore & Bhadra, 2004; Bhadra *et al.*, 2007). Modeling

[2] Most of the work described in this chapter has been published in Joseph, L. and R. J. Butera (2009). "Unmyelinated Aplysia nerves exhibit a nonmonotonic blocking response to high-frequency stimulation." IEEE Transactions on Neural Systems and Rehabilitation Engineering 17(6): 537-44.

studies investigating the ionic mechanisms and the gating variables affected by HFAC waveforms have attributed block induction to different mechanisms that are subject to the model used and the frequency range studied. Many of these studies have been based on axon models that have not been extensively tested with high frequency signals. Since experimental data from axons at these high frequencies has not been used to validate the behavior of the models used in published literature, it is possible that significant discrepancies might exist between simulation results and experimental measurements. Most of these studies have only looked into the ion channel gating mechanisms that prevent action potential propagation during application of HFAC waveforms. The surrounding extracellular environment might play a significant role in block induction but it has been ignored in published literature. It is quite possible that depending on the fiber type, frequency and the amplitude of the HFAC waveform, different or multiple mechanisms might be responsible for inducing block.

Prior experimental work related to conduction block induced by HFAC waveforms have only looked into whether action potential propagation can be blocked or not. The physiological mechanisms that induce block have not been experimentally investigated. It is known that the conduction of impulses dynamically change the extra- and intracellular ionic microenvironment which feeds back in to the axonal activity. Hence by monitoring the axonal activity we should be able to deduce potential mechanisms of block induction.

4.1 Material and Methods

4.1.1 Animal preparation

In vitro experiments were performed on the unmyelinated nerves of *Aplysia.* The propagation of impulses along the nerve was used as an output measure to monitor block status. The animals were dissected according to standard protocol where the animals are anesthetized with isotonic $MgCl_2$ (30% of body weight). The body cavity was incised to expose the nerve connectives leading from the abdominal ganglion. The nervous system, including the circumesophageal ring or head ganglia and the abdominal ganglion, was isolated and pinned to a petri dish with a Sylgard base (Dow Corning). Acute experiments were performed on the left or right pleuroabdominal connectives, which are usually about 4-6 cm in length and provide ample distance for the placement of four suction electrodes. Care was taken to ensure that the nerves of interest were not stretched or damaged during dissection. Spontaneous bidirectional neural activity was present between the ganglia. A high-magnesium, low-calcium saline solution was used in the bath to synaptically isolate the neurons in the ganglia (Nowotny *et al.*, 2003) and suppress the spontaneous activity. The preparation typically allowed for 3-4 hours of experimentation time. All experiments were conducted at room temperature.

4.1.2 Electrophysiological setup

Suction electrodes, commonly used for extracellular recording and stimulation, were used in our experiments. Glass electrodes with tip diameters about the same as that of the nerve fiber (200-500 μm) were pulled and attached to an electrode holder. Typical

electrode impedances for suction electrodes are in the kOhms range. A 400μm tip electrode was found to have an impedance of 30 kOhm. The suction electrodes were positioned along the nerve by micromanipulators (SD Instruments, Narishige). Negative pressure was applied via a syringe mechanism to draw the nerve into the electrode for *en passant* recording and stimulation. Bath solution drawn into the electrode maintained electrical contact and minimized noise in the recordings. Suction electrodes allow for the continuous immersion of the nerve in the saline solution, thus preventing the nerve from drying out. These electrodes also allow localized stimulation and a higher signal to noise ratio for recording. A total of four electrodes were used in our experiments. A schematic of the experimental setup is shown in Figure 2.1. Two suction electrodes were used for the continuous monitoring of the propagation of action potentials (APs) along the nerve. One suction electrode, placed between the recording electrode and the head ganglia, was used to trigger an action potential in the nerve. Another electrode positioned between the two recording electrodes, was used to provide the block-inducing HFAC stimulus. The distance between each of the suction electrodes was 5-10 mm.

A healthy and viable preparation was identified as one in which the activity observed in one electrode was reflected in the other with a delay proportional to the conduction velocity. We used a 10k gain on the amplifier and the bandwidth was limited from 100Hz-1 kHz to filter out the noise that would arise from the high frequency stimulation without affecting the unmyelinated nerve signal. This range of band pass filtering also allowed for recording of traces that did not require any averaging or post-data digital filtering. The input stimuli were transmitted through battery-powered stimulation isolation units (AM Systems-Analog Stimulus Isolator, Model 2200,

Carlsborg, WA) that provided voltage controlled current waveforms. We verified the apparatus response and found that it matches with the advertised specifications, including at frequencies up to 50 kHz (above the specs of 40 kHz).1-3DB attenuation was found at frequencies above 30 kHz. For the range of parameters in our experiments, the output was not limited by the slew rate.

A suprathreshold stimulus pulse of 2V for 0.4ms, converted to current stimulation through the stimulus isolation unit (0.1mA/V), was used to trigger an action potential. Based on previously published work, current-controlled, sinusoidal or biphasic rectangular waveforms in the frequency range of 3 kHz-20 kHz were hypothesized and found to produce the most effective block (Kilgore & Bhadra, 2004). Higher frequencies had not been previously tested due to physical limitations of the instruments. In our study, sinusoidal waveforms in the frequency range of 5-50 kHz, generated by a function generator (Stanford Research Systems, Model DS345) were used to induce block. These waveforms were sent to a similar stimulus isolation unit (1mA/V) to produce current waveforms which were found to be more effective in inducing block than voltage waveforms. This experimental set up was used to investigate the effect of HFAC waveforms in the unmyelinated pleuro-abdominal nerves of *Aplysia*.

4.1.3 Block Thresholds

For each frequency, the amplitude of the waveform was varied until the propagation of action potentials could not be observed. A range of amplitudes was tested to identify the threshold at which block was observed, beginning at lower amplitudes and incrementing the amplitude in discrete steps of 0.1-0.5mA. In our experiments, after the

HFAC stimulus was applied on the nerve, a test pulse was injected at the proximal end near the head ganglia to trigger an action potential in the nerve. If the amplitude of the HFAC waveform was at or above the threshold for inducing conduction block, the action potentials were arrested at the site of injection of the blocking stimulus. The minimum amplitude of the HFAC waveform at which an action potential was not observed in the distal recording electrode, though observed in the proximal recording electrode, was identified as the threshold for inducing block and termed as the 'block threshold'. By monitoring the arrival of action potentials at the distal end, axonal conduction block was detected and the minimum threshold for blocking propagation was determined for a particular frequency. This procedure of identifying block threshold was repeated for different frequencies. The order of frequency tested was randomized to avoid any cumulative effects of fatigue or time. The nerve was allowed to rest for at least a minute between individual trials.

4.1.4 Recovery time

20 animals were used to investigate the minimum amount of time required for normal action potential propagation to recover from conduction block induced by HFAC waveforms of different frequencies. In these 20 animals, block thresholds at different frequencies were first determined as described above. Once the block threshold for a particular frequency was determined, HFAC waveforms with an amplitude greater than the block threshold were applied for randomized durations of 30s, 60s, 90s and 120s. Action potentials were triggered at intervals of 10ms, 20ms, 50ms,100ms, 200ms, 500ms, 1s, 2s and 3s after the HFAC signal was turned off and propagation along the nerve was

monitored to determine recovery time. The electrical activity along the nerve was continuously monitored during this entire procedure. A schematic of the protocol used to measure recovery time is shown in Figure 4.1.

4.2 Results

Normal conduction properties of the nerves were verified and the block thresholds at different frequencies were determined for the *Aplysia* unmyelinated nerve as detailed in chapter 2. All experimental preparations were initially tested for normal conduction properties to determine if action potentials could be repetitively triggered and transmitted along the axon. The conduction properties of the preparation were also constantly tested during the experiment in the absence of the HFAC stimulus to determine whether the preparation was healthy and viable. If a dramatic change in the AP amplitude or shape was observed or if the AP could not be observed in both the recording electrodes or if recovery of the AP did not occur to its pre-block amplitude and shape, the experiment was terminated and the last dataset deleted.

4.2.1 Partial and complete recovery

Experiments were conducted to determine the recovery time for action potential propagation after the blocking stimulus was switched off. Action potentials were triggered at intervals of 100ms, 200ms, 500ms, 1s, 2s and 3s and complete recovery time was identified as the time when the observed compound action potential was similar in shape, size and latency to the compound action potential observed prior to application of the HFAC waveform.

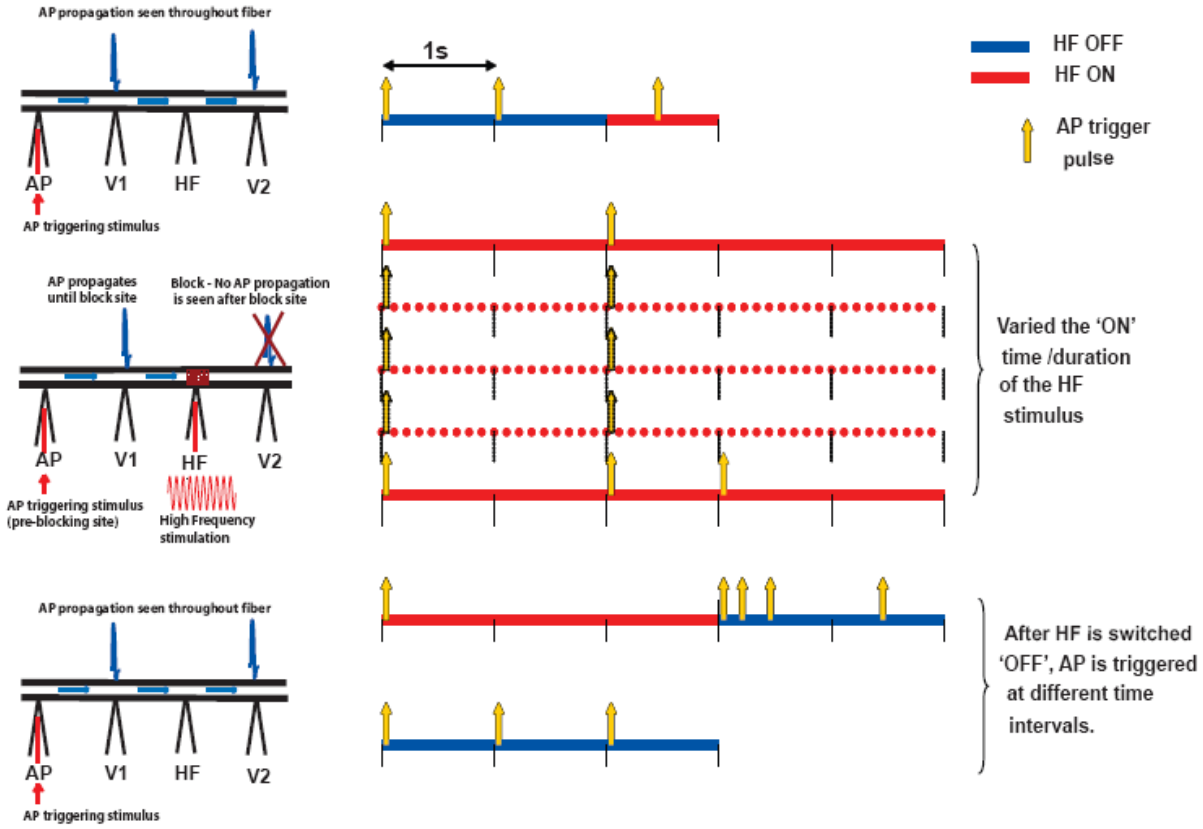

Figure 4.1: The experimental protocol used to determine the recovery time of AP propagation along the nerve after block induction by high frequency stimulation.

Partial recovery of the nerve was observed in certain cases, prior to complete recovery. Partial recovery times were identified as the time when some components of the compound action potential were missing or the amplitude of the compound action potential was smaller than that of the pre-block compound action potential, as depicted in Figure 4.2. Since the nerve connective is made up of axons of varying diameter, it is possible that some of the axons have a longer recovery time compared to others due to the difference in the blocking thresholds of the individual axons. Complete recovery was determined when the shape, latency and amplitude of the compound action potential were comparable to that of the CAP prior to application of the HFAC stimulus and the response in the second recording electrode was similar to the response in the first recording electrode (but with a time delay).

4.2.2 Duration dependence of recovery time

Recovery times were found to be dependent on the duration of application of the HFAC block. In all trials, when the HFAC waveform was applied for a duration of less than 60s, partial recovery occurred within 10-40 ms while complete recovery occurred within 20-225 ms for 67 of 74 trials conducted at different frequencies in the 20 animals. In the remaining 7 trials, complete recovery was seen within 0.5s-3.35s. The pooled data for these 20 animals is plotted in Figure 4.3. Each trial was repeated to verify the recovery time. We can observe that when the extreme outliers (greater than double the median) are removed, as shown in the bottom graph of Figure 4.3, complete recovery always occurred within 225ms with a mean of about 100ms.

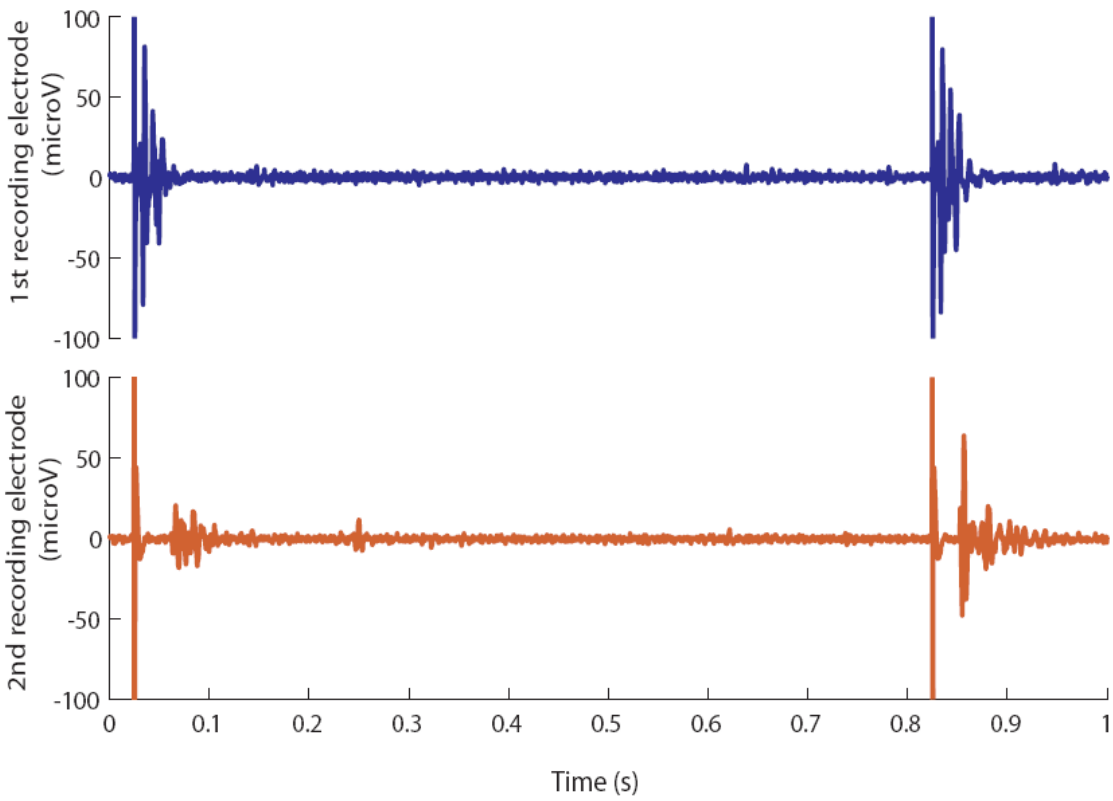

Figure 4.2: Sample trace showing partial and complete recovery of the compound action potential. The top trace shows the CAP recording from the 1st recording electrode between the AP triggering electrode and the block electrode, while the bottom trace depicts the CAP recording in the 2nd recording electrode after the block electrode. Only partial recovery can be seen in the CAP at 0-0.1 s, while complete recovery has occurred in the CAP at 0.8-0.9s.

When the HFAC waveform was applied for a duration longer than 60s, complete recovery occurred within 225ms-5s for 51 of 60 trials, while in the remaining 9 trials complete recovery occurred almost instantaneously within 30ms-150ms. The average recovery time was 1.137s when the HFAC waveform was applied for greater than 60s. Figure 4.4 represents the pooled recovery times at different frequencies when the HFAC waveform was applied for less than 60 seconds (Figure 4.4A) and greater than 60 s (Figure 4.4 B). Figure 4.5A shows a box plot comparison of the data for less than 60 s and greater than 60 seconds and Figure 4.5 B shows the average recovery times.

Statistical analysis of the pooled data reveal that a significant difference in the recovery time exists depending on the duration of application of the HFAC stimulus ($p<0.0001$) as shown in Table 4.1. However, recovery time, was found to be independent of the frequency of HFAC waveform ($p>0.1$). The same number of data points for all frequencies in the range of 10-50 kHz could not be obtained, making statistical analysis of the dependence of recovery time on the frequency of the HFAC waveform difficult. However, as observed in Figure 4.6 and 4.7, we do note that at higher frequencies duration of application of HFAC waveform significantly affected the recovery time. Multiple trials for different durations of application of a 30 kHz waveform were conducted to determine the average recovery time as shown in Figure 4.6. Figure 4.7 represents the recovery time data from single trials at different frequencies and different durations of application of the HFAC waveform. We can observe that at higher frequencies, recovery time significantly increases with the duration of application of the HFAC waveform.

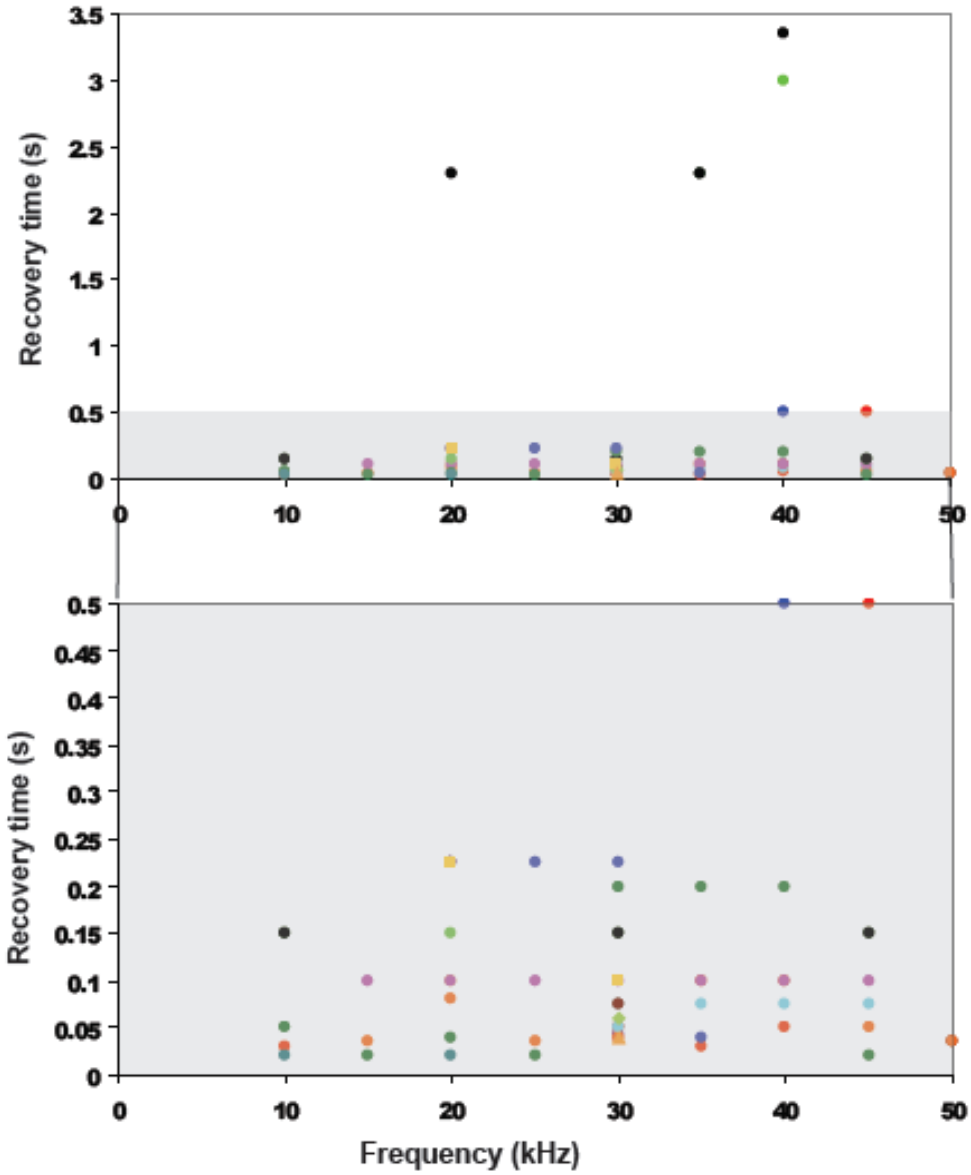

Figure 4.3: Recovery for HFAC application for less than 60 s. In the bottom graph, removing the outliers (possibly due to improper stimulation), we observe that recovery time was always less than 250 ms.

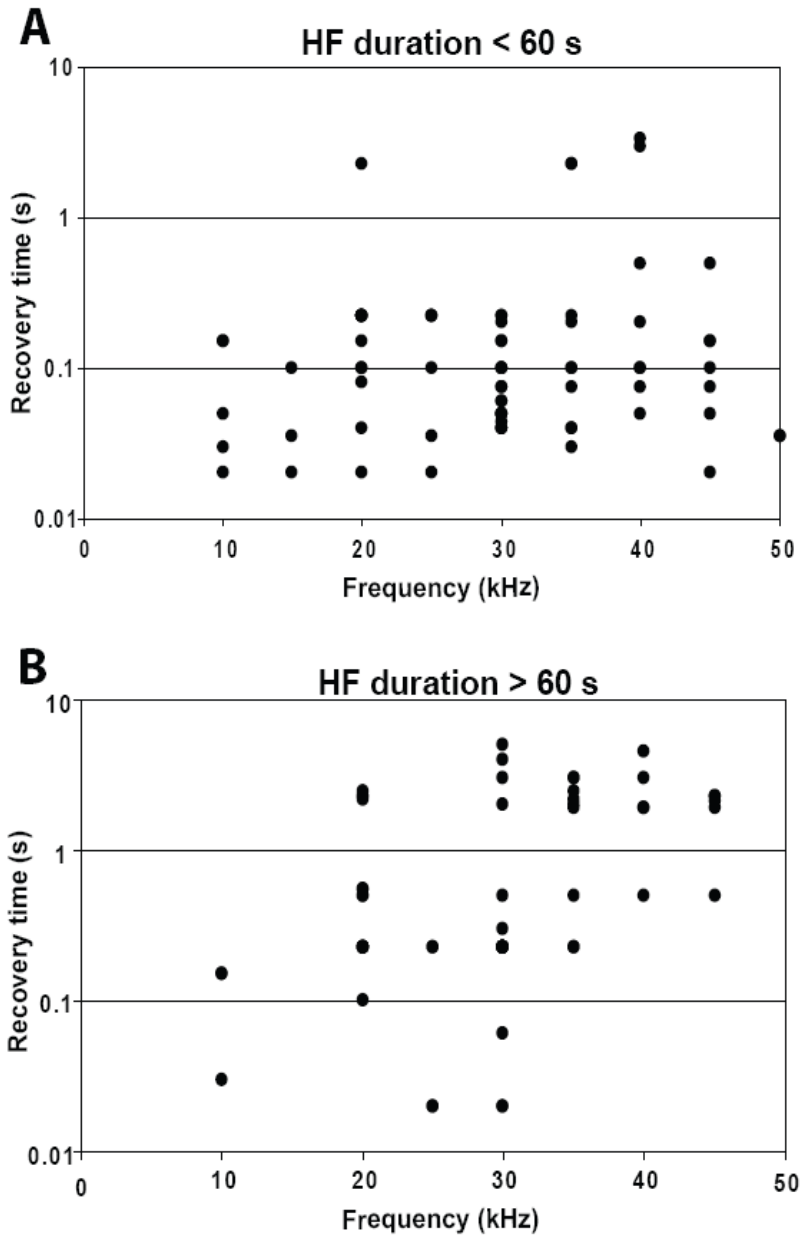

Figure 4.4: Recovery time for different frequencies. Recovery times are represented on a logarithmic scale. **A:** Recovery time for different frequencies when HFAC waveform is applied for less than 60s. **B:** Recovery time for different frequencies when the HFAC waveform is applied for greater than 60s.

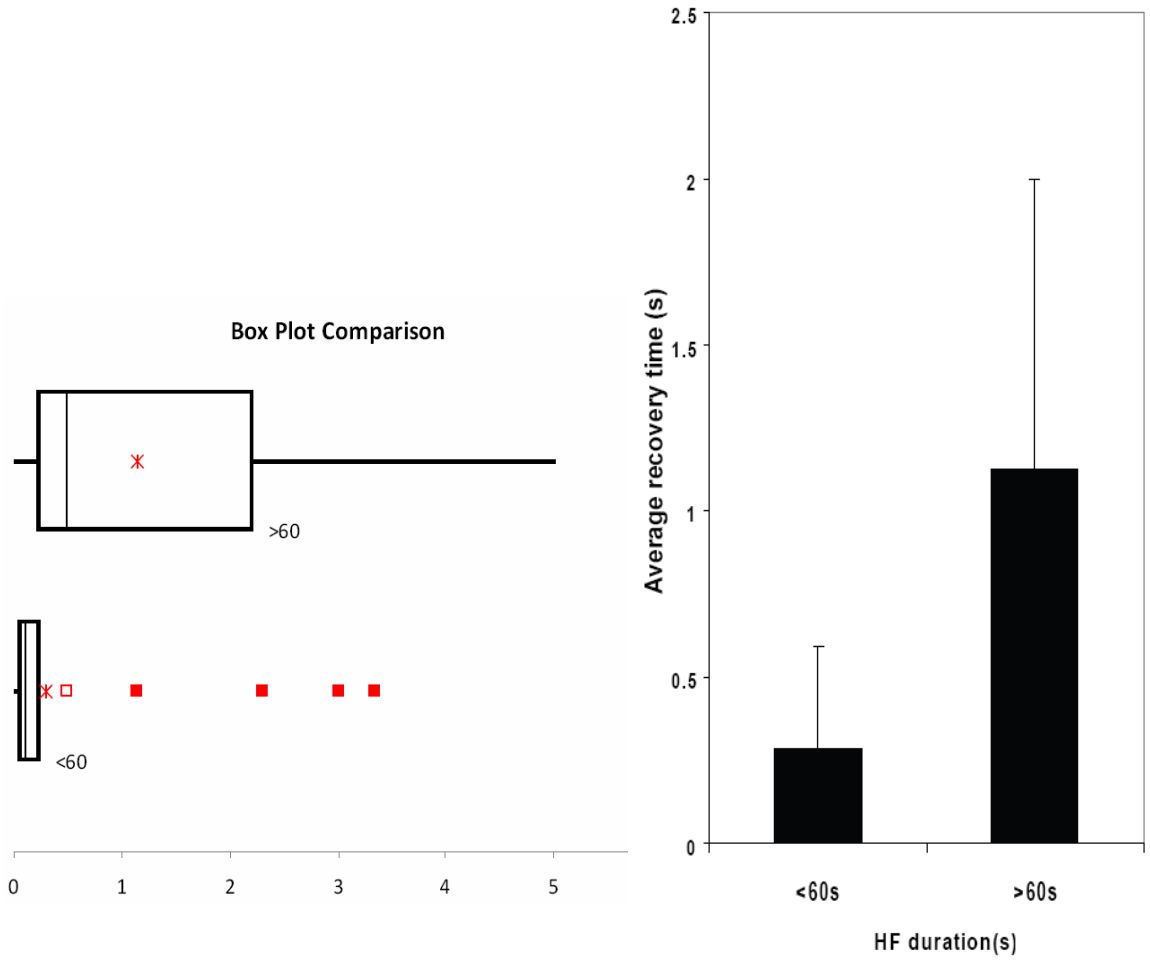

Figure 4.5: A: Box plot comparisons of the recovery time for different durations of application of the HFAC waveform. The red filled squares indicate the extreme outliers while the red hollow squares show mild outlier points. The mean of the data is shown by an asterisk (*) sign. The left and right edges of the box correspond to the interquartile range while the vertical line in the box indicates the median of the data. B: Average recovery time when the HFAC waveform is applied for less than and greater than 60s.

Table 4.1: ANOVA analysis of recovery time data for different durations of application of the HFAC waveform.

ANOVA Summary	
Total Sample Size	133
Grand Mean	0.6720
Pooled Std Dev	0.9834
Pooled Variance	0.9670
Number of Samples	2
Confidence Level	95.00%

ANOVA Sample Stats	<60 Data Set #2	>60 Data Set #2
Sample Size	74	59
Sample Mean	0.3015	1.137
Sample Std Dev	0.6647	1.276
Sample Variance	0.4418	1.628
Pooling Weight	0.5573	0.4427

OneWay ANOVA Table	Sum of Squares	Degrees of Freedom	Mean Squares	F-Ratio	p-Value
Between Variation	22.9047	1	22.9047	23.6862	< 0.0001
Within Variation	126.6774	131	0.9670		
Total Variation	149.5821	132			

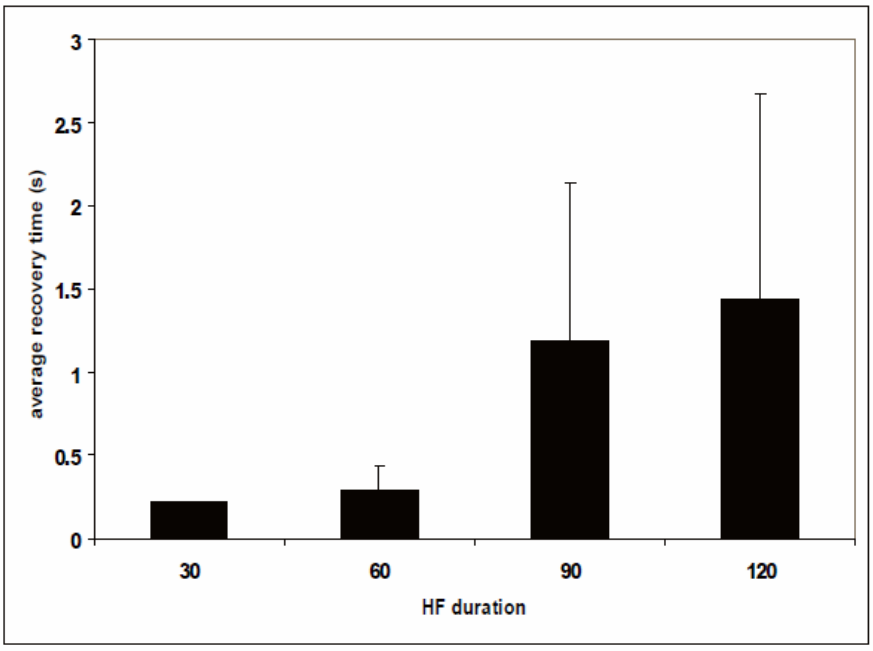

Figure 4.6: Average recovery time of 3 trials for different durations of application (30s, 60s, 90s, 120s) of a 30kHz HFAC waveform. For durations greater than 60s, recovery time was significantly greater.

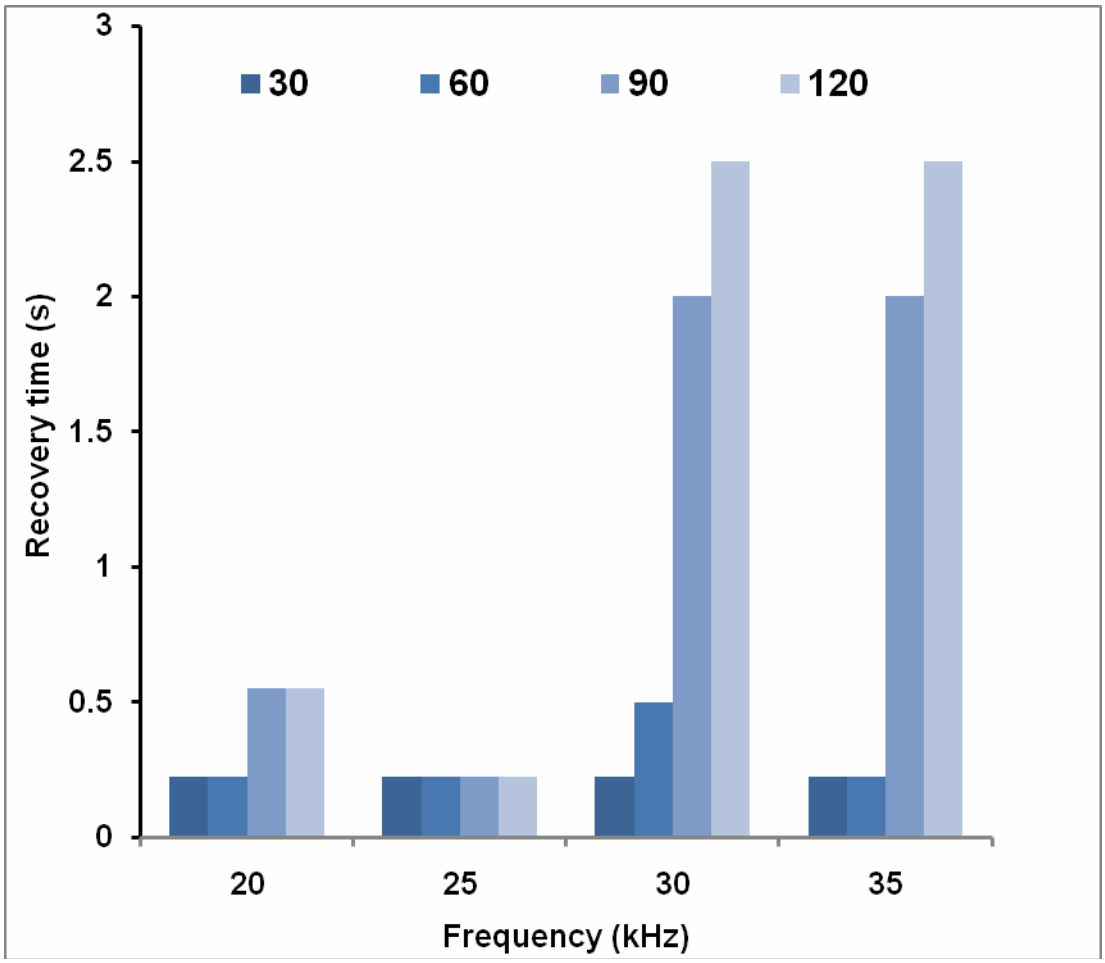

Figure 4.7: Single trial recovery times during application of different frequencies of the HFAC waveform for different durations.For frequencies above 30 kHz, recovery time is significantly greater when HFAC is applied for a duration greater than 60s.

4.3 Discussion

Although no previous study has actually measured the exact time for recovery from nerve block, previously published animal experiments conducted on amphibians and mammalian nerves have shown that normal conduction of action potentials or muscle contraction returns within 1s after the termination of the high frequency blocking stimulus (Rosenblueth & Reboul, 1939; Kilgore & Bhadra, 2004; Williamson & Andrews, 2005). To date, the mechanisms of block induction using HFAC waveforms have only been evaluated through computational modeling studies. In some studies, the inactivation of the sodium channel were found to be responsible for block induction (Kilgore & Bhadra, 2004; Bhadra *et al.*, 2007), while in others the activation of the potassium channels (Tai *et al.*, 2005; Tai *et al.*, 2005) has been credited to block conduction through the peripheral nerves using HFAC waveforms. Simulation studies investigating the mechanisms of block induction have never looked at the effect of duration on the physiological mechanisms of block induction. This study demonstrated that recovery time is dependent on the duration of application of the high frequency stimulus. No other study, experimental or simulation, reported in literature has quantified the recovery time after block induction and the duration effects of the application of the high frequency waveforms.

In our experiments, the recovery time in the unmyelinated nerves of the sea-slug *Aplysia* , was found to be in the range of 20-225 ms for different frequencies, when the HFAC waveform was applied for less than 60s. This indicated that an ion channel gating mechanisms could potentially be responsible for block induction. However, longer recovery times were observed when the duration of application of the HFAC waveform

was above 60s. This bimodal distribution of the recovery times and the non-monotonic response of the block threshold with respect to frequency cannot be explained by a simple ionic mechanism, suggesting that other secondary mechanisms might also be involved in block

Electrical currents have been used to block conduction for various other electrophysiological applications. It should be noted that the term 'high-frequency block' has been used in other fields, like the Deep Brain Stimulation (DBS) field for blocking conduction through the central nervous system fibers (Durand & Bikson, 2001; Jensen & Durand, 2007), and in invertebrate neurophysiology for differential conduction along bifurcating axons (Grossman *et al.*, 1979; Smith, 1983). Modulation of the extracellular potassium concentration has been shown to cause the depolarization block in these studies. (Grossman *et al.*, 1979; Durand & Bikson, 2001). The recovery time after cessation of the blocking stimulus, in these cases, was in the order of several seconds to several minutes. Though these stimuli have been termed 'high-frequency' in literature, the mechanism involved in inducing conduction block in these fields probably differs from the local block observed in peripheral nerves where the frequency of stimulation is typically above 3 kHz and recovery time is faster.

Nonetheless, as shown in our experiments, application of HFAC waveforms for longer durations (above a minute) increased the average recovery time to the order of several seconds, indicating that some additional mechanisms , analogous to those seen DBS and invertebrate neurophysiology field, might be involved in block induction in peripheral nerves. Computer simulations demonstrating block induction via HFAC waveforms have shown that during application of the HFAC waveforms, the membrane

voltage increases dramatically beyond the physiological range and most models have not been validated for those regimes. The drastic change in the membrane voltage during application of the HFAC waveform could lead to imbalances in the Na+-K+ pumps, which could lead to an accumulation of K+ in the extracellular environment and impede action potential propagation. The models used in computational models of HFAC block induction, cannot account for these extracellular changes due to which previous studies have ignored the effect of duration of application of HFAC waveforms on the nerve. Monitoring the changes in the extracellular environment during application of the HFAC waveforms and characterizing the recovery times after block induction in different fiber type populations may enable us to gain an understanding of the physiological mechanisms of block induction using HFAC waveforms.

Our experimental setup serves as an amenable preparation for investigating the ionic mechanisms of high frequency induced conduction block and future studies are aimed at identifying these mechanisms. Our technique also provides the advantage of the directly monitoring neural activity to determine the recovery of the different components of the compound action potential at a resolution not possible with force transducers measurements of muscle force which is conventionally used in high frequency block experiments. In this study we used an unmyelinated nerve preparation to identify recovery times. Future studies are aimed at investigating the recovery times of different components of the compound action potential in a mixed nerve to gain a better understanding of the effect of different nerve properties on block induction during application of HFAC waveforms.

4.4 Conclusion

This study investigated the recovery time after block induction to understand the physiological mechanisms preventing action potential conduction. Most simulation studies have hypothesized an ion channel mechanism, but out experiments reveal that other secondary mechanisms are also involved. We found that conduction block is dependent on the duration of application of the HFAC waveform and even though initially an ionic mechanism may be responsible for block induction, secondary mechanisms prevent instantaneous recovery after removal of the HFAC waveform. No other study has previously looked into the effect of duration of application of the HFAC waveform. Our experimental techniques involving direct measurements of neural activity via compound action potential measurement provide a convenient method for future biological experiments related to understanding the physiological mechanisms of block induction. Our work also highlights the need for modifying existing computational models and developing extensive models that can account for changes in the extracellular space and capacitance, during application of the HFAC waveforms.

CHAPTER 5

CONCLUSIONS & FUTURE DIRECTIONS

The human nervous system and its complex communication mechanisms have mystified scientists for ages. Accurate transmission of information through the nervous system via electrical and chemical signals is critical for the proper functioning of the human body Even though various chemical, electrical and mechanical techniques have been developed to observe behavior, the underlying mechanisms causing those behaviors are often unknown or are difficult to characterize. Electrophysiological techniques have been frequently used to gain insight into the signals and communication pathways between neurons. In this dissertation I have demonstrated that studying the neural activity of the nerve by observing extracellularly recorded compound action potentials can be a useful technique for understanding the behavior of the nerve and specifically of individual fiber types during application of HFAC waveforms.

A major challenge in designing effective neural prosthetic systems is stimulating specific fibers analogous to the physiological recruitment order without affecting the extraneous nerves. Reversible conduction block using high frequency alternating current (HFAC) stimulation has been shown to be completely effective, repeatable and quickly reversible in various amphibian and mammalian animal models (Tanner, 1962; Kilgore & Bhadra, 2004; Bhadra & Kilgore, 2005; Tai *et al.*, 2005; Williamson & Andrews, 2005; Bhadra *et al.*, 2006). Voltage controlled waveforms from 1-30 kHz induced a complete and reversible motor block at all frequencies. The block threshold defined was found to increase linearly with frequency in frog, rat and cat nerves.

The experimental conditions used to induce block varied considerably in these investigations producing inconsistencies in the hypothesized ideal frequency for block induction. Computer simulations coupled with *in-vivo* studies have failed to identify the ideal frequency range or the ionic mechanism of block induction, primarily because the models used were not developed for the nerves and frequencies being studied. Also, only the effect on motor nerve fibers has been traditionally studied while the effects on the smaller diameter, unmyelinated fibers have been ignored. Understanding the effect of HFAC waveforms on whole nerves and specifically on individual fiber type populations is essential if HFAC waveforms are eventually to be used in clinical applications. In this dissertation we characterized the neural activity of individual fiber type populations in whole nerves during application of HFAC waveforms and showed that HFAC stimulation can potentially be used to exploit innate attributes of peripheral nerves for applications related to pain management and neural prostheses.

5.1 Effect of HFAC waveforms on unmyelinated nerves

In Chapter 2, we characterized the effect of applying HFAC waveforms on purely unmyelinated nerves and found a unique behavior never previously reported in literature. This was the first study to investigate the effect of HFAC waveforms in homogenous nerves and in unmyelinated nerves even though models based on an unmyelinated nerve (HH model) have been widely used for understanding the mechanism of block induction by HFAC waveforms. Our experiments revealed that a reversible, local block can be induced in unmyelinated nerves but unlike published studies on myelinated nerves, these nerves demonstrated a non-monotonic block threshold relationship with frequency. This behavior has never before been reported in literature and contradicts findings from

various computational studies based on the Hodgkin-Huxley model. Incorporating a frequency-dependent capacitance (based on experimental data from squid axons), into a HH model caused the threshold to frequency behavior to deviate at higher frequencies away from the linear trend observed in a normal HH model. Though this FDC model could not completely replicate the results from *Aplysia* nerves, it provided evidence that current models were insufficient to explain neuronal behavior during application of frequencies in the kilohertz range. Significant modifications to existing models will have to be made before they can be used to investigate the mechanisms of block induction.

5.2 Effect of HFAC waveforms on mixed nerves

In order to validate our results from the unmyelinated nerves of *Aplysia* we repeated our experiments on the frog sciatic nerve, composed of both myelinated and unmyelinated nerve fibers, as detailed in Chapter 3. Examining the larger diameter myelinated or A-fiber response and the smaller diameter unmyelinated or C-fiber response by extracting the corresponding components of the compound action potential, revealed that the A-fibers had a linearly increasing relationship between block threshold and frequency of the waveform, as previously reported in literature. But contrary to simulation work on unmyelinated nerves, the C-fibers demonstrated a non-monotonic relationship of block threshold to frequency analogous to that seen in the invertebrate nerve preparation. This study not only established the unique behavior of unmyelinated nerves to HFAC waveforms at higher frequencies, but also demonstrated the potential of using HFAC waveforms for selective stimulation, by selectively blocking conduction through specific fiber type populations in mixed nerves. Our results revealed that two distinct regions exist in the HFAC space, where one type of nerve fiber can be selectively blocked over another

type of nerve fiber. We demonstrated that only the A-fibers can be stimulated while keeping the C-fibers blocked and vice-versa. This method of selective stimulation can be extremely useful for various neurophysiological and neuroprosthetic applications.

5.3 Effect of duration of application of HFAC waveforms

In Chapter 4, we again used the unmyelinated *Aplysia* nerve preparation to explore recovery time after block induction using HFAC waveforms. This is the first investigation to utilize data from animal nerves to understand plausible mechanisms of block induction using HFAC waveforms. Estimating the recovery time after the HFAC waveform was switched off provided insight into the physiological mechanisms of block. The recovery times were found to be time be dependent on the duration of application of the HFAC waveform. These results show that a simple ion-channel gating mechanism, as described by several previous computational studies, cannot explain the phenomena of block induction using HFAC waveforms in entirety. Significant modifications to existing models along with additional computational and biological studies are needed to gain a complete understanding of the physiological mechanisms of block induction via HFAC waveforms.

5.4 Future work

Besides contributing to the scientific understanding of the effect of HFAC waveforms on specific fiber type populations, this body of work has also laid the foundation for several future studies that would aid in the development of a clinically implementable technique. We know that experimental and computational studies are complementary methodologies that provide a thorough understanding of various

scientific phenomena. Modeling studies provide us with the flexibility to isolate important parameters while experimental data from animals are essential to give us a realistic view of physiological behavior and validate the modeling results. Though this dissertation work focused mainly on animal experiments, many computational modeling studies are being concurrently carried out in our lab and at other labs to gain insight into the mechanisms of block induction using HFAC waveforms. Several interesting questions related to HFAC block induction are yet unanswered and the following studies outline some methods of addressing them.

5.4.1 Development of physiologically accurate computational models to investigate the mechanism of HFAC induced conduction block.

Qualitative differences exist between myelinated and unmyelinated nerve fibers which can account for the differences observed in the response of different nerve fibers to HFAC stimulation (Kilgore & Bhadra, 2004; Bhadra & Kilgore, 2005; Tai *et al.*, 2005; Williamson & Andrews, 2005; Joseph & Butera, 2009). Membrane models like the Hodgkin-Huxley model (Hodgkin & Huxley, 1952) provide an easy understanding of the physiological mechanism and membrane behavior during electrical excitation of the nerve. Prior modeling studies in the field have found that HFAC waveforms cause repetitive stimulation and a local block of the transmission of action potentials in axon simulations (Tai *et al.*, 2005; Tai *et al.*, 2005; Williamson & Andrews, 2005; Zhang *et al.*, 2006; Zhang *et al.*, 2006; Bhadra *et al.*, 2007). These studies, however, have not been able to provide a conclusive mechanism for the induction of block.

A group from the University of Pittsburgh (Tai *et al.*, 2005; Tai *et al.*, 2005; Zhang *et al.*, 2006; Zhang *et al.*, 2006) worked with different models including the

Hodgkin-Huxley model (Hodgkin & Huxley, 1952) and the Frankenhaeuser-Huxley model (Frankenhaeuser & Huxley, 1964) to understand the physiological mechanisms underlying HFAC induced block. They concluded that the accumulation of potassium due to the sustained activation of potassium channels causes a shift in the average membrane potential preventing the propagation of action potentials. Another group from Case Western Reserve University (Kilgore & Bhadra, 2004; Bhadra *et al.*, 2007), modeled the nerve using the McIntyre and Grill myelinated nerve model in the NEURON simulation environment (Hines & Carnevale, 1997). They found that block is caused by the failure of the inactivating sodium channels to close causing a depolarizing shift in the average membrane potential that prevents conduction. Though most of these models have claimed to have found a mechanism that induces block, they are simply model based observations and causality of the supposed mechanisms was not shown in any of the models.

Our experimental results obtained from the unmyelinated fibers of *Aplysia* are the closest work that are similar to the Hodgkin-Huxley model (based on an unmyelinated nerve) yet show a different behavioral relationship for block threshold with frequency compared to the simulation studies. This difference in behavior could be because the Hodgkin-Huxley model assumes that membrane capacitance is constant at all frequencies while experimental measurements of membrane capacitance show that it actually decreases for frequencies above 1kHz (Haydon & Urban, 1985). Modifying the Hodgkin-Huxley model by incorporating a frequency-dependent capacitance (FDC) altered the linear threshold behavior of the classical HH model, but did not completely account for the biologically observed behavior (Haeffele & Butera, 2007). We hypothesize that since the HH model has not been tested for frequencies from 5-50 kHz,

and since changes in the extracellular factors are not accounted for in the classical HH model, other extracellular factors might contribute to changes in the conduction properties of the axon at higher frequencies causing the experimentally observed non-monotonic behavior. Future work in our lab aims at further modifying the FDC model to explain the experimentally observed behavior and then investigate the ionic mechanisms and gating variables affected when HFAC waveforms are applied.

Recent studies have highlighted the effect of glial cells on neuronal signaling (Coles & Abbott, 1996; Inoue *et al.*, 2002) via glutamate, that increases the K^+ channel activity (Coles & Abbott, 1996; Kane *et al.*, 2000; Inoue *et al.*, 2002). The effect of the extracellular environment and the surrounding glial cells on neuronal activity during HFAC application has not been previously studied. Accumulation of ions in the extracellular environment has often been attributed to causing conduction block. This effect has not been simulated in existing models studying HFAC mechanisms. Incorporating features of the extracellular environment, including Na^+-K^+ pumps, into the model may help explain the trend seen in unmyelinated fibers. Modeling nerve conduction block will enable us to investigate the physiological mechanism that induces HFAC block and ultimately identify optimum conditions for clinical implementation of the technique.

5.4.2 Development of biological experiments to investigate characteristic features of specific fiber types to HFAC induced conduction block.

This dissertation work employed some characteristic animal preparations that were amenable for electrophysiological investigation. Besides revealing unique and significant properties of specific fiber type populations during HFAC stimulation, this

work established the use of CAP recordings as a reliable method to monitor neural activity and determine block status during application of HFAC waveforms. These extracellular electrophysiological techniques can be used with other animal nerve preparations to augment our understanding of the phenomena. Some animal experiments that could help answer key questions are detailed below.

Intraaxonal impalements of nerve axons from various animals can be used to understand the effect on ion channels during application of HFAC waveforms. The giant axon of the squid would be an ideal preparation for these studies. Unfortunately, the seasonal and geographical availability of the squid axon make it inconvenient for use in our lab. Cultured single axons of the *Lymnaea* could serve as amenable preparations for testing the ionic mechanisms of block induction via HFAC waveforms. Preliminary results show that structurally and functionally viable axons of *Lymnaea* can be obtained in culture even when the axon is severed from the cell soma. *Lymnaea* neurons can be successfully cultured to obtain electrophysiologically active axons with lengths greater than 1 cm (Meems, 2005). The procedure is described in Appendix A. The cultured axons will enable intracellular measurements of the membrane potential at any point along the axon as shown in Figure 5.1 and should enable us to characterize the effect of high frequency AC stimulation on an unmyelinated nerve. The effect of high frequency stimulation on an individual axon has not been previously studied, though similar modeling studies exist. Hence, application of HFAC waveforms on the cultured *Lymnaea* axon preparation should provide us with a better understanding of the phenomena. This preparation should also enable us to investigate the ionic mechanisms of block induction using intracellular recordings along different points of the axon.

Various pharmacological methods including using specific channel blockers and ion channel toxins are commonly used to test the role of specific ions (Catterall *et al.*, 2007) and have been suggested as plausible methods for determining the physiological mechanisms of block induction using HFAC waveforms. However, changing the concentration of the local environment around the block site or selectively blocking specific ion channels may affect the conduction of action potentials along the axon which in turn can affect the block thresholds and other characteristic features of HFAC induced block, making it difficult to conclusively demonstrate causality between a mechanism and the induction of HFAC block. If stable electrophysiological recordings can be obtained from single axons via intra-axonal impalements, then pharmacological agents might be able to provide some insight into the ionic mechanisms of conduction block and would be an interesting area for future work.

This dissertation work has described differences in block thresholds between the larger diameter myelinated A-fibers and the smaller diameter unmyelinated C-fibers, at different frequencies. One interesting future line of research would be to specifically investigate whether the observed non-monotonic behavior is function of axon diameter or of myelination. Additional experiments using longer amphibian or mammalian (rat/rabbit) nerves with higher averaging and data sampling rates would enable detailed observations of the different fiber type populations in mixed nerves. Specifically, characterizing the threshold behavior of the A-delta and B-fibers at higher frequencies might explain whether the non-monotonic threshold behavior observed in the unmyelinated *Aplysia* nerves and C-fibers is a property of smaller axon size or absence of myelination.

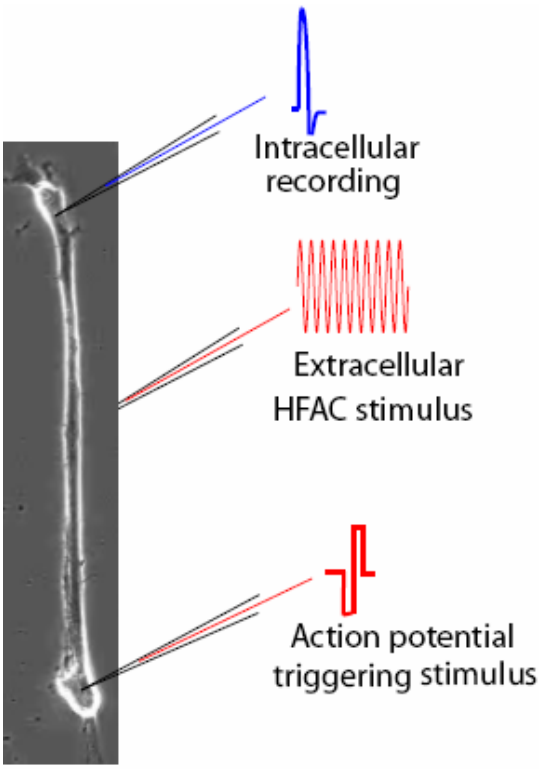

Figure 5.1: Intraaxonal impalement of the culture Lymnaea axon can aid in investigations related to mechanism of block induction using HFAC waveforms.

The earthworm has been found to have giant nerve fibers with diameters in the range of about 90-160 μm in diameter (Gunther, 1976; Roberts, 1986). These nerves have also been found to be myelinated with average conduction velocities of 30-45 m/s (Gunther, 1976; Drewes *et al.*, 1978; Roberts, 1986). Repeating our experiments in the myelinated nerves of earthworms may provide insight into whether the non-monotonicity can be attributed to myelination. The earthworm giant axon would also be a convenient preparation to investigate intracellular neural activity for myelinated nerves during application of HFAC waveforms, analogous to the proposed studies on the unmyelinated *Lymnaea* axon. Comparing the neural activity of the earthworm giant axon and *Lymnaea* axon should provide insight into the intracellular ionic changes in different fiber types during application of HFAC waveforms.

5.5 Conclusion

High frequency waveforms in the range of 5-50 kHz, used for reversible conduction block have numerous applications in the treatment of unwanted peripheral neural activity. Arresting the propagation of superfluous signals will be useful in alleviating disease symptoms such as blocking chronic peripheral pain and stopping pathological hyperactivity of neuronal signals. Varying the frequency of stimulation may allow the selective blocking and unblocking of certain fibers of varying diameters and provide more control on the type of stimulation given to restore functionality, and thus improve the current state of extracellular stimulation in neural prostheses. Selective blocking of specific fibers would also enable the blocking of specific peripheral paths in multiple feedback loops circuits and provide a useful neurophysiological tool for

understanding the behavior of various neural pathways. This dissertation work has shown that dissimilar fiber type populations have different behaviors to HFAC waveforms which can be exploited to selectively stimulate specific fibers. In particular, we found that unmyelinated nerves demonstrate a non-monotonic threshold behavior that can be potentially useful for applications related to pain management. Another finding of this work is that the mechanism of block induction is dependent on duration of application of the stimulus which was never previously studied. The bimodal distribution in recovery time indicates that a simple ion channel gating mechanism, as proposed in current literature, cannot sufficiently explain the phenomena of block induction via HFAC waveforms. Computational and biological experimental studies can be used collectively to decipher complex phenomena. Future studies in our lab and as proposed in this dissertation are aimed at using these techniques to gain a complete understanding of the phenomena of block induction using HFAC waveforms. This dissertation work has set the stage for future computational and biological investigations into the application of HFAC waveforms to develop a clinically feasible technique for selective stimulation and selective conduction block in peripheral nerves.

APPENDIX A

CULTURING LYMNAEA AXONS TO STUDY

MECHANISMS OF HFAC INDUCED CONDUCTION BLOCK

Conventional cell culture techniques make neurons more accessible and provide a method for directly studying the conduction properties of individual cells and isolated nerve fibers. *Lymnaea stagnalis* has proven to be a useful model for studies related to synaptic and axonal electrophysiology because functionally well-defined neurons can be identified in vivo and their synapses reconstructed in cell culture (Ridgway *et al.*, 1991). The ability of *Lymnaea* neurons to regenerate their axonal and synaptic connections makes it advantageous as it enables the direct measurement of intracellular features at a resolution not possible in other species. Another advantage of the *Lymnaea* system is that their axons can function both structurally and functionally for some time in the absence of their cell body, thus allowing us to explore the role of various extrasomal compartments in different phenomena (Meems *et al.*, 2003).

We are interested in the conduction blocking effect of HFAC waveforms. Culturing individual nerve axons will enable us to develop a stable preparation to electrophysiologically investigate the conduction properties of an individual unmyelinated axon under high frequency stimulation and use the corresponding data to modify the HH model. The procedure involves 4 main steps: (1) Isolating the central ganglionic ring from the snail, (2) isolating individual cells from the brain, (3) culturing

individual cells and then (4) obtaining electrophysiological recording from the cultured axons. These are depicted in Figure 5.1.

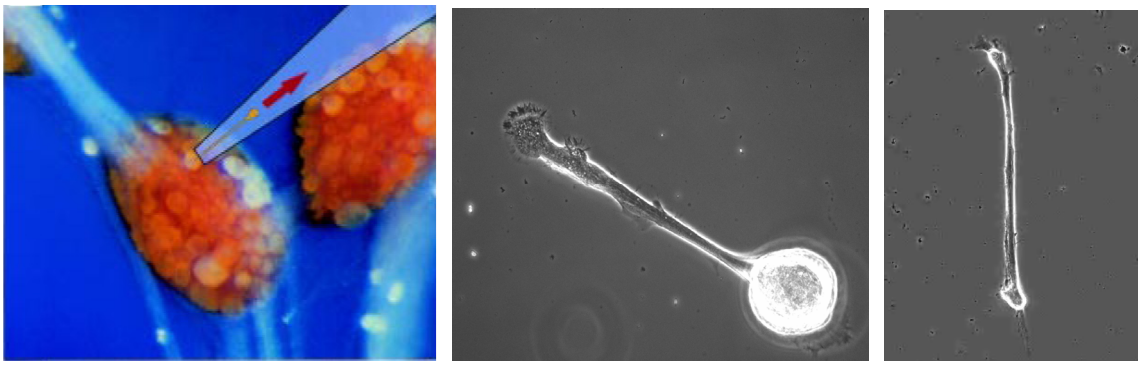

Figure A.1: (a) Isolating a single cell from the *Lymnaea* ganglion (Syed *et al.*, 1999) (b) a cultured *Lymnaea* neuron (c) a *Lymnaea* axon severed from the soma (40X magnification) . Data obtained from work done at Dr. Syed's lab, University of Calgary.

Neuronal activity along the cultured axon can be monitored using conventional intracellular recording techniques. After obtaining stable cultured axons, we will then determine whether complete nerve conduction block can be consistently and repeatedly obtained in the unmyelinated axon using HFAC waveforms. The experimental setup will be similar to that used for the *Aplysia* nerve fibers. Once reversible block can be consistently obtained, we will determine the block thresholds for the nerve for frequencies ranging from 5-50 kHz and compare them with the results obtained in the Aplysia nerves. This study should shed some light on the role of the extracellular components on the non-monotonic threshold behavior observed in the unmyelinated nerve fibers. This preparation can also be used for future studies related to investigating the ionic mechanisms of block induction using HFAC waveforms.

REFERENCES

Abbruzzese G. **2002.** The medical management of spasticity. *European Journal of Neurology*, **9 Suppl 1**:30-34; discussion 53-61.

Ackerman D M. **2010.** Reduction of the onset response in high frequency nerve block. *Department of Biomedical Engineering, Case Western Reserve University*, **PhD**.

Ackermann D M, Jr., Foldes E L, Bhadra N and Kilgore K L. **2009.** Effect of bipolar cuff electrode design on block thresholds in high-frequency electrical neural conduction block. *IEEE Transactions on Neural Systems and Rehabilitation Engineering*, **17**:469-477.

Ackermann D M, Jr., Foldes E L, Bhadra N and Kilgore K L. **2010.** Conduction block of peripheral nerve using high-frequency alternating currents delivered through an intrafascicular electrode. *Muscle & Nerve*, **41**:117-119.

Ashburn M A and Staats P S. **1999.** Management of chronic pain. *Lancet*, **353**:1865-1869.

Baratta R, Ichie M, Hwang S K and Solomonow M. **1989.** Orderly stimulation of skeletal muscle motor units with tripolar nerve cuff electrode. *IEEE Transactions on Biomedical Engineering*, **36**:836-843.

Beard S, Hunn A and Wight J. **2003.** Treatments for spasticity and pain in multiple sclerosis: a systematic review. *Health Technol Assess*, **7**:iii, ix-x, 1-111.

Bhadra N, Bhadra N, Kilgore K and Gustafson K J. **2006.** High frequency electrical conduction block of the pudendal nerve. *Journal of Neural Engineering*, **3**:180-187.

Bhadra N, Foldes E L, Ackermann D and Kilgore K L. **2009.** Reduction of the onset response in high frequency nerve block with amplitude ramps from non-zero amplitudes. *Conf Proc IEEE Eng Med Biol Soc*, **2009**:650-653.

Bhadra N and Kilgore K L. **2004.** Direct current electrical conduction block of peripheral nerve. *IEEE Transactions on Neural Systems and Rehabilitation Engineering*, **12**:313-324.

Bhadra N and Kilgore K L. **2005.** High-frequency electrical conduction block of mammalian peripheral motor nerve. *Muscle & Nerve*, **32**:782-790.

Bhadra N, Lahowetz E A, Foldes S T and Kilgore K L. **2007.** Simulation of high-frequency sinusoidal electrical block of mammalian myelinated axons. *Journal of Computational Neuroscience*, **22**:313-326.

Binstock L and Goldman L. **1967.** Giant Axon of Myxicola - Some Membrane Properties as Observed under Voltage Clamp. *Science*, **158**:1467-&.

Binstock L and Goldman L. **1969.** Current- and Voltage-Clamped Studies on Myxicola Giant Axons - Effect of Tetrodotoxin. *Journal of General Physiology*, **54**:730-&.

Blair E A and Erlanger J. **1933.** A Comparison of the characteristics of axons through their individual electrical responses *American Journal of Physiology*, **106**:524-564.

Bowman B R and McNeal D R. **1986.** Response of Single Alpha-Motoneurons to High-Frequency Pulse Trains - Firing Behavior and Conduction Block Phenomenon. *Applied Neurophysiology*, **49**:121-138.

Bullock T H and Turner R S. **1950.** Events associated with conduction failure in nerve fibers. *J Cell Physiol*, **36**:59-81.

Cattell M and Gerard R W. **1935.** The inhibitory effect of high-frequency stimulation and the excitation state of nerve. *Journal of Physiology*, **83**:407-415.

Catterall W A, Cestele S, Yarov-Yarovoy V, Yu F H, Konoki K and Scheuer T. **2007.** Voltage-gated ion channels and gating modifier toxins. *Toxicon*, **49**:124-141.

Chen Z L, Yu W M and Strickland S. **2007.** Peripheral regeneration. *Annual Review of Neuroscience*, **30**:209-233.

Coles J A and Abbott N J. **1996.** Signalling from neurones to glial cells in invertebrates. *Trends in Neurosciences*, **19**:358-362.

Drewes C D, Landa K B and McFall J L. **1978.** Giant nerve fibre activity in intact, freely moving earthworms. *Journal of Experimental Biology*, **72**:217-227.

Durand D M and Bikson M. **2001.** Suppression and control of epileptiform activity by electrical stimulation: A review. *Proceedings of the IEEE*, **89**:1065-1082.

Flett P J. **2003.** Rehabilitation of spasticity and related problems in childhood cerebral palsy. *Journal of Pediatrics and Child Health*, **39**:6-14.

Foldes E L, Ackermann D, Bhadra N and Kilgore K L. **2009.** Counted cycles method to quantify the onset response in high-frequency peripheral nerve block. *Conference Proceedings of IEEE Engineering in Medicine and Biology Society*, **2009**:614-617.

Frankenhaeuser B and Huxley A F. **1964.** Action Potential in Myelinated Nerve Fibre of Xenopus Laevis as Computed on Basis of Voltage Clamp Data. *Journal of Physiology-London*, **171**:302-&.

Franz D N and Iggo A. **1968.** Conduction Failure in Myelinated and Non-Myelinated Axons at Low Temperatures. *Journal of Physiology-London*, **199**:319-&.

Gaunt R A and Prochazka A. **2009.** Transcutaneously coupled, high-frequency electrical stimulation of the pudendal nerve blocks external urethral sphincter contractions. *Neurorehabilitation and Neural Repair*, **23**:615-626.

Grossman Y and Kendig J J. **1987.** Modulation of Impulse Conduction through Axonal Branchpoint by Physiological, Chemical and Physical Factors. *Israel Journal of Medical Sciences*, **23**:107-114.

Grossman Y, Parnas I and Spira M E. **1979.** Differential conduction block in branches of a bifurcating axon. *J Physiol*, **295**:283-305.

Grossman Y, Parnas I and Spira M E. **1979.** Ionic Mechanisms Involved in Differential Conduction of Action Potentials at High-Frequency in a Branching Axon. *Journal of Physiology-London*, **295**:307-&.

Gu X N. **1991.** Effect of Conduction Block at Axon Bifurcations on Synaptic Transmission to Different Postsynaptic Neurons in the Leech. *Journal of Physiology-London*, **441**:755-778.

Gunther J. **1976.** Impulse conduction in the myelinated giant fibers of the earthworm. Structure and function of the dorsal nodes in the median giant fiber. *Journal of Comparative Neurology*, **168**:505-531.

Guven M, Bozdemir H, Gunay I, Sarica Y, Kahraman I and Koc F. **2006.** The actions of lamotrigine and levetiracetam on the conduction properties of isolated rat sciatic nerve. *European Journal of Pharmacology*, **553**:129-134.

Guven M, Ozgunen K and Gunay I. **2005.** Conduction blocks of lidocaine on crushed rat sciatic nerve: An in-vitro study. *International Journal of Neuroscience*, **115**:725-734.

Haeffele B D and Butera R J. **2007.** Modifying the Hodgkin-Huxley Model for High Frequency AC Stimulation. *CNE '07. 3rd International IEEE/EMBS Conference on Neural Engineering, 2007*:550-552.

Hatsopoulos N G and Donoghue J P. **2009.** The science of neural interface systems. *Annual Review of Neuroscience*, **32**:249-266.

Haydon D A and Urban B W. **1985.** The Admittance of the Squid Giant-Axon at Radio Frequencies and Its Relation to Membrane-Structure. *Journal of Physiology-London*, **360**:275-291.

Henneman E and Olson C B. **1965.** Relations between Structure and Function in Design of Skeletal Muscles. *Journal of Neurophysiology*, **28**:581-&.

Hines M L and Carnevale N T. **1997.** The NEURON simulation environment. *Neural Computation*, **9**:1179-1209.

Hodgkin A L and Huxley A F. **1952.** A Quantitative Description of Membrane Current and Its Application to Conduction and Excitation in Nerve. *Journal of Physiology-London*, **117**:500-544.

Inoue I, Tsutsui I, Abbott N J and Brown E R. **2002.** Ionic currents in isolated and in situ squid Schwann cells. *Journal of Physiology-London*, **541**:769-778.

Ishigooka M, Hashimoto T, Sasagawa I, Izumiya K and Nakada T. **1994.** Modulation of the Urethral Pressure by High-Frequency Block Stimulus in Dogs. *European Urology*, **25**:334-337.

Jensen A L and Durand D M. **2007.** Suppression of axonal conduction by sinusoidal stimulation in rat hippocampus in vitro. *Journal of Neural Engineering*, **4**:1-16.

Joseph L and Butera R J. **2007.** Conduction block in unmyelinated nerves using high frequency AC stimulation. *CNE '07. 3rd International IEEE/EMBS Conference on Neural Engineering, 2007*:575 - 577.

Joseph L and Butera R J. **2009.** Unmyelinated Aplysia nerves exhibit a nonmonotonic blocking response to high-frequency stimulation. *IEEE Transactions on Neural Systems and Rehabilitation Engineering*, **17**:537-544.

Joseph L, Haeffele B D and Butera R J. **2007.** Conduction block induced by high frequency AC stimulation in unmyelinated nerves. *Conference Proceedings IEEE Engineering in Medicine and Biology Society*:1719-1722.

Kandel E R. **1979.** *Behavioral biology of Aplysia : a contribution to the comparative study of opisthobranch molluscs*, San Francisco: W. H. Freeman.

Kandel E R, Schwartz J H and Jessell T M. **2000.** *Principles of neural science*, New York: McGraw-Hill, Health Professions Division.

Kane L S, Buttram J G, Urazaev A K, Lieberman E M and Grossfeld R M. **2000.** Uptake and metabolism of glutamate at non-synaptic regions of crayfish central nerve fibers: Implications for axon-glia signaling. *Neuroscience*, **97**:601-609.

Kilgore K L and Bhadra N. **2004.** Nerve conduction block utilising high-frequency alternating current. *Medical & Biological Engineering & Computing*, **42**:394-406.

Kilgore K L, Foldes E A, Ackermann D M and Bhadra N. **2009.** Combined direct current and high frequency nerve block for elimination of the onset response. *Conference Proceedings of IEEE Engineering in Medicine and Biology Society*, **2009**:197-199.

Lertmanorat Z, Gustafson K J and Durand D M. **2006.** Electrode array for reversing the recruitment order of peripheral nerve stimulation: experimental studies. *Annals of Biomedical Engineering*, **34**:152-160.

Levi R, Hultling C, Nash M S and Seiger A. **1995.** The Stockholm spinal cord injury study: 1. Medical problems in a regional SCI population. *Paraplegia*, **33**:308-315.

Martinov V N and Nja A. **2005.** A microcapsule technique for long-term conduction block of the sciatic nerve by tetrodotoxin. *Journal of Neuroscience Methods*, **141**:199-205.

McIntyre C C, Richardson A G and Grill W M. **2002.** Modeling the excitability of mammalian nerve fibers: Influence of afterpotentials on the recovery cycle. *Journal of Neurophysiology*, **87**:995-1006.

McMullan S, Simpson D A A and Lumb B M. **2004.** A reliable method for the preferential activation of C- or A-fibre heat nociceptors. *Journal of Neuroscience Methods*, **138**:133-139.

Meems R, Munno D, van Minnen J and Syed N I. **2003.** Synapse formation between isolated axons requires presynaptic soma and redistribution of postsynaptic AChRs. *Journal of Neurophysiology*, **89**:2611-2619.

Meems R W. 2005. Synapse Formation on the role of extrasomal compartments. In *Department of Cell Biology and Anatomy*.

Mendell L M. **2005.** The size principle: a rule describing the recruitment of motoneurons. *Journal of Neurophysiology*, **93**:3024-3026.

Miles J D, Kilgore K L, Bhadra N and Lahowetz E A. **2007.** Effects of ramped amplitude waveforms on the onset response of high-frequency mammalian nerve block. *Journal of Neural Engineering*, **4**:390-398.

Nowotny T, Zhigulin V P, Selverston A I, Abarbanel H D I and Rabinovich M I. **2003.** Enhancement of synchronization in a hybrid neural circuit by spike-timing dependent plasticity. *Journal of Neuroscience*, **23**:9776-9785.

O'Dwyer N J, Ada L and Neilson P D. **1996.** Spasticity and muscle contracture following stroke. *Brain*, **119 (Pt 5)**:1737-1749.

Peng C W, Chen J J, Lin C C, Poon P W, Liang C K and Lin K P. **2004.** High frequency block of selected axons using an implantable microstimulator. *Journal of Neuroscience Methods*, **134**:81-90.

Perot P L and Stein S N. **1956.** Conduction Block in Peripheral Nerve Produced by Oxygen at High Pressure. *Science*, **123**:802-803.

Perot P L and Stein S N. **1959.** Conduction Block in Mammalian Nerve Produced by O-2 at High Pressure. *American Journal of Physiology*, **197**:1243-1246.

Petruska J C, Hubscher C H and Johnson R D. **1998.** Anodally focused polarization of peripheral nerve allows discrimination of myelinated and unmyelinated fiber input to brainstem nuclei. *Exp Brain Res*, **121**:379-390.

Prochazka A, Mushahwar V K and McCreery D B. **2001.** Neural prostheses. *Journal of Physiology-London*, **533**:99-109.

Reboul L and Rosenblueth A. **1939.** The action of alternating currents upon the electrical excitability of nerve. *American Journal of Physiology*, **125**:205-215.

Richardson A G, McIntyre C C and Grill W M. **2000.** Modelling the effects of electric fields on nerve fibres: influence of the myelin sheath. *Medical & Biological Engineering & Computing*, **38**:438-446.

Ridgway R L, Syed N I, Lukowiak K and Bulloch A G M. **1991.** Nerve Growth-Factor (Ngf) Induces Sprouting of Specific Neurons of the Snail, Lymnaea-Stagnalis. *Journal of Neurobiology*, **22**:377-390.

Roberts M B V. **1986.** *Biology:a functional approach*: Nelson Thornes.

Rosenblueth A and Reboul J. **1939.** The blocking and deblocking effects of alternating currents on nerve. *American Journal of Physiology*, **125**:251-264.

Rushton D N. **1997.** Functional electrical stimulation. *Physiological Measurement*, **18**:241-275.

Scriven D R. **1981.** Modeling repetitive firing and bursting in a small unmyelinated nerve fiber. *Biophysical Journal*, **35**:715-730.

Smith D O. **1983.** Axon Conduction Failure under Invivo Conditions in Crayfish. *Journal of Physiology-London*, **344**:327-333.

Solomonow M. **1984.** External Control of the Neuromuscular System. *IEEE Transactions on Biomedical Engineering*, **31**:752-763.

Solomonow M, Eldred E, Lyman J and Foster J. **1983.** Control of Muscle Contractile-Force through Indirect High-Frequency Stimulation. *American Journal of Physical Medicine & Rehabilitation*, **62**:71-82.

Strichartz G. **1976.** Molecular Mechanisms of Nerve Block by Local-Anesthetics. *Anesthesiology*, **45**:421-441.

Syed N I, Zaidi H and P.Lovell. **1999.** *Modern Techniques in Neuroscience Research*.

Tai C, Roppolo J R and de Groat W C. **2004.** Block of external urethral sphincter contraction by high frequency electrical stimulation of pudendal nerve. *Journal of Urology*, **172**:2069-2072.

Tai C F, de Groat W C and Roppolo J R. **2005.** Simulation analysis of conduction block in unmyelinated axons induced by high-frequency biphasic electrical currents. *IEEE Transactions on Biomedical Engineering*, **52**:1323-1332.

Tai C F, de Groat W C and Roppolo J R. **2005.** Simulation of nerve block by high-frequency sinusoidal electrical current based on the Hodgkin-Huxley model. *IEEE Transactions on Neural Systems and Rehabilitation Engineering*, **13**:415-422.

Tai C F, Roppolo J R and De Groat W C. **2005.** Response of external urethral sphincter to high frequency biphasic electrical stimulation of pudendal nerve. *Journal of Urology*, **174**:782-786.

Tai C F, Smerin S E, de Groat W C and Roppolo J R. **2006.** Pudendal-to-bladder reflex in chronic spinal-cord-injured cats. *Experimental Neurology*, **197**:225-234.

Tanner J A. **1962.** Reversible blocking of nerve conduction by alternating-current excitation. *Nature*, **195**:712-713.

Wang J, Shen B, Roppolo J R, de Groat W C and Tai C. **2008.** Influence of frequency and temperature on the mechanisms of nerve conduction block induced by high-frequency biphasic electrical current. *Journal of Computational Neuroscience*, **24**:195-206.

Williamson R P and Andrews B J. **2005.** Localized electrical nerve blocking. *IEEE Transactions on Biomedical Engineering*, **52**:362-370.

Woo M Y and Campbell B. **1964.** Asynchronous Firing and Block of Peripheral Nerve Conduction by 20 Kc Alternating Current. *Bulletin of the Los Angeles Neurological Society*, **29**:87-94.

Zhang X, Roppolo J R, de Groat W C and Tai C F. **2006.** Mechanism of nerve conduction block induced by high-frequency biphasic electrical currents. *IEEE Transactions on Biomedical Engineering*, **53**:2445-2454.

Zhang X, Roppolo J R, de Groat W C and Tai C F. **2006.** Simulation analysis of conduction block in myelinated axons induced by high-frequency biphasic rectangular pulses. *IEEE Transactions on Biomedical Engineering*, **53**:1433-1436.

VITA

Laveeta Joseph was born in Kerala, India and grew up in Hyderabad, India. After completing her Bachelor of Engineering degree in Biomedical Engineering from Osmania Univeristy, Hyderabad, where she ranked first among the graduating class of 2004, she joined the Interdisciplinary Bioengineering Graduate Program at the Georgia Institute of Technology, Atlanta.

During her PhD, Laveeta presented her research work at several international conferences, both in the form of posters and talks for which she received various awards including the SfN Graduate Student Travel Award in 2007, the Neural Engineering Conference Graduate Student Travel Award in 2007 and the NIC 2010 Excellence in Neural Interfacing Award. She was also awarded the Schlumberger Faculty for the Future Fellowship from 2007-2010 for her research and teaching skills. In Fall 2008, Laveeta joined the Dual-degree Technology Leadership Program at Georgia Tech to concurrently pursue an MBA along with her PhD.

Laveeta also found her future husband in the Bioengineering Program at Georgia Tech in 2006 and they got married in February 2009. She graduated with her MBA in May 2010 and successfully defended her PhD in June 2010. In the future, she hopes to pursue a career in the medical device industry so that she can contribute to making a difference in the lives of patients.